

C.P. No. 1079

C.P. No. 1079



LIBRARY ESTABLISHMENT
AERONAUTICAL RESEARCH COUNCIL
BEDFORD

MINISTRY OF TECHNOLOGY

AERONAUTICAL RESEARCH COUNCIL

CURRENT PAPERS

Gusts, Discrete and Indiscrete

by

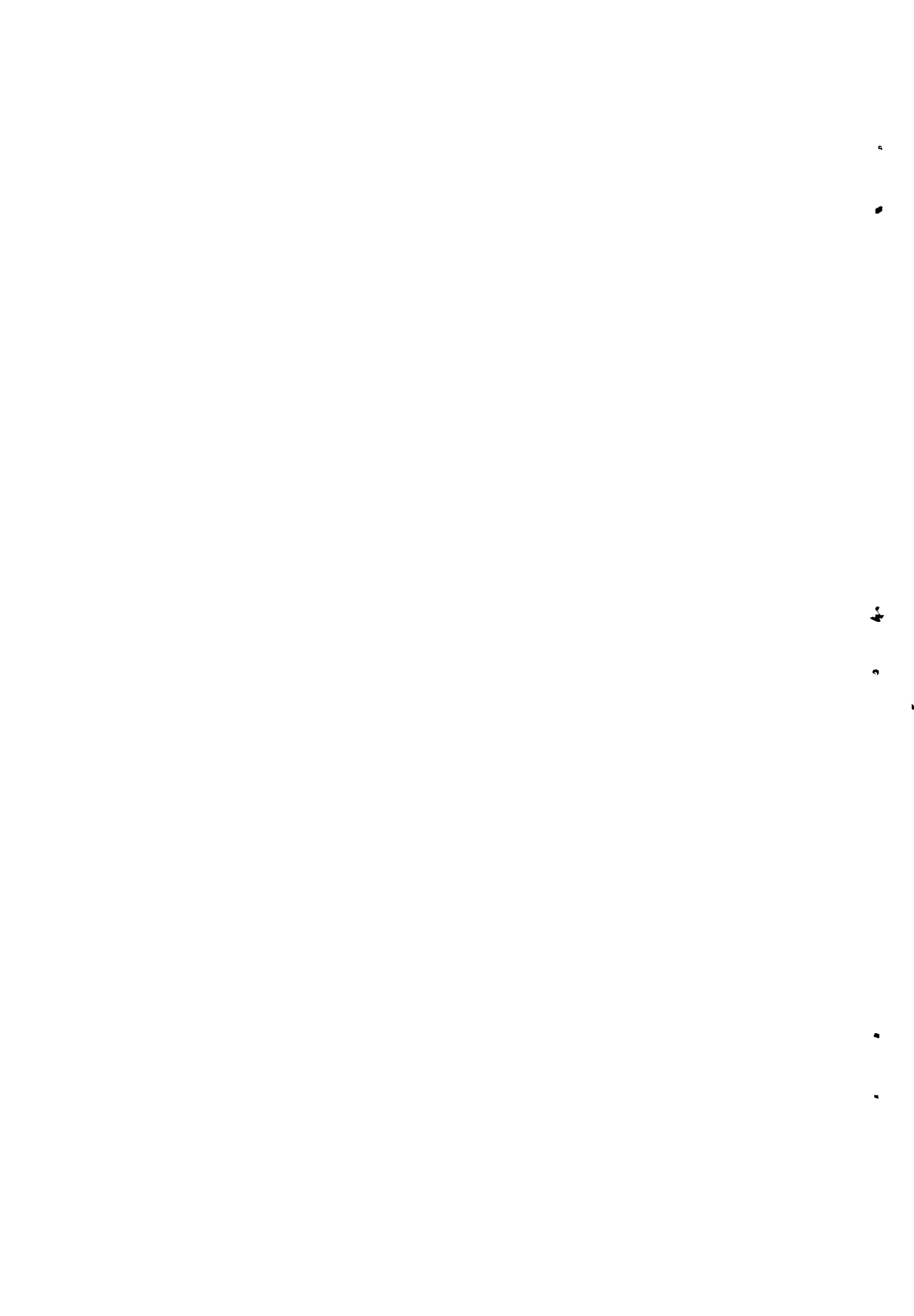
N. I. Bullen

Structures Dept., R.A.E., Farnborough

LONDON · HER MAJESTY'S STATIONERY OFFICE

1970

PRICE 17s 6d [87½p] NET



U.D.C. 533.6.048.5 : 551.551 : 519.242 : 519.251 : 5.001.57

C.P. No.1079*
March 1969

GUSTS, DISCRETE AND INDISCRETE

by

N. I. Bullen

Structures Department, R.A.E., Farnborough

SUMMARY

For the analysis of gust loads on aircraft, a method is described in which the occurrence and magnitude of the loads are represented as random variables.

The paper begins with the discrete gust, and goes on to treat the case in which the disturbances are too frequent to be considered singly and become indiscrete. In the limit this leads to the usual results obtained from the spectral approach, but in the observational material examined this limit is not reached. The simple mathematical model developed here gives a consistent picture of the properties of observed gust load frequency distributions.

CONTENTS

	<u>Page</u>
1 INTRODUCTION	3
2 MATHEMATICAL ANALYSIS OF SIMPLE CASE	4
3 EXTENSIONS OF THE SIMPLE CASE	8
4 GENERAL MATHEMATICAL ANALYSIS	11
5 POSSIBLE EXTENSIONS OF THE MODEL	23
6 R.F. JONES'S THUNDERSTORM DATA	24
7 'SWIFTER' MIDDAY FLIGHTS OVER FLAT DESERT	27
8 'SWIFTER' STACKED SORTIES	30
9 DISCUSSION OF OBSERVATIONAL RESULTS	32
10 CONCLUSIONS	33
Appendix A Summary of mathematical model	34
Appendix B Note on curve fitting	36
Tables 1-7	38-51
Symbols	52
References	54
Illustrations	Figures 1-13
Detachable abstract cards	-

1 INTRODUCTION

When making comparisons between aircraft of the loads imposed by atmospheric turbulence it is useful to set up a theoretical model representing the statistical properties of the turbulence.

The usual procedure is to observe, say, the normal acceleration on an instrumented aircraft; from these observations deduce the parameters of the assumed model, and finally to estimate the response of a second aircraft. Quantities of particular importance are the magnitudes of the high loads, from the point of view of ultimate strength, and the number of the smaller loads for fatigue considerations.

Since the steps taken in deducing the parameters of the model from the observations are retraced when making further predictions, most models work reasonably well for aircraft of similar geometrical and dynamic properties.

Some years ago what is called the 'discrete gust' model was widely used. This assumes that the aircraft normal acceleration increments - bumps - are all caused by discrete gusts of a standard shape; knowing the aircraft characteristics, their frequency and distribution of magnitudes is determined from the observations.

More recently, the atmosphere has been defined in terms of a spectrum, usually of a standard shape, the disposable parameters being a scale-length and an intensity or root-mean-square value. Given this 'input' spectrum and the aircraft response characteristics (i.e. its 'transfer function') the output spectrum is deduced. Subject to certain conditions, from the output spectrum may be determined the root-mean-square value of the quantity under examination, and the number of times its mean value is crossed in the positive direction per unit time (or distance), usually designated by the symbol N_0 .

When the disturbances encountered by the aircraft occur in isolation, a discrete gust approach is appropriate. As the disturbances become more numerous so that their effects become superimposed, the discrete gust approach is no longer satisfactory.

If, in these conditions, spectral methods are used without establishing to what extent the conditions under which they are valid are satisfied in practice, then little reliance can be placed on the results, particularly in the case of the number of zero crossings.

It is the purpose of this paper to examine these problems from a new standpoint. Rice¹, in his paper to which we refer in detail later, bases most of his results on the representation of a random process in terms of a large number of sinusoidal disturbances. He remarks, however, that its representation as a 'shot effect' may also be used as a starting point. In this, the random process is represented by the superposition of a large number of identical pulses occurring randomly with respect to time.

This idea is pursued here and compared with the spectral approach. The simple model developed is also found to be successful in explaining many aspects of observed gust distributions, and this is illustrated by observational material.

The paper falls into two main parts. Sections 2 to 5 deal with the theoretical aspects and derive a simple model for gust loads which is summarised in Appendix A. Sections 6 to 9 deal with the observational material illustrating various aspects of the model. Readers mainly interested in practical applications may prefer to read Appendix A in place of sections 2 to 5. Finally, broad conclusions are given in section 10 and some remarks on curve fitting are made in Appendix B.

2 MATHEMATICAL ANALYSIS OF SIMPLE CASE

2.1 When an aircraft is in turbulence, a response quantity under consideration can be examined by means of random process theory. The representation often adopted for the random process is a spectral one. An alternative representation is considered here, in which the random process x consists of the sum of a number of identical pulses occurring at random with respect to time. The pulse shape is given by $F(t)$ and

$$x = \sum_k F(t - t_k) \quad (1)$$

where the k th pulse arrives at time t_k and the summation is over all pulses.

Initially, the pulse shape considered is defined by

$$F(t) = a e^{-\lambda t} \quad (2)$$

for values of $t \geq 0$ and zero for $t < 0$.

The pulse shape is illustrated in Fig.1a. (A range of pulse shapes considered in section 4.3 is also shown in Fig.1b.) Each pulse thus consists of

instantaneous build-up of magnitude a and an exponential decay of rate λ per unit time*. Let the average number of pulses per unit time be ν .

Then, by Campbell's theorem, the mean value of the random process is given by

$$\bar{x} = \nu \int_0^{\infty} a e^{-\lambda t} dt$$

i.e.

$$\bar{x} = \nu a / \lambda \quad (3)$$

(see Rice¹ 1.2-2); and the variance about the mean value is given by

$$\sigma^2 = \nu \int_0^{\infty} a^2 e^{-2\lambda t} dt$$

i.e.

$$\sigma^2 = \nu a^2 / (2\lambda) \quad (4)$$

(Rice 1.2-3).

Furthermore, for large values of ν/λ the distribution tends to become of Gaussian form and is then given by

$$f(x) = \frac{1}{\sigma \sqrt{2\pi}} \exp \left\{ - (x - \bar{x})^2 / (2\sigma^2) \right\} \quad (5)$$

The rate at which positive crossings of the mean value occur, for the case of ν/λ large, is determined as follows. At all times except for the

* This pulse shape has a bearing on the aircraft problem. If we consider a rigid aircraft flying without pitching into a sharp-edged gust, and assume that the lift builds up instantaneously, (i.e. neglecting Kussner and Wagner effects) then its normal acceleration is given by

$$\ddot{z} = \frac{UV}{\mu_g c} e^{-\frac{s}{\mu_g c}}$$

where c is the aircraft chord
 s is the distance flown into the gust
 U is the gust velocity
 V is the aircraft velocity
 \ddot{z} is the aircraft normal acceleration
 μ_g is the aircraft mass parameter.

infinitesimal time when the pulses build up, the value of x approaches zero at a rate λx . A crossing of the mean value in a positive direction can only occur at the build-up of a pulse, and then only if the variable x is in a range of width a below the mean value, immediately before its occurrence.

The fraction of time the variable x spends between $\bar{x} - a$ and \bar{x} is given by

$$\frac{1}{\sigma \sqrt{2\pi}} \int_{\bar{x}-a}^{\bar{x}} \exp \left\{ - (x - \bar{x})^2 / (2\sigma^2) \right\} dx . \quad (6)$$

Since ν/λ is large, a is small compared with σ and the integral (6) is approximately equal to

$$a / (\sigma \sqrt{2\pi}) . \quad (7)$$

The number of positive zero crossings per unit time, N_0 , is thus

$$\nu a / (\sigma \sqrt{2\pi})$$

and substituting for σ from (4) gives finally

$$N_0 = \sqrt{(\lambda \nu / \pi)} . \quad (8)$$

It is seen that N_0 depends partly on λ , the rate at which x returns to zero, and partly on ν , the number of pulses per unit time, each of these being of dimensions $[T]^{-1}$.

2.2 An alternative approach is now considered. The autocorrelation function of the random variable x is first derived. Since the pulses occur at random, cross contributions to the autocorrelation function vanish so that the autocorrelation function depends only on the shape a single pulse itself.

Using Rice (2.6-2) and finding the autocorrelation function for x about its mean value gives

$$R(\tau) = \frac{\nu a^2}{2\lambda} e^{-\lambda\tau} \quad (9)$$

where $R(\tau)$ is the unnormalised autocorrelation function so that when $\tau = 0$, $R(\tau) = \nu a^2 / (2\lambda)$, that is, the variance.

The Fourier transform of $R(\tau)$ gives the spectrum $S(\omega)$ which is

$$S(\omega) = \frac{va^2}{2\lambda} \times \frac{2\lambda}{\pi(\lambda^2 + \omega^2)} \quad (10)$$

If this function is used in Rice's formula for the number of zero crossings (Rice 3.3-11), as $\int_0^{\infty} \omega^2 S(\omega) d\omega$ is infinite, an infinite number of zero crossings per unit time is predicted, in contradiction of (8) above.

2.3 Rice himself discusses the problem in connection with "a broad band noise voltage" applied to a resistance and condenser in series. This is analogous to the case discussed here. The arrival of an electron at the condenser corresponds to the initial build-up of the pulse and the total charge on the condenser decays exponentially. Rice attempts to explain the difficulty by considering the spectrum as consisting of two bands of noise and discusses this aspect in some detail. It is also argued that in a physical system there is always a high frequency cut-off to the spectrum which prevents the required integral becoming infinite in practice. These arguments however, do not resolve the theoretical problem which is of an entirely different origin.

In deriving his formula for the number of zero crossings, Rice (3.3-7) takes as his representation of the random process

$$\xi = \sum_{n=1}^N c_n \cos(\omega_n t - \phi_n) \quad (11)$$

and uses the fact that ξ and η , its first derivative with respect to time, each have a Gaussian distribution and are independent. (Rice's ξ and η correspond to our x and \dot{x} .) However, in the case under consideration, x and \dot{x} are not independent, since, apart from the infinitesimal time during which pulses arrive, x and \dot{x} are related by the equation

$$\dot{x} = -\lambda x \quad (12)$$

and, furthermore, the distribution of \dot{x} is by no means Gaussian. It appears from the analysis given in section 4, that the latter fact plays

the greater part in invalidating the procedure. It may be concluded that the representation given in (11) is not a satisfactory one for the random process under consideration here.

2.4 We return to a more general discussion of the problem in section 4.

Section 3 digresses to some extent from the main argument to consider a few simple extensions of the above treatment, making it somewhat more representative of the gust problem, and to derive a number of formulae illustrating limiting cases of the subsequent analysis.

3 EXTENSIONS OF THE SIMPLE CASE

3.1 If the pulses, (2) are assumed to be positive or negative at random, as well as being random in time, the process will have zero mean. For an average pulse rate ν , ($\nu/2$ positive, $\nu/2$ negative), the variance as before is $\nu a^2/(2\lambda)$.

Positive zero crossings occur at a rate $\nu/2$ times the fraction of time spent in the range $-a$ to 0 , where a is small compared with σ . Proceeding as before then gives

$$N_0 = \frac{1}{2} \sqrt{\frac{\nu\lambda}{\pi}} . \quad (13)$$

This process is symmetrical while that of section 2.1 is markedly skew for moderate values of ν/λ .

It may be useful to have a second-order approximation for N_0 . If in (6) we put $x - \bar{x} = y$, keep the first two terms in the expansion of the exponential, and integrate, we obtain

$$N_0 = \frac{1}{2} \sqrt{\frac{\nu\lambda}{\pi}} \left(1 - \frac{\lambda}{3\nu} \right) . \quad (14)$$

The number of crossings of any value x can be found by a similar method. When the distribution of x approaches the Gaussian form and a is small compared with σ , the distribution of x -crossings tends to that of x itself. As will be shown (section 4.1) this is also the case generally, when x and \dot{x} are independent.

3.2 As a further extension, let a vary from pulse to pulse, having a distribution given by

$$f(a) = \frac{1}{\rho \sqrt{2\pi}} \exp \left\{ -\frac{a^2}{(2\rho^2)} \right\} . \quad (15)$$

Again the mean is zero and the variance is given by

$$\sigma^2 = \nu \rho^2 / (2\lambda) . \quad (16)$$

This follows from an extension of Campbell's Theorem derived by Rice (1.5-2).

A positive zero crossing occurs when the variable is in the range $-x$ to $-x + dx$ and receives a pulse of magnitude x or greater. The probability of the first event is

$$\frac{1}{\sigma \sqrt{2\pi}} \exp \left\{ -\frac{x^2}{(2\sigma^2)} \right\} dx \quad (17)$$

and the probability that a pulse is of magnitude x or greater is

$$\frac{1}{\rho \sqrt{2\pi}} \int_x^\infty \exp \left\{ -\frac{a^2}{(2\rho^2)} \right\} da . \quad (18)$$

Integrating the joint probability and multiplying by ν gives:-

$$N_o = \frac{\nu}{2\pi \rho \sigma} \int_0^\infty \int_x^\infty \exp \left(-\frac{x^2}{2\sigma^2} - \frac{a^2}{2\rho^2} \right) da dx . \quad (19)$$

To evaluate the integral substitute

$$\begin{aligned} x &= \sigma r \sin \theta \\ a &= \rho r \cos \theta . \end{aligned}$$

The area of integration is a sector bounded by $\theta = 0$ (when $x = 0$) and $\theta = \arctan(\rho/\sigma)$ (when $a = x$), and extending from $r = 0$ to $r = \infty$.

Thus

$$N_o = \frac{\nu}{2\pi} \int_0^{\arctan(\rho/\sigma)} \int_0^\infty e^{-\frac{r^2}{2}} r dr d\theta . \quad (20)$$

Integrating and putting $\rho/\sigma = \sqrt{(2\lambda/\nu)}$ gives finally

$$N_o = \frac{\nu}{2\pi} \arctan \sqrt{(2\lambda/\nu)} \quad (21)$$

or for large ν/λ

$$N_o = \frac{1}{\pi} \sqrt{\frac{\lambda\nu}{2}} \left(1 - \frac{2\lambda}{3\nu}\right) \quad (22)$$

as far as second-order terms.

3.3 As a final example in this section, the case when a is distributed exponentially is considered. Let

$$f(a) = \frac{1}{2\rho} e^{-\frac{|a|}{\rho}} \quad (23)$$

so that

$$\overline{a^2} = 2\rho^2 \quad (24)$$

and

$$\sigma^2 = \nu\rho^2/\lambda \quad (25)$$

The probability that a exceeds a value x is $\frac{1}{2} e^{-x/\rho}$, and the probability that x lies between $-x$ and $-x + dx$ is

$$\frac{1}{\sigma\sqrt{2\pi}} \exp\{-x^2/(2\sigma^2)\} dx \quad .$$

Thus,

$$N_o = \frac{\nu}{2\sqrt{2\pi}} \int_0^{\infty} \exp\left\{-\frac{x^2}{2\sigma^2} - \frac{x}{\rho}\right\} d\left(\frac{x}{\rho}\right) \quad (26)$$

The integral reduces to Mills' ratio for σ/ρ . Kendall and Stuart² (Vol.1 p 137) give for this ratio an asymptotic expansion in which the remainder at any point in the summation is less in absolute value than the last term taken into account. Keeping the first two terms in the asymptotic series gives

$$N_o = \frac{\nu}{2\sqrt{2\pi}} \left(\frac{\rho}{\sigma} - \frac{\rho^3}{\sigma^3}\right) \quad (27)$$

and using (25) to substitute for σ/ρ we have finally

$$N_o = \frac{1}{2} \sqrt{\frac{\nu\lambda}{2\pi}} \left(1 - \frac{\lambda}{\nu}\right) \quad (28)$$

3.4 All the formulae for N_0 derived in this section are, to the first order of small quantities, of the form

$$N_0 = \text{constant} \times \sqrt{\nu\lambda}$$

and although the distributions assumed for a differ considerably, the constant shows comparatively small differences. Evaluating the constant in (14), (22) and (28) gives 0.2824, 0.2244, and 0.1995 respectively.

4 GENERAL MATHEMATICAL ANALYSIS

4.1 In general, it is necessary to derive for the random process not only the rate of zero crossings, but also the rate of crossing of any value x and hence, the frequency distribution of crossings. In order to do this, knowledge is required of the joint frequency distribution of x and \dot{x} . It can then be shown that the number of x -crossings in the positive direction, N_x , is given by

$$N_x = \int_0^{\infty} \dot{x} f(x, \dot{x}) d\dot{x} \quad (29)$$

where $f(x, \dot{x})$ is the joint frequency distribution of x and \dot{x} . (See for example, Crandall and Mark³ p 45).

Thus, N_x is the average positive value of \dot{x} at the value x , multiplied by $\int_0^{\infty} f(x, \dot{x}) d\dot{x}$, which is the value of the one-dimensional distribution of x for positive values of \dot{x} .

When x and \dot{x} are independent, then

$$f(x, \dot{x}) = f_1(x) f_2(\dot{x}) \quad (30)$$

and

$$N_x = f_1(x) \int_0^{\infty} \dot{x} f_2(\dot{x}) d\dot{x} \quad (31)$$

The integral is independent of x and depends only on the function f_2 , so that the rate of x -crossings is proportional to $f_1(x)$; that is, to the original distribution of x .

4.2 In order to determine the joint distribution of x and \dot{x} use is made of a result given by Rice (section 3.11). This states the following.

If,

$$\xi = \sum_k F(t - t_k) \quad (32)$$

and

$$\eta = \sum_k G(t - t_k) \quad (33)$$

where the t_k are the same in (32) and (33), then the cumulant $\kappa_{r,s}$ of the joint distribution of ξ and η is given by

$$\kappa_{r,s} = v \int_{-\infty}^{\infty} F^r(t) G^s(t) dt \quad (34)$$

For the case being considered here, $\xi = x$ and $\eta = \dot{x}$. The characteristic function of the joint distribution is then given by

$$\phi(u, v) = \exp \left\{ \sum \frac{\kappa_{r,s}}{r! s!} (iu)^r (iv)^s \right\} \quad (35)$$

and the joint distribution itself follows by taking the transform of the characteristic function, so that

$$f(x, \dot{x}) = \frac{1}{4\pi^2} \int_{-\infty}^{\infty} \int_{-\infty}^{\infty} e^{-iux - iv\dot{x}} \phi(u, v) du dv \quad (36)$$

A simple extension of the above formulae allows the magnitude distribution of the pulses to be taken into account. Let the magnitude of the pulse be proportional to a variable a of known distribution. It follows from the additive property of cumulants that it is merely necessary to replace a^n where it occurs in (34) by its mean value $\overline{a^n}$. Apart from this, equations (34) are unchanged. For the symmetrical case, $\overline{a^n} = 0$ for n odd and hence $\kappa_{r,s} = 0$ for $(r + s)$ odd. Thus the problem is theoretically solved. The procedure, then, in the aircraft case is as follows. The atmosphere is defined in terms of a population of discrete gusts of standard shape, occurring with a given mean frequency, and with a given magnitude distribution. The aircraft response to a single gust is then determined in as much detail as is necessary, there being no restriction on the number of degrees of freedom considered. From the response to a single gust the cumulants of the joint

distribution of x and \dot{x} , the variable under consideration and its first derivative, are determined from (34). The joint distribution of x and \dot{x} follow from (35) and (36) and any information regarding the crossing distribution from (29).

This procedure will now be illustrated by means of a very simple model, applied to aircraft normal acceleration. However, simple though the model is, we shall see later that it is adequate to explain many of the observed features of gust load distributions.

4.3 The pulse shape assumed in this section is a rough approximation to the response of an aircraft to a discrete gust. If unsteady lift functions are ignored and the gust shape is assumed to be

$$u = U(1 - e^{-\lambda_2 s}) \quad (37)$$

then the aircraft normal acceleration is given by

$$\ddot{z} = \frac{UV}{c \mu_g} \times \frac{\lambda_2}{\lambda_2 - \lambda_1} (e^{-\lambda_1 s} - e^{-\lambda_2 s}) \quad (38)$$

where $\lambda_1 = 1/(c \mu_g)$ and s is the distance.

This is equivalent to assuming a sharp-edged gust with

$$\left. \begin{aligned} \psi &= 1 - e^{-\lambda_2 s} \\ \varphi &= 1 \end{aligned} \right\} \quad (39)$$

for the unsteady lift functions.

In the following analysis the symbol t is retained for the independent variable and $UV/(c \mu_g)$ replaced by the symbol a , so that we let

$$F(t) = \frac{a \lambda_2}{\lambda_2 - \lambda_1} (e^{-\lambda_1 t} - e^{-\lambda_2 t}) \quad (40)$$

and a for the time being is assumed constant.

This pulse shape is illustrated in Fig.1(ii) for $\lambda_2 = 10 \lambda_1$, $\lambda_2 = 5 \lambda_1$ and $\lambda_2 = 2 \lambda_1$. The maximum occurs at time t_m where

$$t_m = \log(\lambda_2/\lambda_1)/(\lambda_2 - \lambda_1) \quad (41)$$

and is of magnitude $ae^{-\lambda_1 t_m}$.

Differentiating (40) we get

$$G(t) = \frac{-a\lambda_2}{\lambda_2 - \lambda_1} (\lambda_1 e^{-\lambda_1 t} - \lambda_2 e^{-\lambda_2 t}) \quad (42)$$

The cumulants of the joint distribution of x and \dot{x} are then given by (34). Up to the fourth order these are listed below in (43) together with the form taken when setting $\lambda_1/\lambda_2 = \alpha$

$$\kappa_{1,0} = va/\lambda_1 \quad (43)(i)$$

$$\kappa_{0,1} = 0 \quad (ii)$$

$$\kappa_{2,0} = \frac{va^2 \lambda_2}{2\lambda_1(\lambda_1 + \lambda_2)} = \frac{va^2}{2\lambda_1(1 + \alpha)} \quad (iii)$$

$$\kappa_{1,1} = 0 \quad (iv)$$

$$\kappa_{0,2} = \frac{va^2 \lambda_2^2}{2(\lambda_1 + \lambda_2)} = \frac{va^2 \lambda_2}{2(1 + \alpha)} \quad (v)$$

$$\kappa_{3,0} = \frac{2va^3 \lambda_2^2}{3\lambda_1(2\lambda_1 + \lambda_2)(\lambda_1 + 2\lambda_2)} = \frac{va^3}{3\lambda_1(1 + 2\alpha)(1 + \alpha/2)} \quad (vi)$$

$$\kappa_{2,1} = 0 \quad (vii)$$

$$\kappa_{1,2} = \frac{va^3 \lambda_2^3}{3(2\lambda_1 + \lambda_2)(\lambda_1 + 2\lambda_2)} = \frac{va^3 \lambda_2}{6(1 + 2\alpha)(1 + \alpha/2)} \quad (viii)$$

$$\kappa_{0,3} = \frac{2va^3 \lambda_2^3 (\lambda_1 + \lambda_2)}{3(2\lambda_1 + \lambda_2)(\lambda_1 + 2\lambda_2)} = \frac{va^3 \lambda_2^2 (1 + \alpha)}{3(1 + 2\alpha)(1 + \alpha/2)} \quad (ix)$$

$$\kappa_{4,0} = \frac{3va^4 \lambda_2^3}{4\lambda_1(\lambda_1 + \lambda_2)(\lambda_1 + 3\lambda_2)(3\lambda_1 + \lambda_2)} = \frac{va^4}{4\lambda_1(1 + \alpha)(1 + 3\alpha)(1 + \alpha/3)} \quad \dots\dots\dots (x)$$

$$\kappa_{3,1} = 0 \quad (xi)$$

$$\kappa_{2,2} = \frac{va^4 \lambda_2^4}{4(\lambda_1 + \lambda_2)(\lambda_1 + 3\lambda_2)(3\lambda_1 + \lambda_2)} = \frac{va^4 \lambda_2}{12(1 + \alpha)(1 + 3\alpha)(1 + \alpha/3)} \dots\dots (xii)$$

$$\kappa_{1,3} = \frac{va^4 \lambda_2^4}{4(\lambda_1 + 3\lambda_2)(3\lambda_1 + \lambda_2)} = \frac{va^4 \lambda_2^2}{12(1 + 3\alpha)(1 + \alpha/3)} \dots\dots (xiii)$$

$$\kappa_{0,4} = \frac{3va^4 \lambda_2^4 (\lambda_1^2 + 3\lambda_1 \lambda_2 + \lambda_2^2)}{4(\lambda_1 + \lambda_2)(\lambda_1 + 3\lambda_2)(3\lambda_1 + \lambda_2)} = \frac{va^4 \lambda_2^3 (1 + 3\alpha + \alpha^2)}{4(1 + \alpha)(1 + 3\alpha)(1 + \alpha/3)} \dots\dots (xiv)$$

When λ_2 is large compared with λ_1 , then $\alpha \rightarrow 0$ and the non-zero cumulants become

$$\kappa_{1,0} = va/\lambda_1 \dots\dots (44)(i)$$

$$\kappa_{2,0} = va^2/(2\lambda_1) \dots\dots (ii)$$

$$\kappa_{0,2} = va^2 \lambda_2/2 \dots\dots (iii)$$

$$\kappa_{3,0} = va^3/(3\lambda_1) \dots\dots (iv)$$

$$\kappa_{1,2} = va^3 \lambda_2/6 \dots\dots (v)$$

$$\kappa_{0,3} = va^3 \lambda_2^2/3 \dots\dots (vi)$$

$$\kappa_{4,0} = va^4/(4\lambda_1) \dots\dots (vii)$$

$$\kappa_{2,2} = va^4 \lambda_2/12 \dots\dots (viii)$$

$$\kappa_{1,3} = va^4 \lambda_2^2/12 \dots\dots (ix)$$

$$\kappa_{0,4} = va^4 \lambda_2^3/4 \dots\dots (x)$$

It is easy to show that for this case we also have

$$\kappa_{r,0} = va^r/(r\lambda_1) \dots\dots (xi)$$

and

$$\kappa_{0,r} = \nu a^r \lambda_2^{r-1} / r \quad \text{for} \quad r > 1 \quad . \quad (\text{xii})$$

In passing, we note that $\kappa_{1,1} = 0$. This, in itself, is not in general sufficient to ensure the independence of x and \dot{x} . It is however, sufficient when x and \dot{x} are both Gaussian. In the general case, x and \dot{x} are independent, though not necessarily Gaussian, when $\kappa_{r,s} = 0$ for all $\kappa_{r,s}$ in which r and s are both non-zero.

To determine the degree to which the distributions of x and \dot{x} tend to Gaussian form, the cumulants are expressed in standard form by dividing by the appropriate power of the standard deviation. Using the approximations of (44), for x

$$\kappa_{3,0} / (\kappa_{2,0})^{3/2} = 2/3 \sqrt{\frac{2\lambda_1}{\nu}} \quad (45)(i)$$

and

$$\kappa_{4,0} / (\kappa_{2,0})^2 = \lambda_1 / \nu \quad . \quad (\text{ii})$$

Thus, the distribution of x tends to the Gaussian form as λ_1 / ν tends to zero. For \dot{x} ,

$$\kappa_{0,3} / (\kappa_{0,2})^{3/2} = 2/3 \sqrt{\frac{2\lambda_2}{\nu}} \quad (46)(i)$$

and

$$\kappa_{0,4} / (\kappa_{0,2})^2 = \lambda_2 / \nu \quad . \quad (\text{ii})$$

Here the cause of the difficulty encountered in section 2 in determining the number of zero crossings is clearly seen. The case considered there is the limiting case of the present one when $\lambda_2 \rightarrow \infty$. It is now apparent that for the distribution of \dot{x} to be Gaussian it is necessary for $\lambda_2 / \nu \rightarrow 0$ and these two conditions are inconsistent unless ν is doubly infinite.

When λ_2 is not infinite and ν is large compared with both λ_1 and λ_2 then the joint distribution of x and \dot{x} is approximately Gaussian and we can use the result that

$$N_0 = \sigma_{\dot{x}} / (2\pi \sigma_x) \quad (47)$$

giving at once

$$N_0 = \sqrt{\lambda_1 \lambda_2} / (2\pi) \quad (48)$$

from (43)(iii) and (v).

When, however, λ_2 is large compared with ν , approximating to the simple case considered in section 2, then it is to be expected that equation (8) will give an approximate value of N_0 .

4.4 Before proceeding with the analysis, it is of interest at this juncture to compare the above approach with the spectral method.

From the pulse shape given in (40) it is found that

$$R(\tau) = \frac{a^2 \lambda_2^2}{2(\lambda_2^2 - \lambda_1^2)} \left\{ \frac{e^{-\lambda_1 \tau}}{\lambda_1} - \frac{e^{-\lambda_2 \tau}}{\lambda_2} \right\} \quad (49)$$

and

$$S(\omega) = \frac{a^2 \lambda_2^2}{(\lambda_1^2 + \omega^2)(\lambda_2^2 + \omega^2)} \quad (50)$$

Also,

$$\int_0^{\infty} \frac{d\omega}{(\lambda_1^2 + \omega^2)(\lambda_2^2 + \omega^2)} = \frac{\pi}{2\lambda_1 \lambda_2 (\lambda_1 + \lambda_2)}$$

and

$$\int_0^{\infty} \frac{\omega^2 d\omega}{(\lambda_1^2 + \omega^2)(\lambda_2^2 + \omega^2)} = \frac{\pi}{2(\lambda_1 + \lambda_2)}$$

so that $N_0 = \sqrt{\lambda_1 \lambda_2} / (2\pi)$, agreeing with (48) above.

In cases where λ_2 is large, this method is not applicable, since the distribution of \dot{x} is no longer approximately Gaussian. In such cases N_0 tends to the value derived in section 2.1, equation (8), which, not surprisingly, differs from that obtained by applying the spectral formula in circumstances in which it is not valid. Thus, before using the spectral method, the distribution of both x and \dot{x} should be examined in

order to establish the fact that the results are valid. It is not sufficient merely to examine the time history of x alone to determine whether it is Gaussian, this may well prove to be a good approximation when ν/λ_1 is large.

Furthermore, it is to be noted that in the simple case considered here, as may often happen in practice, the spectral method gives a finite value for N_0 and so does not arouse suspicion regarding the validity of the procedure, as would an infinite value.

Returning to the main discussion, we continue consideration of the case when λ_2/λ_1 is large but now allow the magnitude a to vary in accordance with a known distribution. As pointed out in section 4.2, the result of this is to replace a^n by $\overline{a^n}$ wherever it occurs in (44). It is assumed that the distribution of a is symmetrical about zero* and $|a|$ is distributed exponentially in accordance with (23). By symmetry, the odd cumulants of the distribution of x alone vanish, and for the even cumulants (44)(xi) becomes

$$\kappa_{2r} = \nu \overline{a^{2r}} / (2r \lambda_1) \quad (51)$$

From (23)

$$\overline{a^{2r}} = (2r)! \rho^{2r} \quad (52)$$

giving

$$\kappa_{2r} = \nu (2r - 1)! \rho^{2r} / \lambda_1 \quad (53)$$

and thus

$$\varphi(u) = \exp \left\{ \frac{\nu}{\lambda_1} \sum_{r=1}^{\infty} \frac{(2r - 1)!}{(2r)!} (ipu)^{2r} \right\} \quad (54)$$

* If a has an exponential distribution, but takes only positive values (up gusts only) a similar analysis to that followed here yields

$$\varphi(u) = (1 - ipu)^{-\nu/\lambda_1}$$

and

$$f(x) = (x/\rho)^{\frac{\nu}{\lambda_1} - 1} e^{-\frac{x}{\rho}} \left\{ \rho \left(\frac{\nu}{\lambda_1} - 1 \right)! \right\}$$

a Pearson Type III distribution.

i.e.

$$\varphi(u) = (1 + \rho^2 u^2)^{-\frac{\nu}{2\lambda_1}} \quad (55)$$

The distribution of x is then given by

$$f(x) = \frac{1}{2\pi} \int_{-\infty}^{\infty} (1 + \rho^2 u^2)^{-\frac{\nu}{2\lambda_1}} e^{iux} du \quad (56)$$

i.e.

$$f(x) = \left(\frac{x}{\rho}\right)^{\frac{\nu}{2\lambda_1} - \frac{1}{2}} \frac{K_{\frac{\nu}{2\lambda_1} - \frac{1}{2}}\left(\frac{x}{\rho}\right)}{\left\{\sqrt{\pi} 2^{\frac{\nu}{2\lambda_1} - \frac{1}{2}} \rho \left(\frac{\nu}{2\lambda_1} - 1\right)!\right\}} \quad (57)$$

for x positive, and the distribution is symmetrical about the origin, (K being the modified Bessel function).

This is the distribution derived by the author by an entirely different approach in an earlier paper⁴. There, the distribution is derived from the assumption that it results from a large number of Gaussian distributions, the variances of which are themselves distributed in a certain way.

For small values of $\nu/(2\lambda_1)$, a plot of $\log \{f(x)\}$ against x is concave upwards. As ν increases the distribution becomes exponential, plotting as a straight line on the logarithmic scale, for $\nu = 2\lambda_1$, and then for larger values of ν becomes concave downwards, tending to a Rayleigh distribution in the limit as $\nu \rightarrow \infty$.

As shown in the earlier paper⁴, if such Rayleigh distributions, with values of ρ^2 distributed in Pearson Type III fashion are combined, as the distribution of ρ becomes more heterogeneous, the series of shapes is retraced in the reverse direction. In this sequence, a given shape may occur twice, so that it is not possible from a cursory examination of $f(x)$ to determine whether it results from a stationary process or not.

Returning to the present model, the cumulants for the distribution of \dot{x} alone, from (44)(x11), are

$$k_{0,2r} = \nu a^{2r} \lambda_2^{2r-1} / (2r)$$

and a similar analysis to that for x yields

$$f(\dot{x}) = \left(\frac{\dot{x}}{\lambda_2 \rho}\right)^{\frac{\nu}{2\lambda_2} - \frac{1}{2}} K_{\frac{\nu}{2\lambda_2} - \frac{1}{2}} \left(\frac{\dot{x}}{\lambda_2 \rho}\right) / \left\{ \sqrt{\pi} 2^{\frac{\nu}{2\lambda_2} - \frac{1}{2}} \left(\frac{\nu}{2\lambda_2} - 1\right)! \lambda_2 \rho \right\} \quad \dots\dots (58)$$

The joint distribution of x and \dot{x} is not of course given by the product of (57) and (58); (57) is the joint distribution integrated with respect to \dot{x} , and (58) is the joint distribution integrated with respect to x . The product would, however, be the correct form if x and \dot{x} were independent and we now examine how far this is likely to be a reasonable approximation.

Independence results when all $\kappa_{r,s} = 0$ for both r and s non-zero. In the symmetrical case, up to the fourth order, there are only two such cumulants, $\kappa_{2,2}$ and $\kappa_{1,3}$, which are not zero. From (43) and (44) the fourth order cumulants are

$$\begin{aligned} \kappa_{4,0} &= \overline{v a^4} / (4\lambda_1) \\ \kappa_{3,1} &= 0 \\ \kappa_{2,2} &= \overline{v a^4} \lambda_2 / 12 \\ \kappa_{1,3} &= \overline{v a^4} \lambda_2^2 / 12 \\ \kappa_{0,4} &= \overline{v a^4} \lambda_2^3 / 4 \end{aligned}$$

The cumulant $\kappa_{4,0}$ is less than $\kappa_{0,4}$ by a factor $1/(\lambda_1 \lambda_2^3)$, and it might be expected that, apart from the numerical factor, the intermediate cumulants would each reduce by the quarter power of this value. This is not the case however; on this basis $\kappa_{1,3}$ is low by a factor $(\lambda_1/\lambda_2)^{\frac{1}{4}}$, and $\kappa_{2,2}$ low by a factor $(\lambda_1/\lambda_2)^{\frac{1}{2}}$.

Thus, since λ_1/λ_2 is small, there may be some grounds for hoping that the assumption that x and \dot{x} are independent is a reasonable approximation to the truth, and this assumption is in fact made.

Putting $f_1(x)$ equal to (57) and $f_2(\dot{x})$ equal to (58), and substituting in (31), gives

$$N_x = \lambda_2 (n_2 - \frac{1}{2})! \left(\frac{x}{\rho}\right)^{n_1 - \frac{1}{2}} K_{n_1 - \frac{1}{2}} \left(\frac{x}{\rho}\right) / \left\{ \pi 2^{n_1 - \frac{1}{2}} (n_1 - 1)! (n_2 - 1)! \right\} \dots (59)$$

where $n_1 = \nu/(2\lambda_1)$ and $n_2 = \nu/(2\lambda_2)$.

In particular

$$N_0 = \lambda_2 (n_1 - 3/2)! (n_2 - \frac{1}{2})! / \{ 2\pi (n_1 - 1)! (n_2 - 1)! \} . \quad (60)$$

When ν is large compared with both λ_1 and λ_2 so that n_1 and n_2 are both large, then

$$(n_1 - 1)! / (n_1 - 3/2)! \approx \sqrt{(n_1 - \frac{1}{2})}$$

and

$$(n_2 - \frac{1}{2})! / (n_2 - 1)! \approx \sqrt{n_2}$$

so that (60) gives

$$N_0 = \lambda_2 \sqrt{n_2} / \{ 2\pi \sqrt{(n_1 - \frac{1}{2})} \} . \quad (61)$$

If, finally, $\frac{1}{2}$ is negligible compared with n_1 , then (61) reduces to

$$N_0 = \sqrt{\lambda_1 \lambda_2} / (2\pi)$$

in agreement with (48).

If ν is large compared with λ_1 and small compared with λ_2 then

$$(n_2 - \frac{1}{2})! \approx \sqrt{\pi}$$

and

$$(n_2 - 1)! \approx 1/n_2 .$$

Again neglecting $\frac{1}{2}$ compared with n_1 , (60) gives

$$N_0 = \frac{1}{2} \sqrt{\frac{\nu \lambda_1}{2\pi}}$$

in agreement with the first order term of (28).

Thus, the formula for the number of zero crossings given in (60) agrees in the two limiting cases considered with those derived more simply. It has already been established⁴ that crossing distributions from aircraft normal acceleration records are satisfactorily described by functions of the form of (57). It therefore seems worthwhile pursuing the model further and examining it in relation to observational data. Before doing so, however, a further modification to the formulae will be made to take more account of the second order terms, as in the examples considered these are often not sufficiently small to be neglected. The procedure adopted is to assume distributions of the form (57) and (58) but with the values of the parameters adjusted to fit exactly the second and fourth cumulants in their full form of (43). This gives

$$f_1(x) = \left(\frac{x}{\rho_1}\right)^{n_1 - \frac{1}{2}} K_{n_1 - \frac{1}{2}}\left(\frac{x}{\rho_1}\right) / \left\{ \sqrt{\pi} 2^{n_1 - \frac{1}{2}} (n_1 - 1)! \rho_1 \right\} \quad (62)$$

and

$$f_2(\dot{x}) = \left(\frac{\dot{x}}{\rho_2}\right)^{n_2 - \frac{1}{2}} K_{n_2 - \frac{1}{2}}\left(\frac{\dot{x}}{\rho_2}\right) / \left\{ \sqrt{\pi} 2^{n_2 - \frac{1}{2}} (n_2 - 1)! \rho_2 \right\} \quad (63)$$

where

$$n_1 = \nu(1 + 3\alpha) (1 + \alpha/3) / \{2\lambda_1(1 + \alpha)\} \quad (64)$$

$$n_2 = \nu(1 + 3\alpha) (1 + \alpha/3) / \{2\lambda_2(1 + \alpha) (1 + 3\alpha + \alpha^2)\} \quad (65)$$

$$\rho_1 = \rho / \sqrt{\{(1 + 3\alpha) (1 + \alpha/3)\}} \quad (66)$$

and

$$\rho_2 = \rho \lambda_2 \sqrt{(1 + 3\alpha + \alpha^2)} / \sqrt{\{(1 + 3\alpha) (1 + \alpha/3)\}} \quad (67)$$

For the x-crossing distribution

$$N_x = \rho_2 (n_2 - \frac{1}{2})! \left(\frac{x}{\rho_1}\right)^{n_1 - \frac{1}{2}} K_{n_1 - \frac{1}{2}}\left(\frac{x}{\rho_1}\right) / \left\{ \rho_1 \pi 2^{n_1 - \frac{1}{2}} (n_1 - 1)! (n_2 - 1)! \right\} \dots (68)$$

and

$$N_0 = \rho_2 (n_1 - 3/2)! (n_2 - \frac{1}{2})! / \{2\pi \rho_1 (n_1 - 1)! (n_2 - 1)!\} \quad (69)$$

The application of these formulae to observational material is considered in sections 6 to 8.

5 POSSIBLE EXTENSIONS OF THE MODEL

5.1 Various extensions of the model immediately suggest themselves. Considering first of all the distribution of the pulses in time, it has been assumed that their arrivals form a Poisson process, and this implies an exponential distribution of time intervals between pulses. Patchiness can be introduced into the pulse occurrences by assuming an alternative distribution of time intervals. A Pearson Type III might prove satisfactory for this, in which the probability of a time interval between t and $t + dt$ is

$$t^{p-1} e^{-\frac{t}{\tau}} dt / \{\tau^p (p-1)!\} \quad (70)$$

The case already considered is for $p = 1$.

For $p < 1$ the distribution of pulses becomes patchy, and for large values of p the pulses tend to occur periodically and so might be used in a description of wave phenomena. In this case, the assumption of the independence of x and \dot{x} would doubtless no longer apply.

5.2 It would also be useful to consider alternative distributions for pulse magnitude other than the exponential and to examine the effect this would have on the distribution of the resulting variable.

5.3 In the examples considered in sections 6 to 8, the model is applied to describe the behaviour of aircraft normal acceleration. There is, of course, no restriction on the variable quantity considered, or on the complexity of the assumed pulse shape, which may take account of as many degrees of freedom in the response of the aircraft as are considered necessary.

A simple extension of the model to include the effect of flexibility on the aircraft normal acceleration can be made by assuming a pulse shape of the form

$$F(t) = a(e^{-\lambda_1 t} - e^{-\lambda_2 t}) + b\{e^{-(\lambda_3 + i\lambda_4)t} - e^{-(\lambda_3 - i\lambda_4)t}\} \quad (71)$$

5.4 It is also necessary to examine in more detail the importance of the cross-cumulants in the joint distribution of x and \dot{x} . Apart from a slender order-of-magnitude argument, the justification for ignoring these cross-cumulants at present lies in the resulting agreement with observation. Certainly, for the treatment of quasi-periodic disturbances as suggested in section 5.1, the cross-cumulants would become important.

6 R.F. JONES'S THUNDERSTORM DATA

6.1 The first application of the theoretical results is to observations in storm clouds with a Spitfire aircraft made by Jones⁵. In this paper, frequency distributions of aircraft peak normal accelerations are given for flights through cumulus and cumulonimbus clouds at heights ranging from 2500 feet to 42400 feet, grouped into eight height bands. These observations are quoted here in Tables 1(i) to (viii) in the form of cumulative frequency distributions, whereas we have been dealing with crossing distributions. However, for such data it has been shown⁶ that the cumulative distribution of peak values gives an acceptable approximation to the crossing distribution, becoming increasingly close as the excursions from the mean become larger. It is therefore assumed in all the examples considered here that the differences between the cumulative peak distribution and the crossing distribution may be ignored.

Curves of the form of (68) are fitted to these data using tables of the function⁷ prepared for the purpose in which the shape parameter n takes half integral values. These appear to give a sufficient gradation of shapes and a reasonable fit was obtained by trial and error*. The values from the fitted curves are also given in Tables 1(i) to (viii), and the observed values and fitted curves are shown plotted in Figs.2a to 2h on a bumps-per-mile basis. The parameters for the fitted curves are given in Table 2, repeated below for convenience.

* The curve fitting for this particular example was done some time before the ideas in the present paper were developed.

Table 2 (repeated)

R.F. Jones's thunderstorm data. Summary of parameters

Height, ft	n_1	ρ_1 g units	N_0	λ_1 per mile	ν per mile	$1/\lambda_2$ ft
2500-7400	$1\frac{1}{2}$	0.1042	5.49	22.97	39.1	89.2
7500-12400	$2\frac{1}{2}$	0.0833	4.70	19.69	56.9	99.2
12500-17400	2	0.1053	5.06	16.77	39.7	61.4
17500-22400	$1\frac{1}{2}$	0.1316	4.86	14.20	33.3	47.6
22500-27400	$2\frac{1}{2}$	0.1220	4.66	11.94	50.4	36.8
27500-32400	$3\frac{1}{2}$	0.1036	4.33	9.97	60.7	35.4
32500-37400	$3\frac{1}{2}$	0.0917	3.78	8.26	51.6	33.8
37500-42400	$4\frac{1}{2}$	0.0858	3.84	6.57	57.0	13.3

(As up and down bumps have been added, the extrapolated value of the fitted curve at zero acceleration gives $2N_0$.)

6.2 An examination of Figs.2a to 2h shows a fairly uniform change of shape of the distributions, close to exponential form at the lower altitudes and increasing in curvature with increasing height. The values of n_1 in Table 2 confirm this impression.

On earlier ideas this might be attributed to the fact that at the higher altitudes the sample is smaller and therefore likely to be more homogeneous. At the lower altitudes any combining of samples of different intensities will lead to a decrease in the curvature. In other words, the trend in the curvature of the distributions is due to a trend in sample size.

The present work suggests an alternative explanation. It has been seen that the shape of the distribution is dependent on the parameter ν/λ_1 (equation (57)). If λ_1 is identified with $1/(c\mu_g)$ then this itself varies very widely with altitude and its variation is sufficient to explain the observed trend. In Fig.3 the values of n_1 are shown plotted against the mass parameter μ_g , showing good agreement with the predicted relationship. The dashed line on the diagram is the best straight line through the origin; the full line is a second-degree curve passing through the origin and the first and last experimental points.

6.3 We can also make some further deductions from the model. If λ_2 is large, so that we can use the first order approximations, then for the highest altitude band $\nu/(2\lambda_1) = 4\frac{1}{2}$ from the observed shape of curve. Putting $\lambda_1 = 1/(c \mu_g)$ gives $\lambda_1 = 6.57$ per mile and $\nu = 59.1$ per mile. From the first order term of (27)

$$N_0 = \frac{1}{2} \sqrt{\frac{\nu \lambda_1}{2\pi}}$$

and substituting the above values for ν and λ_1 gives $N_0 = 3.93$ per mile. This is very close to the observed value of 3.84 per mile.

However, when the same calculations are made for the lowest altitude band the value of N_0 is found to be 7.93 per mile compared with the observed value of 5.48 per mile, the comparison tending to be progressively worse with decreasing height. Clearly the first order approximation is only adequate at the high altitudes and the effect of terms in λ_1/λ_2 become appreciable at the lower altitudes.

6.4 To illustrate this, a model is fitted based on the more complete representation of (57). With a further parameter at our disposal it is now possible to fit n_1 and N_0 exactly by a correct choice of ν and λ_2 .

The values of N_0 based on the observations and the values of λ_1 calculated from values of the mass parameter based on a mean aircraft weight are shown plotted as the circled points in Fig.4 and a smooth curve fitted by eye to the values of N_0 . The experimental values are given in Table 2. From the experimental values of n_1 , N_0 and λ_1 and using equations (64) to (67) and (69) values of ν and $1/\lambda_2$ have been determined, also given in Table 2 and shown by the circled points of Fig.5. (The parameter $1/\lambda_2$ rather than λ_2 itself has been taken as it is closely related to the old gust gradient distance, as shown by (37), although the build-up distance of the pulse itself depends on both λ_1 and λ_2 .) From the curves shown as the full lines in Figs.3 and 4, the full lines of Fig.5 have been calculated, so that the full lines on all the Figs.3, 4, and 5 form a consistent set.

There is a rather large scatter of circled points in Fig.5, but it should be remembered that the experimental errors of both n_1 and N_0 contribute to this. It is more correct to consider the experimental scatter from a different point of view. Postulating the variation of ν and λ_2 given by the full curves of Fig.5, the full curves for n_1 and N_0 shown in Figs.3 and 4 are derived, in reasonably good agreement with experiment.

From Fig.5, it is seen that there is a slight variation in the value of ν , but its small magnitude confirms that almost all the variation in the shape of the bump distributions is due to the large change in λ_1 .

The large change in $1/\lambda_2$ is, at first sight surprising. At 40000 feet the value of λ_1/λ_2 is 0.0292. A small value is to be expected since the first order approximation gives such a good agreement with observation. At 5000 feet the value of λ_1/λ_2 is 0.388; clearly the second order terms are no longer negligible.

A better understanding of the behaviour of $1/\lambda_2$ is obtained if equation (41) is used to calculate the pulse build-up distance, putting $t_m = H$. Values of H calculated from the smoothed values of λ_1 and λ_2 are plotted in Fig.6 and show a linear relationship with height varying from 138 feet at 5000 feet altitude to 85 feet at 40000 feet altitude. The main function of λ_2 is to determine this build-up distance correctly. How far the variation in the build-up distance is due to a change in environment, and how far due to a change in aircraft response has yet to be determined. Comparisons between aircraft will help to throw some light on this problem.

6.5 The important point to be emphasised regarding this example is that the variation in curve shape for the bump distributions follows closely that predicted from the mathematical model, depending almost entirely on the change in aircraft mass parameter.

7 'SWIFTER' MIDDAY FLIGHTS OVER FLAT DESERT

7.1 The second example is taken from an extensive investigation of aircraft normal accelerations experienced when flying at low altitude in North Africa, known as 'Operation Swifter'. This investigation has been described in detail earlier⁸. The observations we now examine, relate to midday flights over the flat desert at 200 feet altitude. The restriction to midday flights has been made because environmental conditions are fairly steady at this time.

The flights have been classified according to the solar radiation being received by the ground, and the cumulative gust distributions are given in Tables 3(i) to (x).

The results are presented in terms of gust velocities derived by Zbrozek's method⁹. As only a single type of aircraft is involved, this merely amounts to making small corrections for aircraft weight and speed,

converting the accelerations to gust velocities by some arbitrary factor, and interpolating to determine the number of gusts at the required velocity level. The gust velocity in Table 3 is therefore treated as proportional to aircraft normal acceleration, and, as before, the cumulative distribution is assumed to provide a satisfactory approximation to the crossing distribution.

Distributions of the form of (68) are fitted to the observations of Table 3, in which the fitted values are also given and a comparison between the experimental points and the fitted curves is shown diagrammatically in Figs.7a to 7j. A summary of parameters is given in Table 4, repeated below.

Table 4 (repeated)

'Swifter' midday flights over flat desert. Summary of parameters

Solar radiation mW/cm ²	n_1	ρ_1 ft/sec	N_0 per mile	ν per mile	$1/\lambda_2$ feet	ρ feet/sec
35-39	$2\frac{1}{2}$	1.543	9.590	101.3	14.38	1.700
40-44	$3\frac{1}{2}$	1.259	8.816	130.7	24.76	1.475
45-49	5	1.171	7.656	166.7	41.62	1.500
50-54	$5\frac{1}{2}$	1.168	7.510	180.2	44.52	1.518
55-59	"	1.202	7.521	180.4	44.33	1.560
60-64	"	1.253	8.032	188.0	37.63	1.573
65-69	"	1.269	8.428	193.5	33.27	1.558
70-74	"	1.351	8.668	196.7	30.85	1.637
75-79	"	1.408	8.632	196.2	31.21	1.710
80-84	"	1.323	9.000	200.9	27.81	1.577

The values of n_1 , ρ_1 and N_0 are those of the curves fitted in Figs.7a to 7j (Tables 3(1) to (x)).

The values of ν , $1/\lambda_2$ and ρ are derived using the relationships given in (64) to (69) with $\lambda_1 = 23.14$ per mile. These values are shown plotted as the circled points in Figs.8 and 9.

7.2 The most striking feature of these observations is the rapid increase in n_1 as the solar radiation increases from 37 mW/cm² to about 50 mW/cm². This is detectable in Figs.7a to 7d as a change of shape and shown more clearly in 8a. For values of solar radiation above 50 mW/cm² the value of n_1 is constant and second order terms produce a

slight trend in ν , although whether in fact it is ν that is constant with a slight trend in n_1 it is difficult to say, as the observations hardly warrant this accuracy, a change from $5\frac{1}{2}$ to 5 in n_1 being barely detectable. (Curve fitting with unrestricted values for n_1 would also entail two way interpolation if only existing tables were used.) During the rapid increase in ν the value of $1/\lambda_2$ also increases rapidly and then falls away slightly. There is a similar but smaller variation in N_0 .

7.3 It is also of interest to consider the observations from an energy standpoint. The energy of the disturbances is proportional to their number and to the square of their magnitude. In Fig.10 the values of $\nu\rho^2$ are shown plotted against solar radiation and the points lie reasonably well on a straight line. This linear relationship has been used in determining the curves of Figs.8c and 9c. The full lines of Fig.8a to 8c, Fig.9a to 9c, and Fig.10, are a consistent set, as are also the circled points.

7.4 We may perhaps do a little guesswork regarding the physical implications of these results. As the solar radiation increases up to 50 mW/cm^2 the number of disturbances ν increases rapidly, the atmosphere "comes to the boil" so to speak. This analogy is not strictly correct as we are dealing with steady conditions at each value of solar radiation.

Accompanying this rapid rise in ν , the behaviour of $1/\lambda_2$ indicates that the size of the disturbances also increases. As the increase in ν is far more rapid than the rise in solar radiation energy requirements lead to a fall in ρ .

Above about 50 mW/cm^2 the number of disturbances is fairly constant and the increase in the influx of energy leads to a gradual increase in ρ . During this stage $1/\lambda_2$ decreases slightly, perhaps because the disturbances become more sharply defined.

7.5 It would be of interest to extend the curves to lower values of solar radiation. 'Swifter' flights at these lower values were made in the early mornings and afternoons, when, of course, the conditions are not as steady as at midday. A cursory examination of these observations indicates that the values of n_1 seldom falls much below unity and the values of $\nu\rho^2$ lie above the straight line of Fig.10. This implies that under these conditions the turbulence is patchy and the model not strictly applicable as ν is not constant. It may be possible to extend the theory to take this into account (see section 11.1). A further difficulty in analysing these results is that

for these small values of n_1 a small change in n_1 leads to a large change in the shape of the distribution and present tables are inadequate.

7.6 The important point in this example is the change in shape of the gust distribution produced by a change in the mean pulse rate ν , while the mass parameter is held constant. This contrasts with the first example in which the change in shape is mainly due to the change in mass parameter.

8 'SWIFTER' STACKED SORTIES

The final example is also taken from the 'Swifter' investigation and refers to the flights known as the 'stacked sorties'. In these flights, which took place near midday, aircraft flew at heights of 200 feet, 400 feet and 600 feet separated by only a short interval of time so that the conditions were, for all practical purposes constant. (If only two aircraft were available the 600 feet flight was omitted.) To take a fairly homogeneous sample for the present analysis the flights considered are those made when the solar radiation exceeded 64 mW/cm^2 . The observed values and fitted distributions are given in Tables 5 and 6, for flights over flat and hilly desert respectively, and are shown plotted in Figs.11 and 12.

Now the mass parameter varies by only just over 1% between 200 feet and 600 feet and disturbances which affect an aircraft at 200 feet probably also affect an aircraft at 600 feet. That is to say, both λ_1 and ν vary very little with altitude. Thus the present theory predicts very little change in the shape of the gust distributions with altitude and this is confirmed by the observations. On the other hand the number of zero crossings shows a marked decrease with altitude and this must therefore be due to a variation in λ_2 . According to our model the variation in λ_2 will produce a small second order variation in n_1 . With the values of the parameters obtained from a first approximation this variation on the value of n_1 is between $\frac{1}{2}$ and 1 for each 200 feet change in altitude, and is barely detectable, if at all. However, in the curve fitting, an allowance has been made for this trend and values of n_1 differing by $\frac{1}{2}$ for each 200 feet change in altitude have been chosen - in effect, the best set of three differing by this amount have been fitted.

The resulting parameters are summarised in Tables 7(i) and 7(ii), repeated below.

Table 7 (repeated)

'Swifter' stacked sorties with solar radiation ≥ 65 mW/cm².Summary of parameters(i) Flat desert

Height ft	n_1	P_1 ft/sec	N_o per mile	λ_1 per mile	ν per mile	$1/\lambda_2$ ft
200	$5\frac{1}{2}$	1.295	9.337	23.14	204.9	25.10
400	6	1.326	7.275	23.01	191.5	48.28
600	$6\frac{1}{2}$	1.337	6.156	22.87	183.0	71.41

(ii) Hilly desert

Height ft	n_1	P_1 ft/sec	N_o per mile	λ_1 per mile	ν per mile	$1/\lambda_2$ ft
200	4	1.706	9.549	23.14	154.7	20.19
400	$4\frac{1}{2}$	1.650	7.892	23.01	153.7	37.13
600	5	1.650	6.817	22.87	153.4	54.49

It will be seen that in the case of the flat desert the assumed change in n_1 is not quite sufficient to maintain ν at a constant value; by comparison, for the hilly desert, the allowance is just sufficient to do so.

The value of n_1 found here for flying at 200 feet over flat desert is the same as the value for all groups in the second example with solar radiation greater than 64 mW/cm². As the range of solar radiation is much wider in the present example and the value of ρ varies slightly the combination of results might have been expected to produce a slight decrease in the value of n_1 , but this is not detectable.

A further small point to note is that the value of $1/\lambda_2$ for flights at 200 feet over the flat desert found here differs slightly from the values in the second example when the solar radiation exceeded 64 mW/cm². As these values are determined from large samples, the difference is rather too great to be explained as due to random sampling and is probably due to a slight difference in routes flown. While all the stacked sorties were made on the routes to the West of El Adam, a good deal of flying over flat desert also took place on the southerly routes towards Giarabub. These are minor points however. The main feature of this example is the striking behaviour of $1/\lambda_2$.

8.2 The values of $1/\lambda_2$ given in Table 7 are shown plotted in Fig.13. These show a linear relationship with height within very close limits (to within 1%). The fact that the lines do not pass exactly through the origin may result partly from a bias between the actual and nominal altitudes and partly from altimeter errors.

In the case of the first example considered, changes in λ_2 are connected with changes in aircraft response. Here, the aircraft response is, for all practical purposes, constant, and the change in $1/\lambda_2$ is clearly due to changes in the environment. The linear relationship with height shown in Fig.13 tends to confirm this opinion.

9 DISCUSSION OF OBSERVATIONAL RESULTS

9.1 The application of the 'shot effect' model to aircraft normal accelerations gives encouraging results in the examples considered.

The three examples illustrate the effect of varying each of the parameters λ_1 , ν and λ_2 in turn. The first example demonstrates a change in shape of the gust distribution due to a variation of λ_1 ; the second, a change in shape of the gust distribution due to a variation in ν ; and the third shows the effect of λ_2 on the number of zero crossings N_0 . The model satisfactorily predicts all these trends and presents a consistent picture of the phenomenon.

9.2 In earlier models the range of shapes in observed distributions was usually explained by postulating a distribution of root-mean-square values for short intervals of Gaussian processes; differing root-mean-square distributions giving rise to differing gust distributions. This procedure suffers from a certain conceptual difficulty. These intervals must necessarily be long enough to be considered stationary and short enough for a continuous distribution of root-mean-square values to give a reasonable approximation to the truth. Furthermore, the process so defined is not stationary in as much as its root-mean-square value varies with time. In many cases, for example, when flying over a hot flat desert at midday, a model which does not rely on non-stationarity to predict the observed gust distributions seems preferable.

The present model does not suffer from these disadvantages. The shape of the gust distribution depends almost entirely on the mass parameter and the frequency of the disturbances, and the process is stationary in the sense that its statistical properties are invariant with time.

10 CONCLUSIONS

10.1 In investigating the behaviour of an aircraft in turbulence the most satisfactory method of analysis depends on the frequency with which the disturbances are encountered.

When the disturbances are rare, then a discrete gust approach may prove adequate. As the occurrence of the disturbances becomes more frequent, so that their effects become superimposed, the discrete gust approach is no longer satisfactory. Finally, the frequency of occurrence becomes so great that spectral methods can be used. Between the two limiting cases, the discrete gust and the spectral approach, there is a wide area in which neither is satisfactory. It is to this region, between the discrete gust on the one hand and the spectral approach on the other, that the method developed here applies.

The examples chosen illustrate its application to aircraft normal accelerations. It would be of interest to examine how far the model is successful in predicting the behaviour of other response variables, with, of course, suitable modification of assumed pulse shape.

However, above all, what is required at the present time is to make comparisons between aircraft to examine the consistency of the various parameters under these conditions and to discover how far predictions based on one aircraft are valid for another. It should always be borne in mind that the purpose of the analysis is to predict, from observations of gust loads on one aircraft, the loads experienced by a second aircraft flying in the same environment. For this purpose it is not necessary for the model to reflect accurately the true physical picture. In fact, it should be as simple as possible consistent with the aim defined above.

Appendix A

SUMMARY OF MATHEMATICAL MODEL

A.1 The mathematical model developed in the paper is summarised here. The equations given all occur in the main text and are quoted with their original equation numbers.

The random variable x , (in the cases considered, the aircraft normal acceleration) is assumed to result from superimposing a large number of pulses of the form

$$F(t) = \frac{a\lambda_2}{\lambda_2 - \lambda_1} (e^{-\lambda_1 t} - e^{-\lambda_2 t}) \quad (40)$$

These pulses occur at random with respect to time at a mean rate ν per unit time. In the aircraft applications considered in the paper, the independent variable is distance rather than time, and the parameter λ_1 is identified with $1/(c\mu_g)$, where c is the aircraft chord and μ_g the aircraft mass parameter.

The magnitude parameter a is assumed to be distributed exponentially:-

$$f(a) = \frac{1}{2\rho} e^{-\frac{|a|}{\rho}} \quad (23)$$

The distributions of x and \dot{x} are assumed to be, respectively

$$f_1(x) = \left(\frac{x}{\rho_1}\right)^{n_1 - \frac{1}{2}} K_{n_1 - \frac{1}{2}} \left(\frac{x}{\rho_1}\right) / \left\{ \sqrt{\pi} 2^{n_1 - \frac{1}{2}} (n_1 - 1)! \rho_1 \right\} \quad (62)$$

and

$$f_2(\dot{x}) = \left(\frac{\dot{x}}{\rho_2}\right)^{n_2 - \frac{1}{2}} K_{n_2 - \frac{1}{2}} \left(\frac{\dot{x}}{\rho_2}\right) / \left\{ \sqrt{\pi} 2^{n_2 - \frac{1}{2}} (n_2 - 1)! \rho_2 \right\} \quad (63)$$

where

$$n_1 = \nu(1 + 3\alpha) (1 + \alpha/3) / \{2\lambda_1(1 + \alpha)\} \quad (64)$$

$$n_2 = \nu(1 + 3\alpha) (1 + \alpha/3) / \{2\lambda_2(1 + \alpha) (1 + 3\alpha + \alpha^2)\} \quad (65)$$

$$\rho_1 = \rho / \sqrt{\{(1 + 3\alpha) (1 + \alpha/3)\}} \quad (66)$$

$$\rho_2 = \rho \lambda_2 \sqrt{(1 + 3\alpha + \alpha^2)/\{(1 + 3\alpha)(1 + \alpha/3)\}} \quad (67)$$

and

$$\alpha = \lambda_1/\lambda_2 .$$

When α can be neglected, (62) and (63) are exact. Otherwise, the parameters in (62) and (63) are so chosen that the second and fourth cumulants have their correct values.

Assuming further that x and \dot{x} are independent, then the x -crossing distribution is given by

$$N_x = \rho_2 (n_2 - \frac{1}{2})! \left(\frac{x}{\rho_1}\right)^{n_1 - \frac{1}{2}} K_{n_1 - \frac{1}{2}} \left(\frac{x}{\rho_1}\right) / \{\rho_1 \pi 2^{n_1 - \frac{1}{2}} (n_1 - 1)! (n_2 - 1)!\} \quad \dots (68)$$

and

$$N_0 = \rho_2 (n_1 - 3/2)! (n_2 - \frac{1}{2})! / \{2\pi \rho_1 (n_1 - 1)! (n_2 - 1)!\} . \quad (69)$$

Appendix B

NOTE ON CURVE FITTING

B.1 All the fitted curves tabulated in this paper have been fitted by trial and error, using the set of functions previously tabulated⁷ for $n = \frac{1}{2}(\frac{1}{2}) 6(1) 12$. These tables give a sufficient range of shapes for most practical purposes, except perhaps near the lower end of the range. The adequacy of the fit has been judged subjectively without recourse to a least-squares or minimum χ^2 procedure. It would be necessary to consider a number of factors if this were done.

When the number of gusts in a class interval is large, most of the error arises from instrumental and like causes, which lead to an error in the range of the interval. This might be of the order of a few per cent. At the other extreme, when the numbers in the classes are small, the largest contribution to the error is due to sampling scatter.

If the instrumental errors amount to, say, 4% then the contribution to the variance from this cause is $N^2/625$, where N is the number in the class (strictly speaking, the expected number). For a given total number in the whole distribution the sampling contribution to the variance of the class is N , making for the total variance $N + N^2/625$.

For classes containing over 625 gusts the instrument errors predominate; below this figure sampling errors predominate.

To minimise χ^2 it is necessary to minimise the squares of the differences between the observed and expected numbers divided by the respective variances, i.e. to minimise

$$\sum \left\{ \frac{(N_{\text{obs}} - N_{\text{exp}})^2}{(N_{\text{exp}} + N_{\text{exp}}^2/625)} \right\}$$

where N_{obs} is the observed number in the class and N_{exp} is the expected number.

It is to be noted that the distributions tabulated here are cumulative before the above procedure can be applied the numbers within each class interval must be found by differencing.

A computer programme for curve fitting based on these considerations and allowing for unrestricted values of the shape parameter n would be useful.

B.2 Two specific points regarding the actual curves fitted should be mentioned.

The first is the appearance on several occasions of a few large gusts not fitting well into the general pattern. No simple expression fitting the main part of the distribution satisfactorily fits these tails and on any simple theory it is necessary to assume that such a tail results from a separate population of rare events. Whether these rare events are gusts, manoeuvres, or a combination of these is not yet established.

The second point concerns the Swifter results only. The observed totals at a gust velocity of $7\frac{1}{2}$ ft/sec show a small positive bias of about one or two per cent. This is not a serious discrepancy and is undetectable on the diagrams, but it is consistent enough to give rise to the suspicion that it may be due in some way to the data processing, possibly the instrument response characteristics, the addition of up and down gusts, or the method of interpolating between the acceleration levels to obtain the number of gusts at a given derived gust velocity.

Table 1

R.F. JONES'S THUNDERSTORM DATACUMULATIVE BUMP DISTRIBUTIONS(i) 2500 feet to 7400 feet; 227.1 miles

g	No. of bumps		Bumps per mile	
	Obs.	Fitted	Obs.	Fitted
0		2494		10.98
0.1	1554	1554	6.84	6.84
0.2	755	745	3.32	3.28
0.3	330	333	1.45	1.47
0.4	147	144	0.647	0.634
0.5	56	60.1	0.247	0.265
0.6	22	25.2	0.0969	0.111
0.7	11	10.3	0.0484	0.0454
0.8	5	4.20	0.0220	0.0185
0.9	2	1.70	0.00881	0.00749
1.0	1	0.683	0.00440	0.00301
1.1	0			

$$n_1 = 1\frac{1}{2}; \quad \rho_1 = 0.1042 \text{ g}$$

(ii) 7500 feet to 12400 feet; 495.3 miles

g	No. of bumps		Bumps per mile	
	Obs.	Fitted	Obs.	Fitted
0		4654		9.40
0.1	3495	3495	7.06	7.06
0.2	1869	1874	3.77	3.78
0.3	823	859	1.66	1.73
0.4	350	360	0.707	0.727
0.5	145	142	0.293	0.287
0.6	54	53.6	0.109	0.108
0.7	18	19.7	0.0363	0.0398
0.8	7	7.05	0.0141	0.0142
0.9	3	2.48	0.00606	0.00501
1.0	3	0.861	0.00606	0.00174
1.1	1	0.295	0.00202	0.000596
1.2	0			

$$n_1 = 2\frac{1}{2}; \quad \rho_1 = 0.0833 \text{ g}$$

Table 1 (Contd)

(iii) 12500 feet to 17400 feet; 241.2 miles

g	No. of bumps		Bumps per mile	
	Obs.	Fitted	Obs.	Fitted
0		2440		10.12
0.1	1839	1839	7.62	7.62
0.2	1064	1058	4.41	4.39
0.3	527	542	2.18	2.25
0.4	251	264	1.04	1.09
0.5	123	122	0.510	0.506
0.6	55	54.8	0.228	0.227
0.7	27	24.2	0.112	0.100
0.8	9	10.5	0.0373	0.0435
0.9	4	4.51	0.0166	0.0187
1.0	2	1.91	0.00829	0.00792
1.1	1	0.811	0.00415	0.00336
1.2	1	0.340	0.00415	0.00141
1.3	1	0.142	0.00415	0.000589
1.4	0			

$$n_1 = 2; \rho_1 = 0.1053 g$$

(iv) 17500 feet to 22400 feet; 108.6 miles

g	No. of bumps		Bumps per mile	
	Obs.	Fitted	Obs.	Fitted
0		1055		9.71
0.1	750	750	6.91	6.91
0.2	441	432	4.06	3.98
0.3	230	234	2.12	2.15
0.4	123	123	1.13	1.13
0.5	59	63.0	0.543	0.580
0.6	30	32.5	0.276	0.299
0.7	18	16.5	0.166	0.152
0.8	9	7.91	0.0829	0.0728
0.9	4	3.90	0.0368	0.0359
1.0	1	1.91	0.00921	0.0176
1.1	0			

$$n_1 = 1\frac{1}{2}; \rho_1 = 0.1316 g$$

Table 1 (Contd)

(v) 22500 feet to 27400 feet; 46.2 miles

g	No. of bumps		Bumps per mile	
	Obs.	Fitted	Obs.	Fitted
0		430		9.31
0.1	372	372	8.06	8.06
0.2	244	264	5.28	5.72
0.3	173	167	3.75	3.62
0.4	104	99.0	2.25	2.14
0.5	60	55.7	1.30	1.21
0.6	30	30.3	0.650	0.656
0.7	16	16.1	0.346	0.349
0.8	7	8.37	0.152	0.181
0.9	5	4.28	0.108	0.0927
1.0	2	2.15	0.0433	0.0466
1.1	0			

$$n_1 = 2\frac{1}{2}; \quad \rho_1 = 0.1220 \text{ g}$$

(vi) 27500 feet to 32400 feet; 22.3 miles

g	No. of bumps		Bumps per mile	
	Obs.	Fitted	Obs.	Fitted
0		193		8.66
0.1	173	173	7.75	7.75
0.2	127	128	5.69	5.76
0.3	79	84.0	3.54	3.76
0.4	50	50.1	2.24	2.25
0.5	30	28.0	1.34	1.25
0.6	15	14.9	0.672	0.668
0.7	7	7.60	0.314	0.341
0.8	5	3.77	0.224	0.169
0.9	5	1.82	0.224	0.0818
1.0	3	0.865	0.134	0.0388
1.1	3	0.403	0.134	0.0180
1.2	2	0.185	0.0896	0.00829
1.3	1	0.0832	0.0448	0.00373
1.4	1	0.0375	0.0448	0.00168
1.5	1	0.0166	0.0448	0.000746
1.6	0			

$$n_1 = 3\frac{1}{2}; \quad \rho_1 = 0.1036 \text{ g}$$

Table 1 (Contd)

(vii) 32500 feet to 37400 feet; 20.4 miles

g	No. of bumps		Bumps per mile	
	Obs.	Fitted	Obs.	Fitted
0		154		7.56
0.1	134	134	6.56	6.56
0.2	93	93.0	4.56	4.56
0.3	49	55.3	2.40	2.71
0.4	28	29.7	1.37	1.45
0.5	15	14.9	0.735	0.730
0.6	8	7.06	0.392	0.346
0.7	3	3.23	0.147	0.158
0.8	2	1.42	0.0980	0.0696
0.9	2	0.608	0.0980	0.0298
1.0	2	0.255	0.0980	0.0125
1.1	2	0.105	0.0980	0.00516
1.2	0			

$$n_1 = 3\frac{1}{2}; \rho_1 = 0.0917 g$$

(viii) 37500 feet to 42400 feet; 13.7 miles

g	No. of bumps		Bumps per mile	
	Obs.	Fitted	Obs.	Fitted
0		105		7.69
0.1	94	94	6.88	6.88
0.2	68	69.1	4.98	5.06
0.3	43	44.0	3.15	3.22
0.4	25	25.0	1.83	1.83
0.5	13	13.1	0.952	0.957
0.6	6	6.40	0.439	0.469
0.7	0			

$$n_1 = 4\frac{1}{2}; \rho_1 = 0.0858 g$$

Table 2R.F. JONES'S THUNDERSTORM DATASUMMARY OF PARAMETERS

Height feet	n_1	ρ_1 g units	N_0	λ_1 per mile	ν per mile	$1/\lambda_2$ feet
2500- 7400	$1\frac{1}{2}$	0.1042	5.49	22.97	39.1	89.2
7500-12400	$2\frac{1}{2}$	0.0833	4.70	19.69	56.9	99.2
12500-17400	2	0.1053	5.06	16.77	39.7	61.4
17500-22400	$1\frac{1}{2}$	0.1316	4.86	14.20	33.3	47.6
22500-27400	$2\frac{1}{2}$	0.1220	4.66	11.94	50.4	36.8
27500-32400	$3\frac{1}{2}$	0.1036	4.33	9.97	60.7	35.4
32500-37400	$3\frac{1}{2}$	0.0917	3.78	8.26	51.6	33.8
37500-42400	$4\frac{1}{2}$	0.0858	3.84	6.57	57.0	13.3

Table 3

'SWIFTER' MIDDAY FLIGHTS OVER FLAT DESERT CLASSIFIED WITH RESPECT TO
SOLAR RADIATION. CUMULATIVE GUST DISTRIBUTIONS

(i) Solar radiation 35-39 mW/cm²; 1620 miles

Gust velocity ft/sec	No. of gusts		Gusts per mile	
	Obs.	Fitted	Obs.	Fitted
0		31073		19.181
5	7337	7337	4.529	4.529
7½	2344	2293	1.447	1.415
10	638	644.3	0.3938	0.3977
15	44	42.58	0.02716	0.02628
20	1	2.457	0.0006173	0.001517

$$n_1 = 2\frac{1}{2}; \rho_1 = 1.543 \text{ ft/sec}$$

(ii) Solar radiation 40-44 mW/cm²; 2953 miles

Gust velocity ft/sec	No. of gusts		Gusts per mile	
	Obs.	Fitted	Obs.	Fitted
0		52070		17.633
5	12667	12667	4.290	4.290
7½	3769	3584	1.276	1.214
10	850	864.4	0.2878	0.2927
15	38	38.16	0.01287	0.01292

$$n_1 = 3\frac{1}{2}; \rho_1 = 1.259 \text{ ft/sec}$$

(iii) Solar radiation 45-49 mW/cm²; 2532 miles

Gust velocity ft/sec	No. of gusts		Gusts per mile	
	Obs.	Fitted	Obs.	Fitted
0		38772		15.313
5	12828	12828	5.066	5.066
7½	4492	4233	1.774	1.672
10	1124	1143	0.4439	0.4514
15	55	57.31	0.02172	0.02263
20	5	2.116	0.001975	0.0008357
25	2		0.0007899	

$$n_1 = 5; \rho_1 = 1.171 \text{ ft/sec}$$

Table 3 (Contd)

(iv) Solar radiation 50-54 mW/cm²; 4994 miles

Gust velocity ft/sec	No. of gusts		Gusts per mile	
	Obs.	Fitted	Obs.	Fitted
0		75008		15.020
5	27501	27501	5.507	5.507
7 $\frac{1}{2}$	10025	9760	2.007	1.954
10	2752	2819	0.5511	0.5645
15	147	158.6	0.02944	0.03176
20	10	6.425	0.002002	0.001287
25	1		0.0002002	

$$n_1 = 5\frac{1}{2}; \quad \rho_1 = 1.168 \text{ ft/sec}$$

(v) Solar radiation 55-59 mW/cm²; 2051 miles

Gust velocity ft/sec	No. of gusts		Gusts per mile	
	Obs.	Fitted	Obs.	Fitted
0		30853		15.043
5	11894	11894	5.799	5.799
7 $\frac{1}{2}$	4441	4420	2.165	2.155
10	1345	1344	0.6558	0.6553
15	85	84.37	0.04144	0.04114
20	7	3.831	0.003413	0.001868
25	1		0.0004876	
30	1		0.0004876	

$$n_1 = 5\frac{1}{2}; \quad \rho_1 = 1.202 \text{ ft/sec}$$

(vi) Solar radiation 60-64 mW/cm²; 2255 miles

Gust velocity ft/sec	No. of gusts		Gusts per mile	
	Obs.	Fitted	Obs.	Fitted
0		36224		16.064
5	14969	14969	6.638	6.638
7 $\frac{1}{2}$	6091	5931	2.701	2.630
10	1928	1938	0.8550	0.8594
15	142	142.0	0.06297	0.06297
20	7	7.579	0.003104	0.003361
25	1	0.3312	0.004435	0.0001469

$$n_1 = 5\frac{1}{2}; \quad \rho_1 = 1.253 \text{ ft/sec}$$

Table 3 (Contd)

(vii) Solar radiation 65-69 mW/cm²; 2691 miles

Gust velocity ft/sec	No. of gusts		Gusts per mile	
	Obs.	Fitted	Obs.	Fitted
0		45359		16.856
5	19122	19122	7.106	7.106
7½	7923	7721	2.944	2.869
10	2510	2575	0.9327	0.9569
15	200	197.5	0.07432	0.07339
20	15	11.05	0.005574	0.004106
25	1	0.5068	0.0003716	0.0001883

$$n_1 = 5\frac{1}{2}; \rho_1 = 1.269 \text{ ft/sec}$$

(viii) Solar radiation 70-74 mW/cm²; 4041 miles

Gust velocity ft/sec	No. of gusts		Gusts per mile	
	Obs.	Fitted	Obs.	Fitted
0		70053		17.336
5	32436	32436	8.027	8.027
7½	14607	14304	3.615	3.540
10	5208	5272	1.289	1.305
15	478	502	0.1183	0.1242
20	54	35.21	0.01336	0.008713
25	7	2.035	0.001732	0.0005036
30	3		0.007424	
35	1		0.0002475	

$$n_1 = 5\frac{1}{2}; \rho_1 = 1.351 \text{ ft/sec}$$

(ix) Solar radiation 75-79 mW/cm²; 2858 miles

Gust velocity ft/sec	No. of gusts		Gusts per mile	
	Obs.	Fitted	Obs.	Fitted
0		49341		17.264
5	24169	24169	8.457	8.457
7½	11483	11251	4.018	3.937
10	4334	4409	1.516	1.543
15	472	479.6	0.1652	0.1678
20	44	38.74	0.01540	0.01355
25	5	2.586	0.001749	0.0009048
30	1		0.003499	

$$n_1 = 5\frac{1}{2}; \rho_1 = 1.408 \text{ ft/sec}$$

Table 3 (Contd)

(x) Solar radiation 80-84 mW/cm²; 2148 miles

Gust velocity ft/sec	No. of gusts		Gusts per mile	
	Obs.	Fitted	Obs.	Fitted
0		38665		18.00
5	17359	17359	8.081	8.081
7 $\frac{1}{2}$	7706	7436	3.588	3.462
10	2586	2651	1.204	1.234
15	237	234.9	0.1103	0.1094
20	23	15.29	0.01071	0.007118
25	3	0.8180	0.001397	0.0003808

$$n = 5\frac{1}{2}; \rho_1 = 1.323 \text{ ft/sec}$$

Table 4

'SWIFTER' MIDDAY FLIGHTS OVER FLAT DESERT
SUMMARY OF PARAMETERS

Solar radiation mW/cm ²	n_1	ρ_1 ft/sec	N_0 per mile	ν per mile	$1/\lambda_2$ feet	ρ ft/sec
35-39	$2\frac{1}{2}$	1.543	9.590	101.3	14.38	1.700
40-44	$3\frac{1}{2}$	1.259	8.816	130.7	24.76	1.475
45-49	5	1.171	7.656	166.7	41.62	1.500
50-54	$5\frac{1}{2}$	1.168	7.510	180.2	44.52	1.518
55-59	$5\frac{1}{2}$	1.202	7.521	180.4	44.33	1.560
60-64	$5\frac{1}{2}$	1.253	8.032	188.0	37.63	1.573
65-69	$5\frac{1}{2}$	1.269	8.428	193.5	33.27	1.558
70-74	$5\frac{1}{2}$	1.351	8.668	196.7	30.85	1.637
75-79	$5\frac{1}{2}$	1.408	8.632	196.2	31.21	1.710
80-84	$5\frac{1}{2}$	1.323	9.000	200.9	27.81	1.577

The values of n_1 , ρ_1 and N_0 are those of the curves fitted in Figs.7a to 7j (Tables 3(i) to (x)). The values of ν , $1/\lambda_2$ and ρ are derived from these using the relationships given in (64) to (69) with $\lambda_1 = 23.14$ per mile.

Table 5

'SWIFTER' STACKED SORTIES WITH SOLAR RADIATION ≥ 65 mW/cm² OVER FLAT DESERT

CUMULATIVE GUST DISTRIBUTIONS

(i) 200 feet; 2103 miles

Gust velocity ft/sec	No. of gusts		Gusts per mile	
	Obs.	Fitted	Obs.	Fitted
0		39272		18.674
5	17089	17089	8.126	8.126
7 $\frac{1}{2}$	7365	7108	3.502	3.380
10	2401	2452	1.142	1.166
15	198	202.1	0.09415	0.09610
20	10	12.20	0.004755	0.005801

$$n_1 = 5\frac{1}{2}; \rho_1 = 1.295 \text{ ft/sec}$$

(ii) 400 feet; 2174 miles

Gust velocity ft/sec	No. of gusts		Gusts per mile	
	Obs.	Fitted	Obs.	Fitted
0		31633		14.551
5	15351	15351	7.061	7.061
7 $\frac{1}{2}$	7111	7009	3.271	3.224
10	2641	2665	1.215	1.226
15	285	265.6	0.1311	0.1222
20	17	19.15	0.007820	0.008809

$$n_1 = 6; \rho_1 = 1.326 \text{ ft/sec}$$

(iii) 600 feet; 1342 miles

Gust velocity ft/sec	No. of gusts		Gusts per mile	
	Obs.	Fitted	Obs.	Fitted
0		16522		12.311
5	8617	8617	6.421	6.421
7 $\frac{1}{2}$	4229	4193	3.151	3.124
10	1672	1703	1.246	1.269
15	208	192.9	0.1550	0.1437
20	20	15.63	0.01490	0.01165
25	2	1.017	0.001490	0.0007578

$$n_1 = 6\frac{1}{2}; \rho_1 = 1.337 \text{ ft/sec}$$

Table 6

'SWIFTER' STACKED SORTIES WITH SOLAR RADIATION ≥ 65 mW/cm² OVER HILLY DESERT

CUMULATIVE GUST DISTRIBUTIONS

(i) 200 feet; 1221 miles

Gust velocity ft/sec	No. of gusts		Gusts per mile	
	Obs.	Fitted	Obs.	Fitted
0		23319		19.098
5	11256	11256	9.219	9.219
7 $\frac{1}{2}$	5534	5404	4.532	4.426
10	2189	2261	1.793	1.852
15	319	305.2	0.2613	0.2500
20	45	33.17	0.03686	0.02717
25	6	3.149	0.004914	0.002579

$$n_1 = 4; \rho_1 = 1.706 \text{ ft/sec}$$

(ii) 400 feet; 1252 miles

Gust velocity ft/sec	No. of gusts		Gusts per mile	
	Obs.	Fitted	Obs.	Fitted
0		19762		15.784
5	10077	10077	8.049	8.049
7 $\frac{1}{2}$	5228	4997	4.176	3.991
10	2175	2144	1.737	1.712
15	276	297.2	0.2204	0.2374
20	31	32.41	0.02476	0.02589
25	2	3.035	0.001597	0.002424
30	1	0.2561	0.0007987	0.0002046

$$n_1 = 4\frac{1}{2}; \rho_1 = 1.650 \text{ ft/sec}$$

Table 6 (Contd)(iii) 600 feet; 688 miles

Gust velocity ft/sec	No. of gusts		Gusts per mile	
	Obs.	Fitted	Obs.	Fitted
0		9381		13.635
5	5174	5174	7.520	7.520
7½	2745	2730	3.990	3.968
10	1204	1245	1.750	1.810
15	194	192.6	0.2820	0.2799
20	32	23.06	0.04651	0.03352
25	4	2.340	0.005814	0.003401
30	2	0.2116	0.002907	0.0003076

$$n_1 = 5; \rho_1 = 1.650 \text{ ft/sec}$$

Table 7

'SWIFTER' STACKED SORTIES WITH SOLAR RADIATION ≥ 65 mW/cm²

SUMMARY OF PARAMETERS

(i) Flat desert

Height feet	n_1	ρ_1 ft/sec	N_0 per mile	λ_1 per mile	ν per mile	$1/\lambda_2$ feet
200	$5\frac{1}{2}$	1.295	9.337	23.14	204.9	25.10
400	6	1.326	7.275	23.01	191.5	48.28
600	$6\frac{1}{2}$	1.337	6.156	22.87	183.0	71.41

(ii) Hilly desert

Height feet	n_1	ρ_1 ft/sec	N_0 per mile	λ_1 per mile	ν per mile	$1/\lambda_2$ feet
200	4	1.706	9.549	23.14	154.7	20.19
400	$4\frac{1}{2}$	1.650	7.892	23.01	153.7	37.13
600	5	1.650	6.817	22.87	153.4	54.49

SYMBOLS

a	a magnitude parameter in the definition of pulse shape $F(t)$
c	aircraft chord
$F(t)$	the defined pulse shape, a function of t
$f(x)$	the frequency distribution of x , similarly $f(\dot{x})$ etc.
$G(t)$	a further function of t , used mainly as the first derivative of $F(t)$
H	the pulse build up distance
K	the modified Bessel function
N_{exp}	the expected number in a class
N_{obs}	the observed number in a class
N_x	the number of positive crossings per unit time (or distance) of the value x
n, n_1, n_2	parameters determining the shape of frequency distributions
p	a parameter in the distribution of time intervals between pulses
$R(\tau)$	the autocorrelation function
$S(\omega)$	the spectrum
s	distance
t	time
t_m	the pulse build up time
U	gust velocity
u	dummy variable in characteristic function
V	aircraft forward velocity
v	dummy variable in characteristic function
x	a random variable
z	aircraft height
α	the ratio λ_1/λ_2
κ	cumulant of distribution (with suffix or suffices)
$\lambda, \lambda_1, \lambda_2$	parameters in the definition of pulse shape etc.
μ	moment of distribution (with suffix or suffices)
μ_g	aircraft mass parameter
ρ, ρ_1, ρ_2	scale parameters of distributions
σ	standard deviation (with appropriate suffix)
τ	time variable in autocorrelation function (in (71), a scale parameter)
ν	mean pulse rate per unit time or distance
φ	a characteristic function, (or in (39) an unsteady lift function)

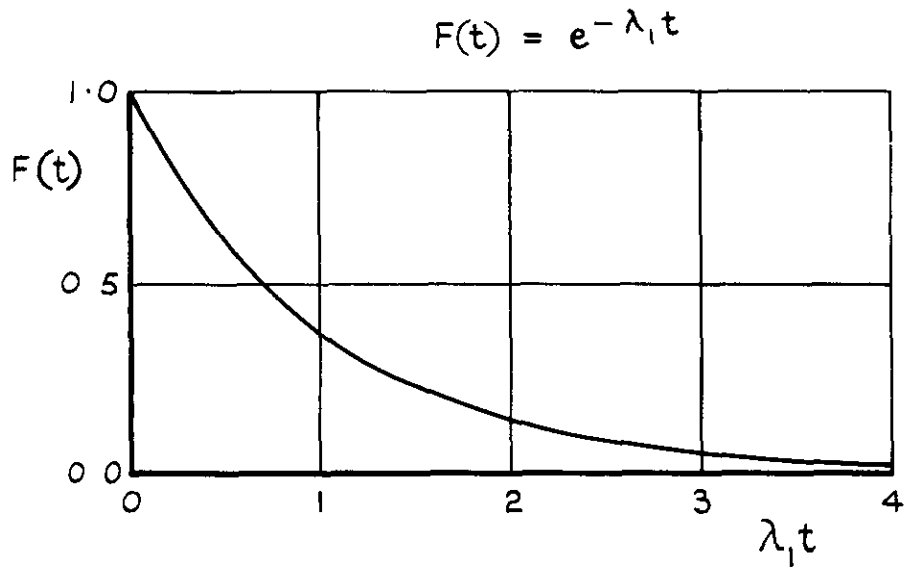
SYMBOLS (Contd)

ψ unsteady lift function
 ω frequency variable in spectrum

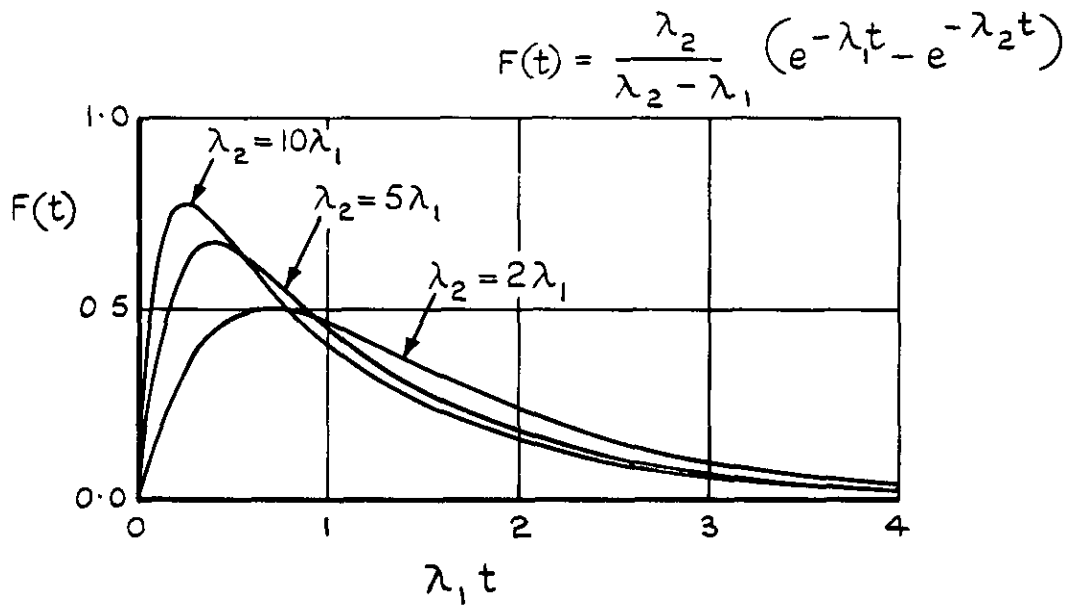
An extended use is made of the factorial sign, writing $x!$ for $\Gamma(x + 1)$.

REFERENCES

<u>No.</u>	<u>Author</u>	<u>Title, etc</u>
1	S. I. Rice	Mathematical analysis of random noise. Bell System Technical Journal XXIII, pp 282-332 XXIV pp 46-156
2	M. G. Kendall A. Stuart	The advanced theory of statistics, 2 edition. Griffin and Co. Ltd
3	S. H. Crandall W. D. Mark	Random vibration in mechanical systems. Academic Press (1963)
4	N. I. Bullen	The combination of statistical distributions of random loads. A.R.C. R&M 3513
5	R. F. Jones	Radar echoes from and turbulence within cumulus and cumulonimbus clouds. Meteorological Office Professional Notes 109
6	H. Press May T. Meadows I. Hadlock	Estimates of probability distribution of root- mean-square gust velocity of atmospheric turbu- lence from operational gust load data by random process theory. NACA Technical Note 3362
7	N. I. Bullen Elizabeth Busby	Tables of the function $x^n K_n(x)/\{2^{n-1}(n-1)!\}$ for use as cumulative frequency distributions. A.R.C. C.P. 765
8	N. I. Bullen	Gusts at low altitude in North Africa. A.R.C. C.P. 581
9	J. K. Zbrozek	Gust alleviation factor. A.R.C. R&M 2970

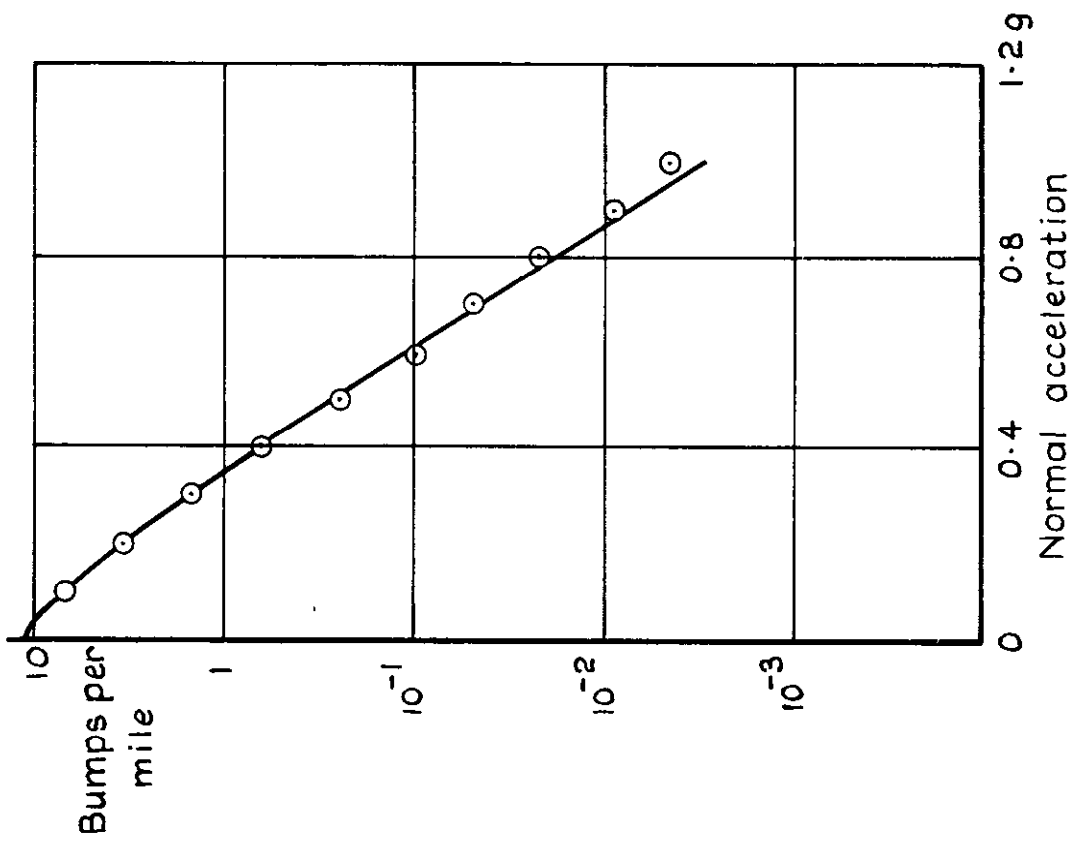


a Exponential pulse

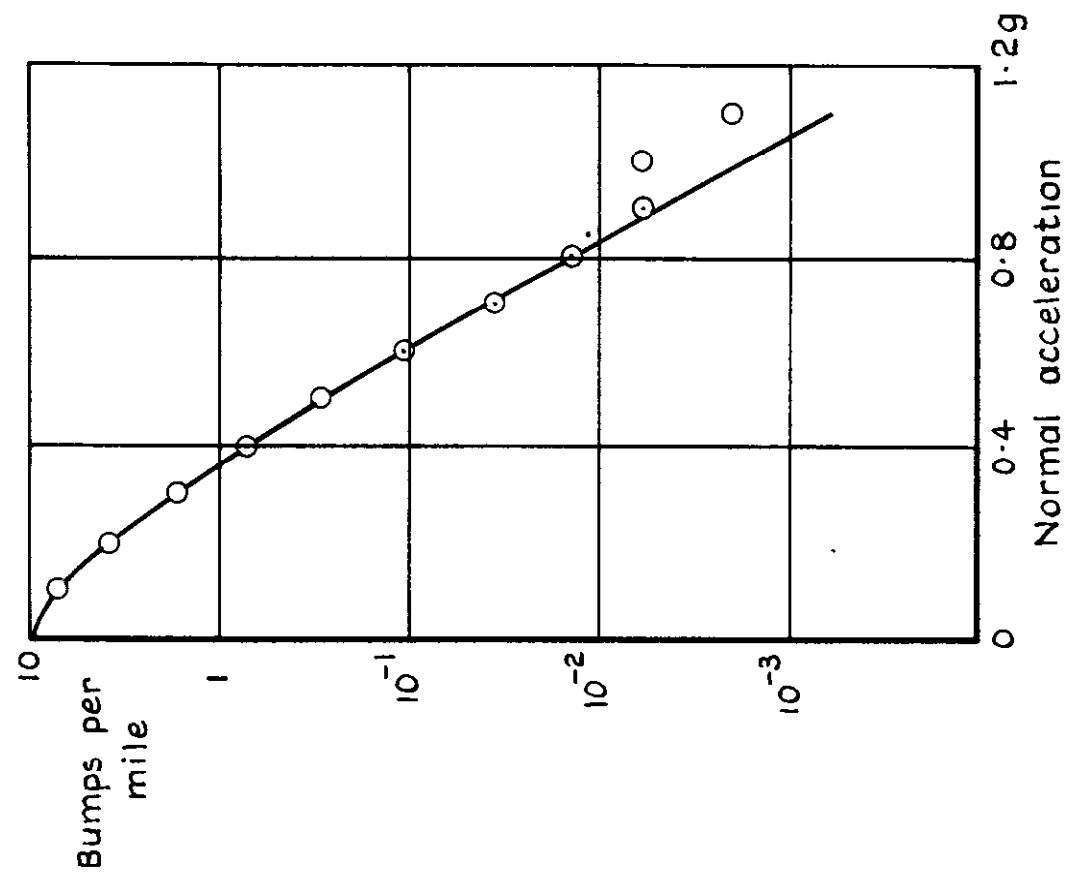


b Pulse shapes for a range of values of λ_2

Fig.1 Pulse shapes

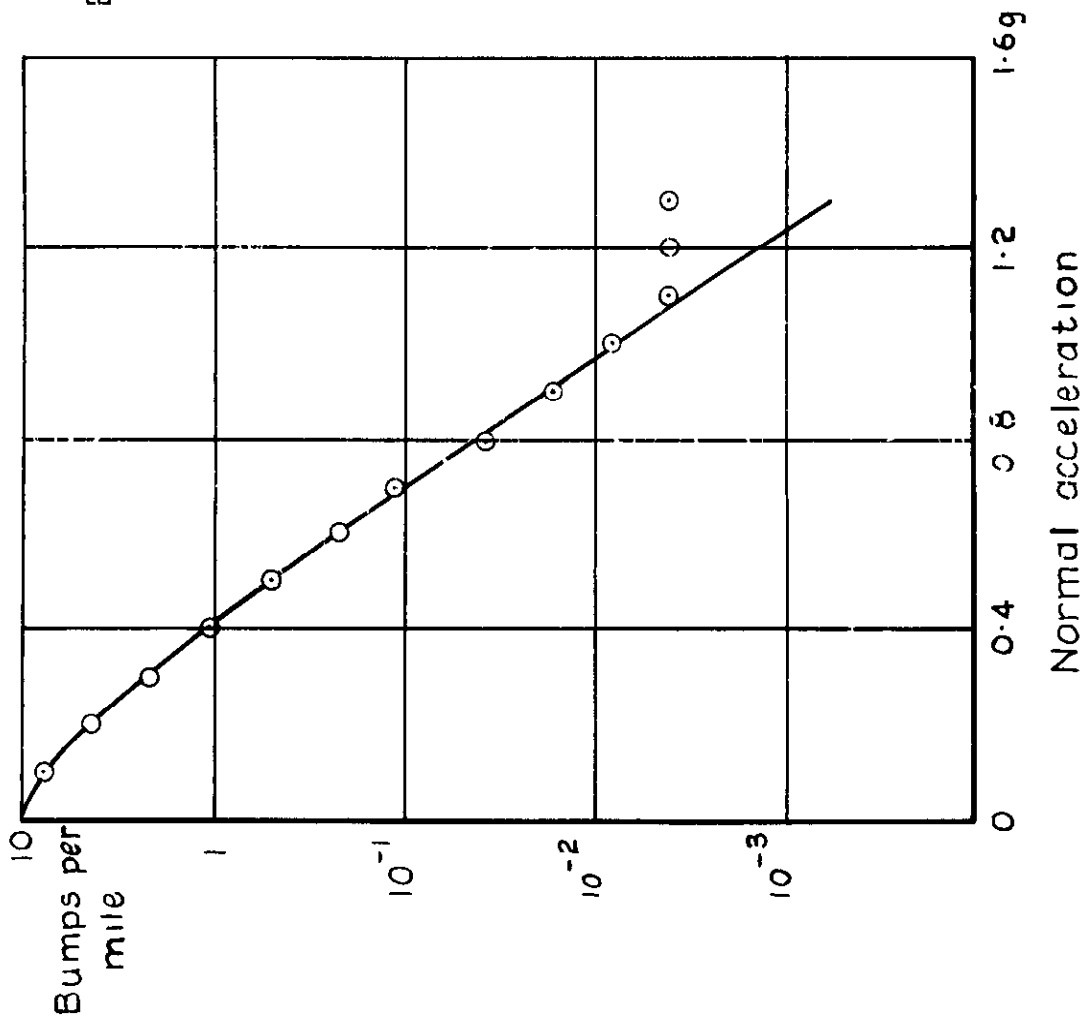


a 2500ft to 7400 ft

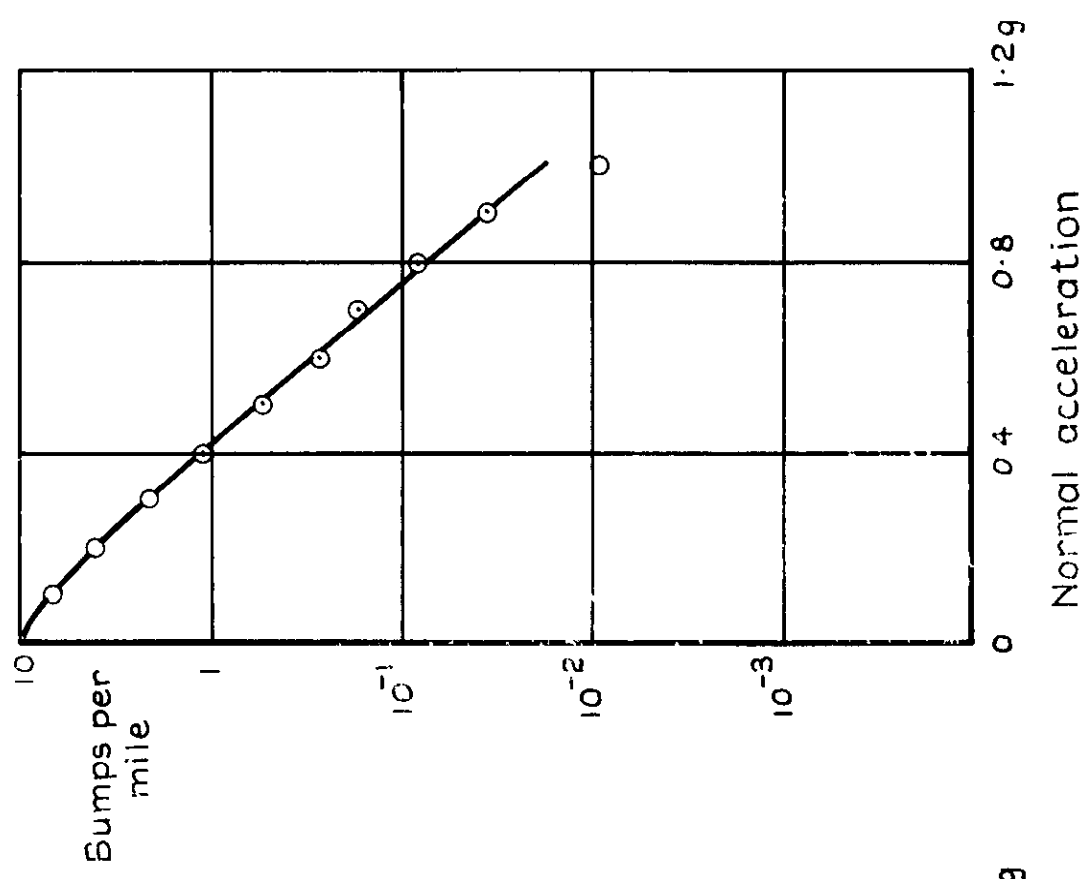


b 7500ft to 12400ft

Fig. 2 Cumulative bump distributions from R.F. Jones's thunderstorm data

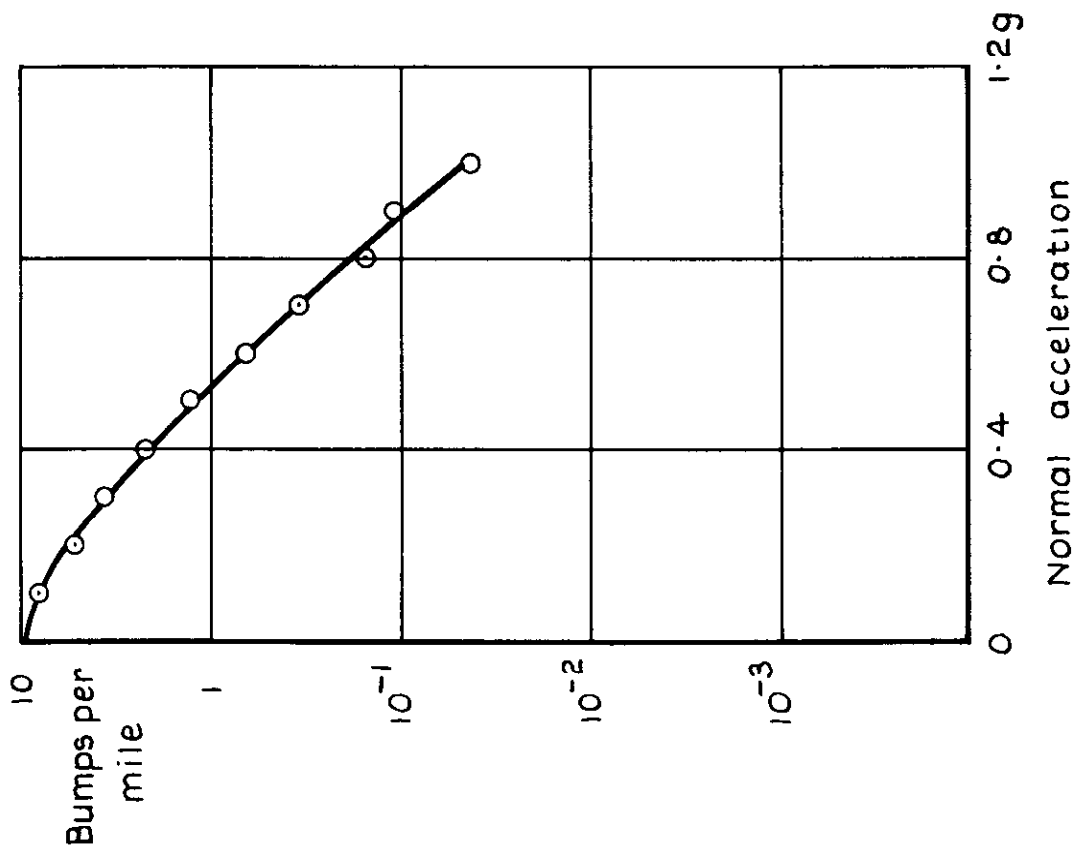


c 12500ft to 17400ft

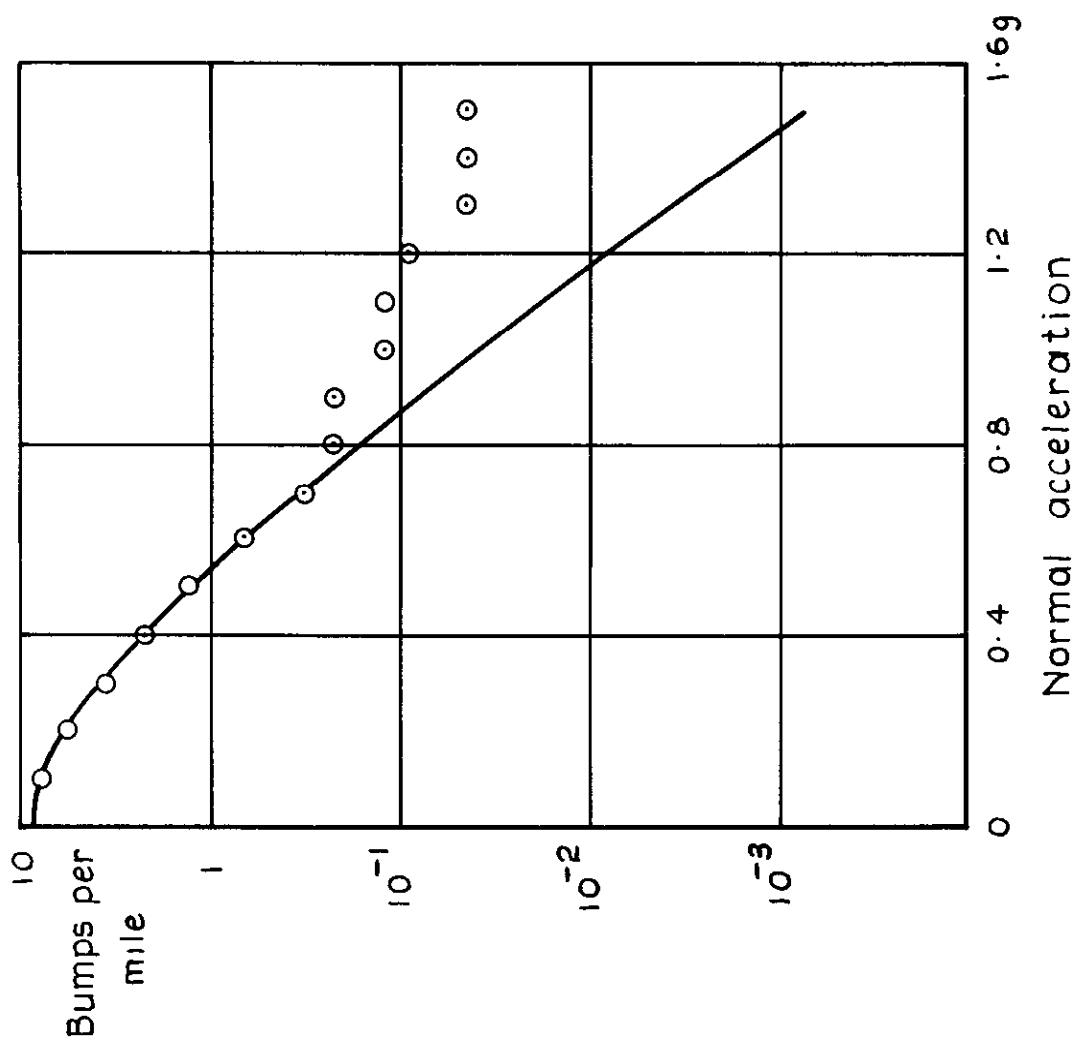


d 17500ft to 22400ft

Fig.2 contd

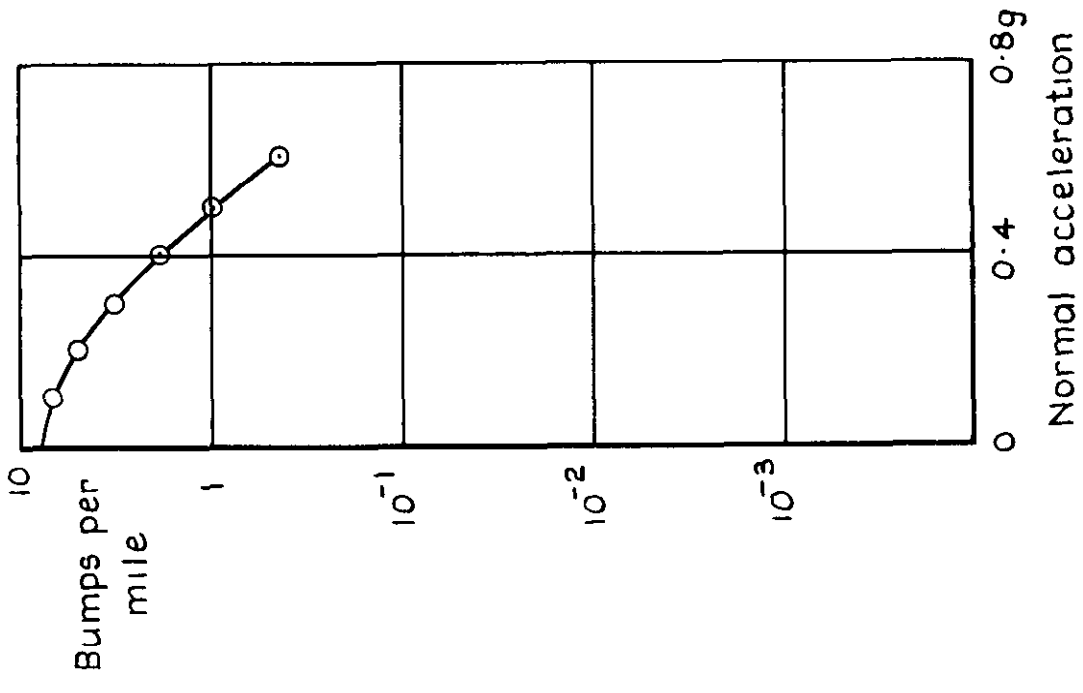


e 22500ft to 27400ft

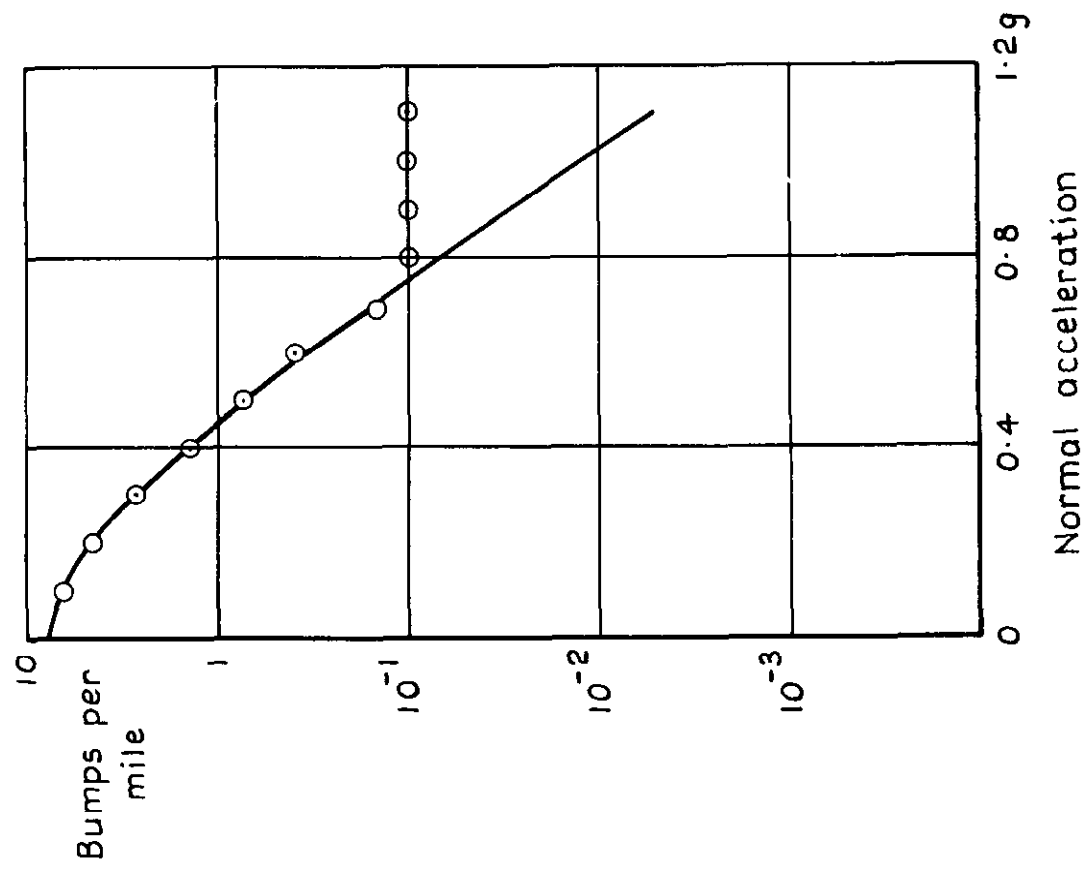


f 27500ft to 32400ft

Fig.2 contd



h 37500ft to 42400ft



g 32500ft to 37400ft

Fig. 2 conold

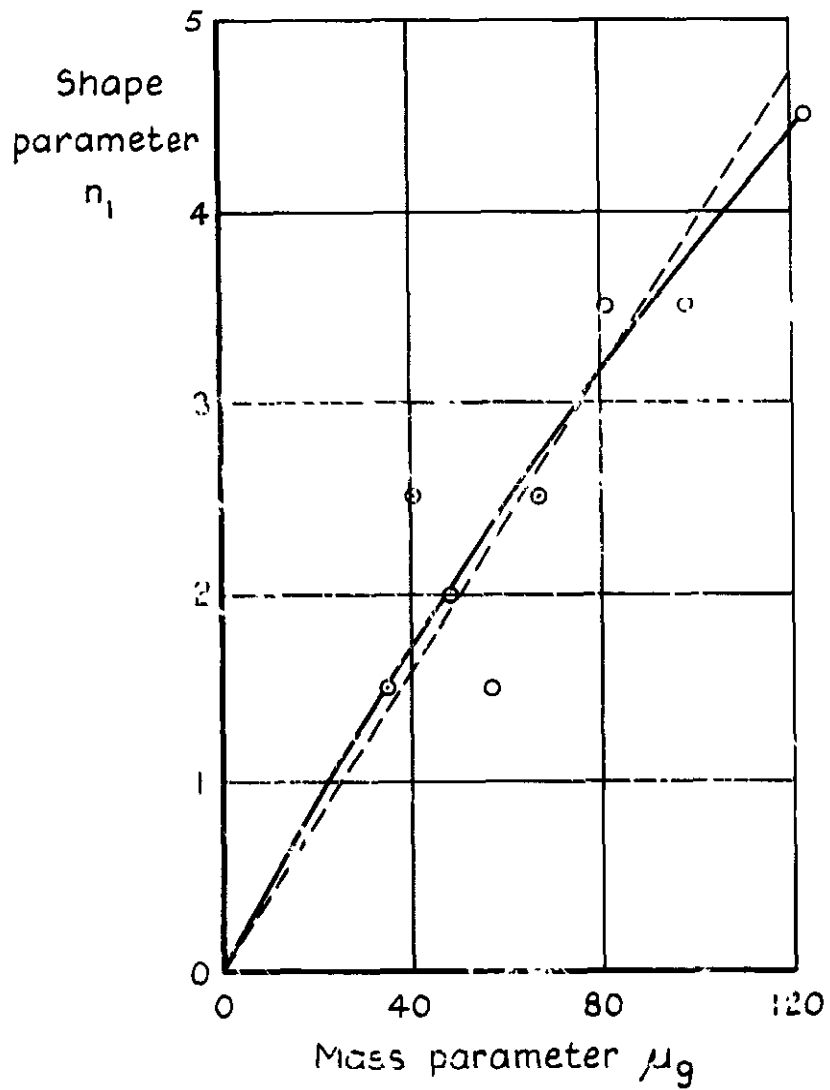


Fig.3 R.F Jones's thunderstorm data. Variation of the shape of the bump distribution with mass parameter

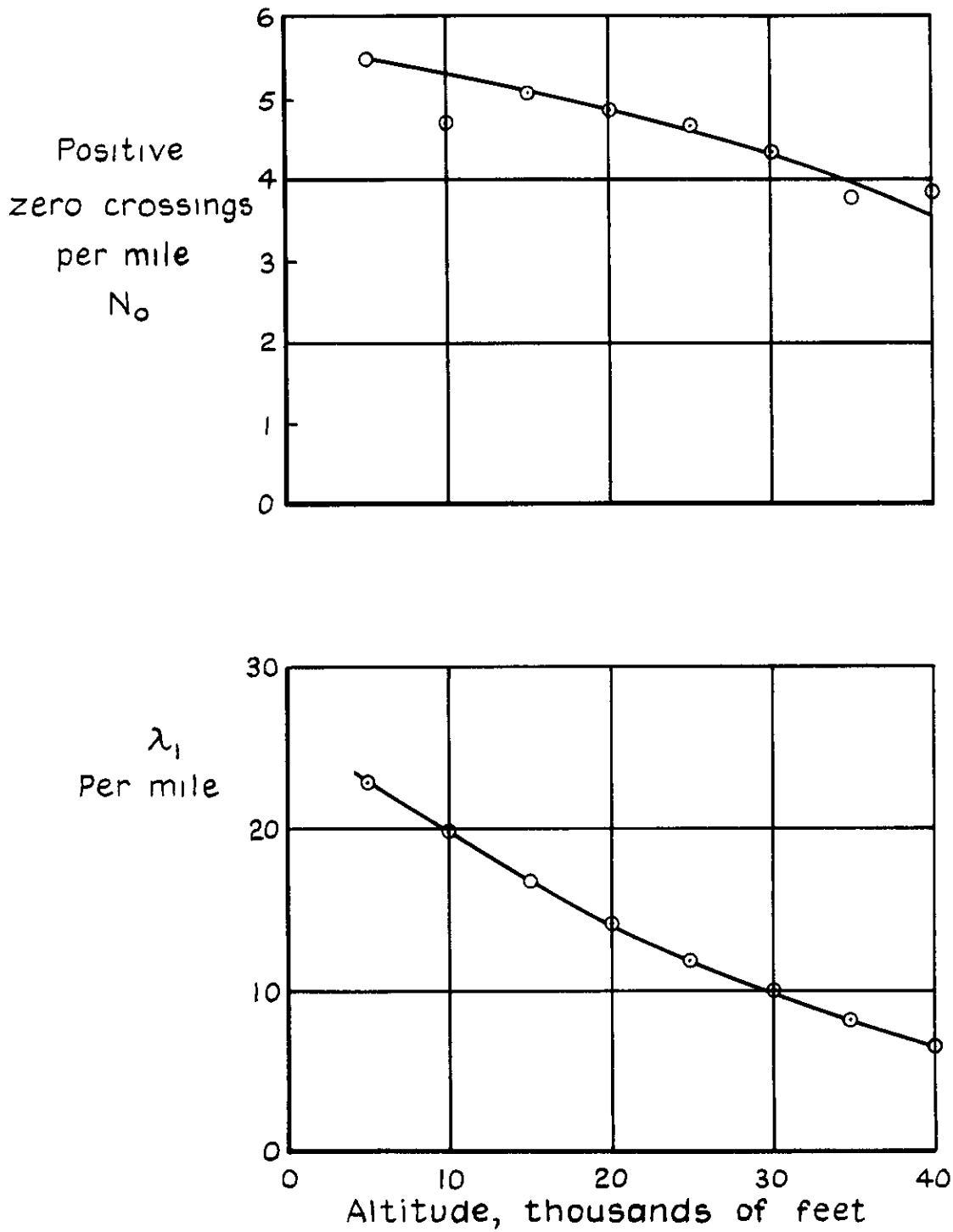


Fig. 4 R.F. Jones's thunderstorm data. Variation of N_0 and λ_1 with altitude

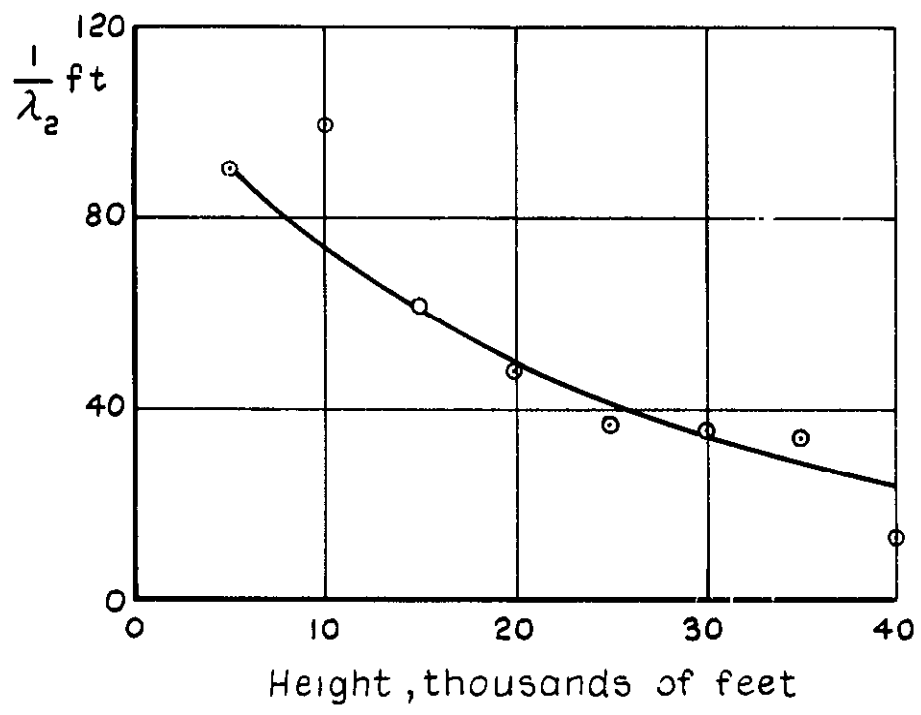
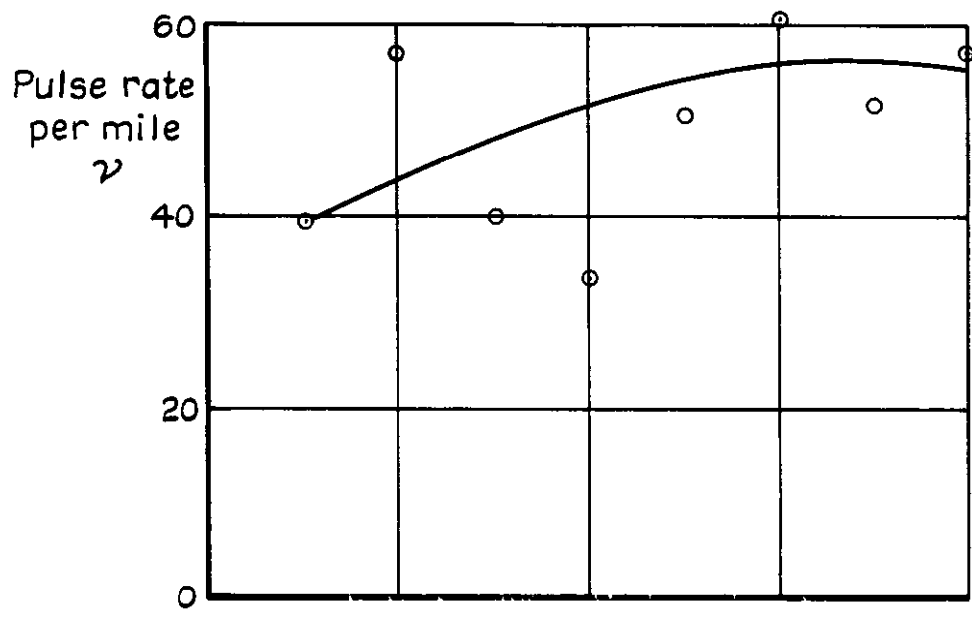


Fig. 5 R.F. Jones's thunderstorm data. Variation of ν and $1/\lambda_2$ with altitude

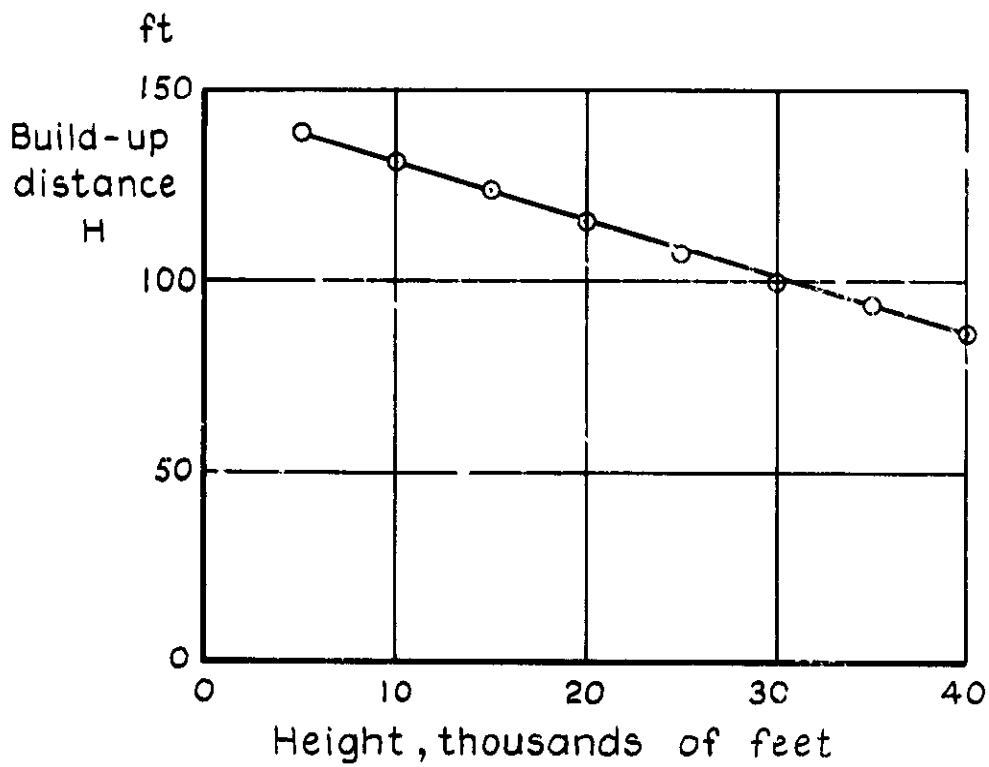
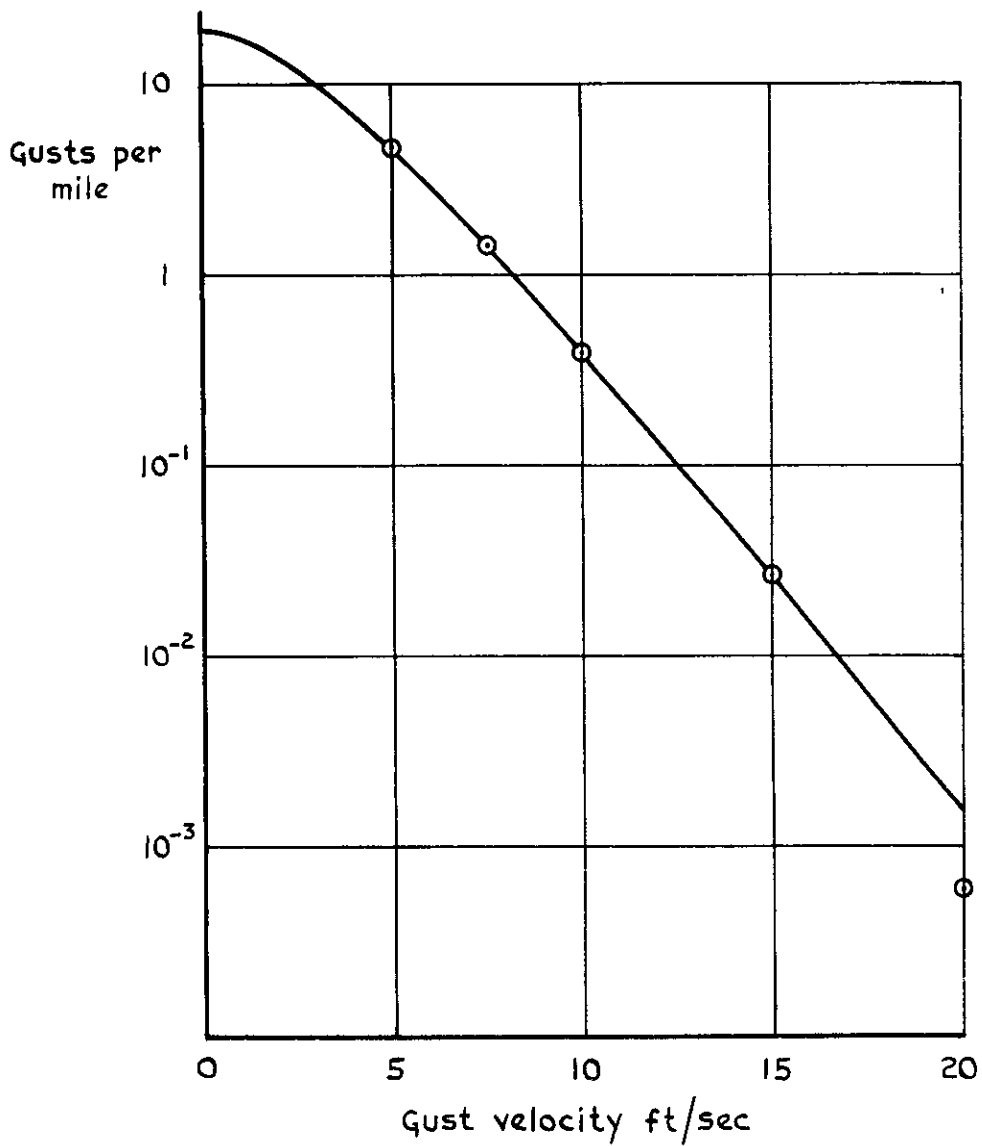
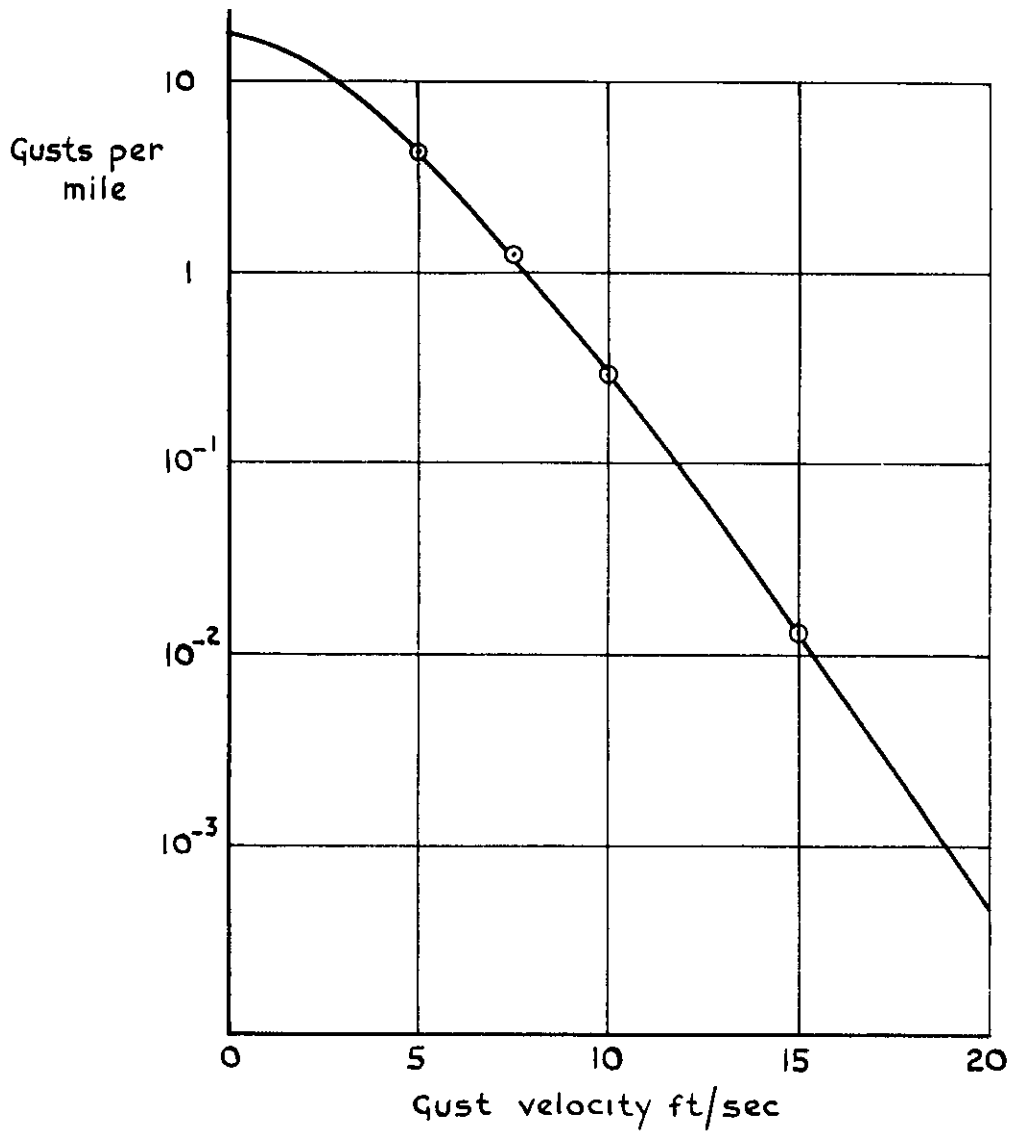


Fig. 6 R.F. Jones's thunderstorm data. Variation of pulse build-up distance with height



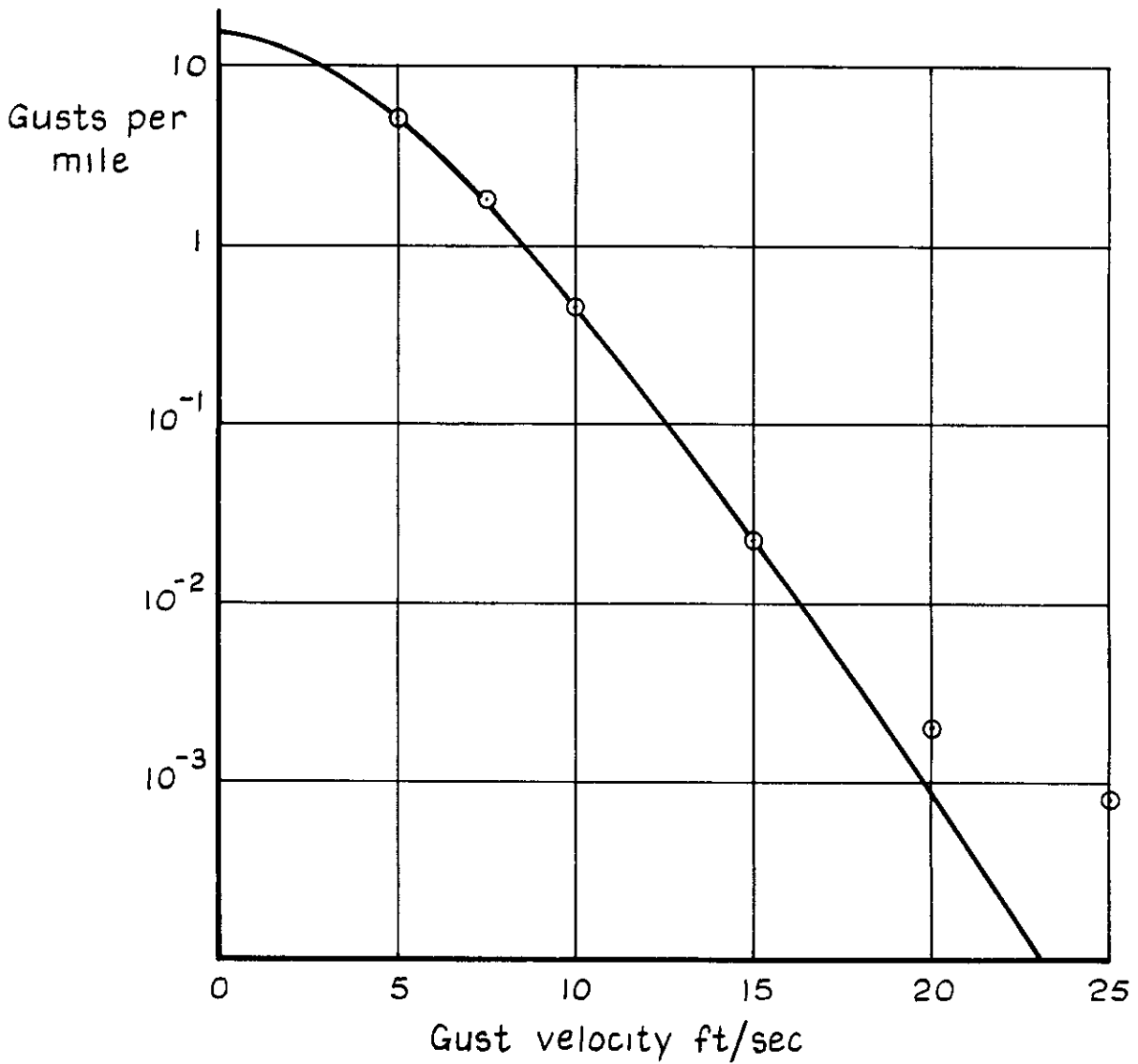
a Solar radiation 35-39 mW/cm²

Fig.7 "Swifter" midday flights over flat desert classified with respect to solar radiation. Cumulative gust distributions



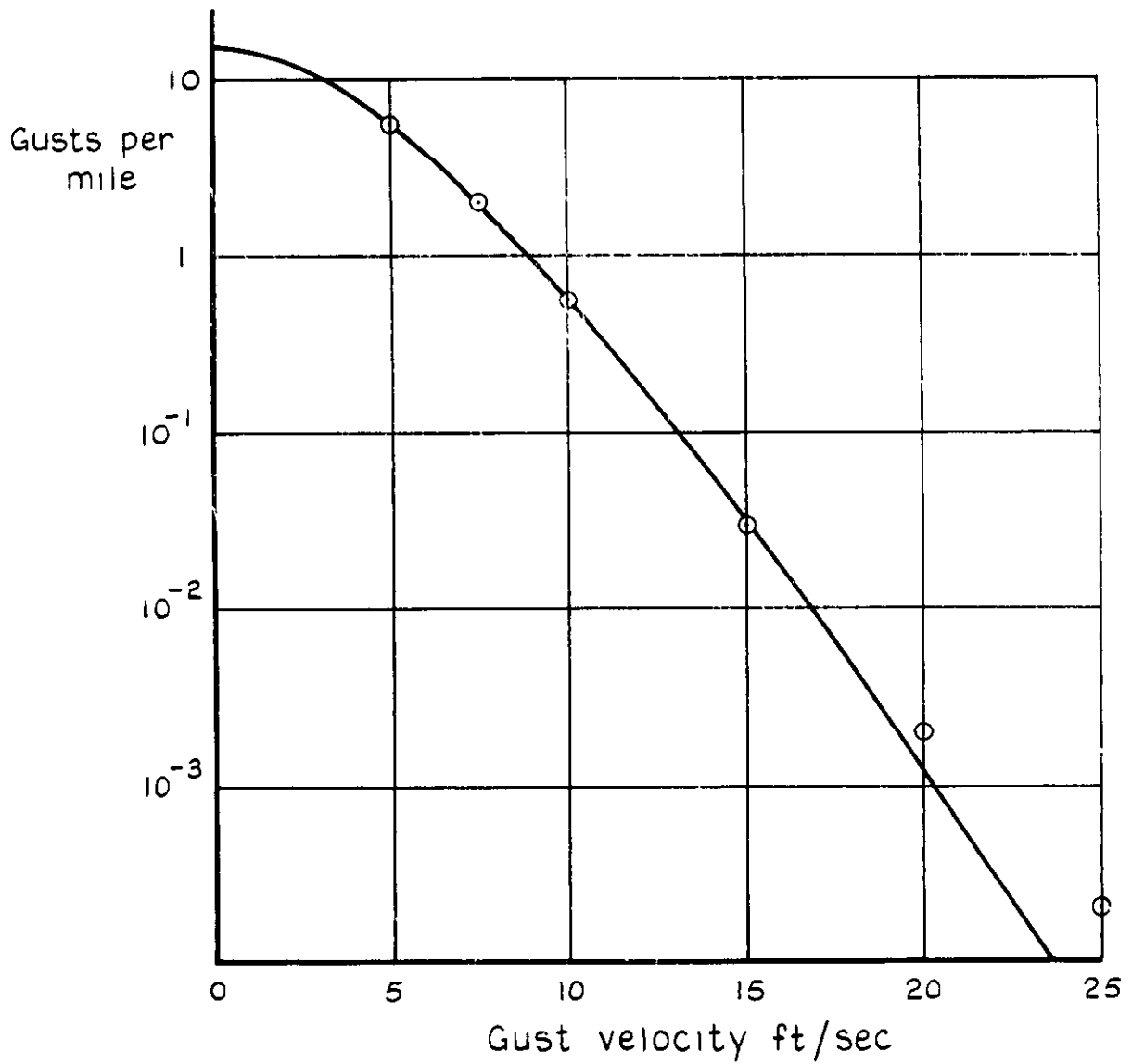
b Solar radiation 40-44 mW/cm²

Fig. 7 contd



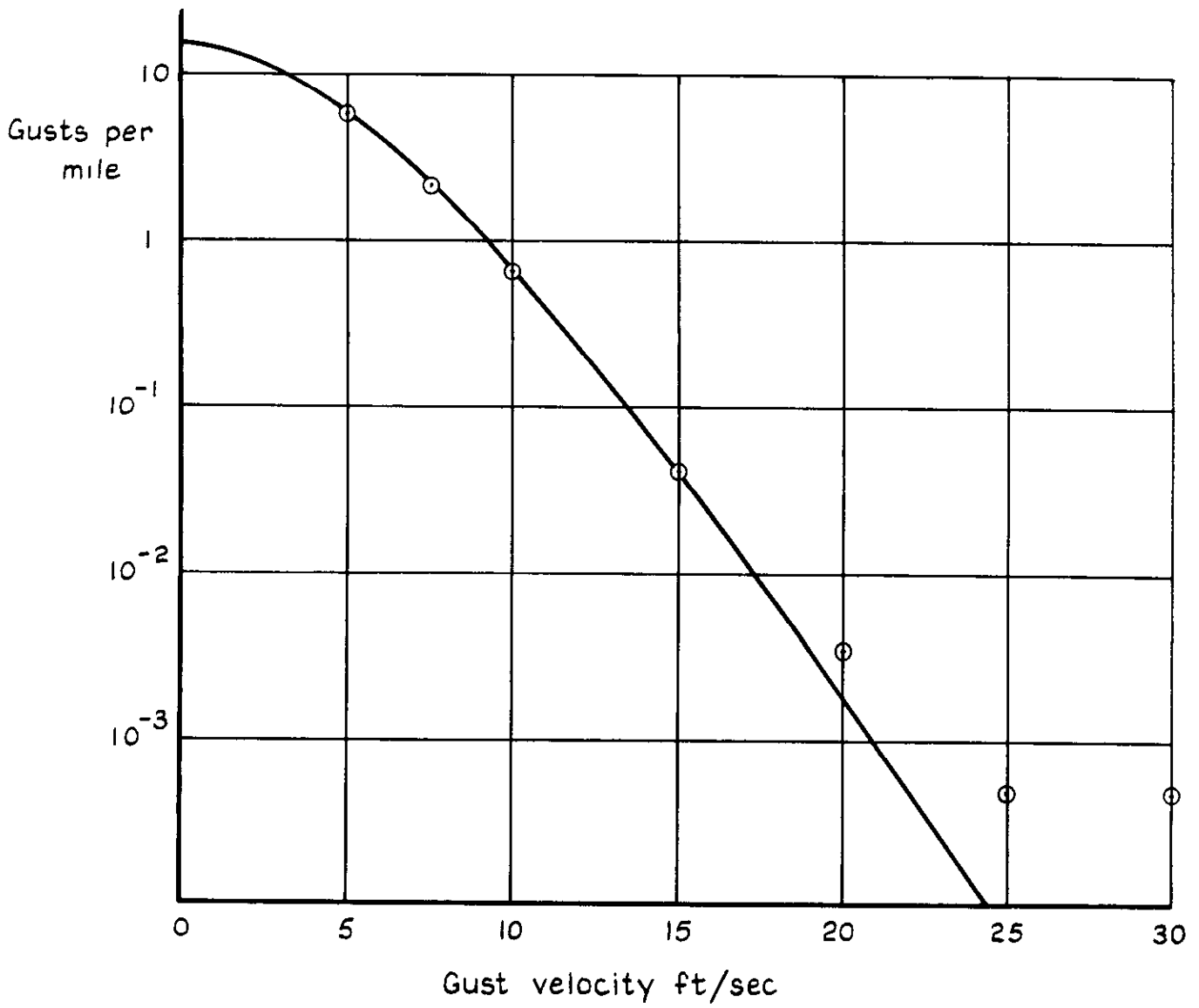
c Solar radiation 45-49 mW/cm^2

Fig. 7 contd



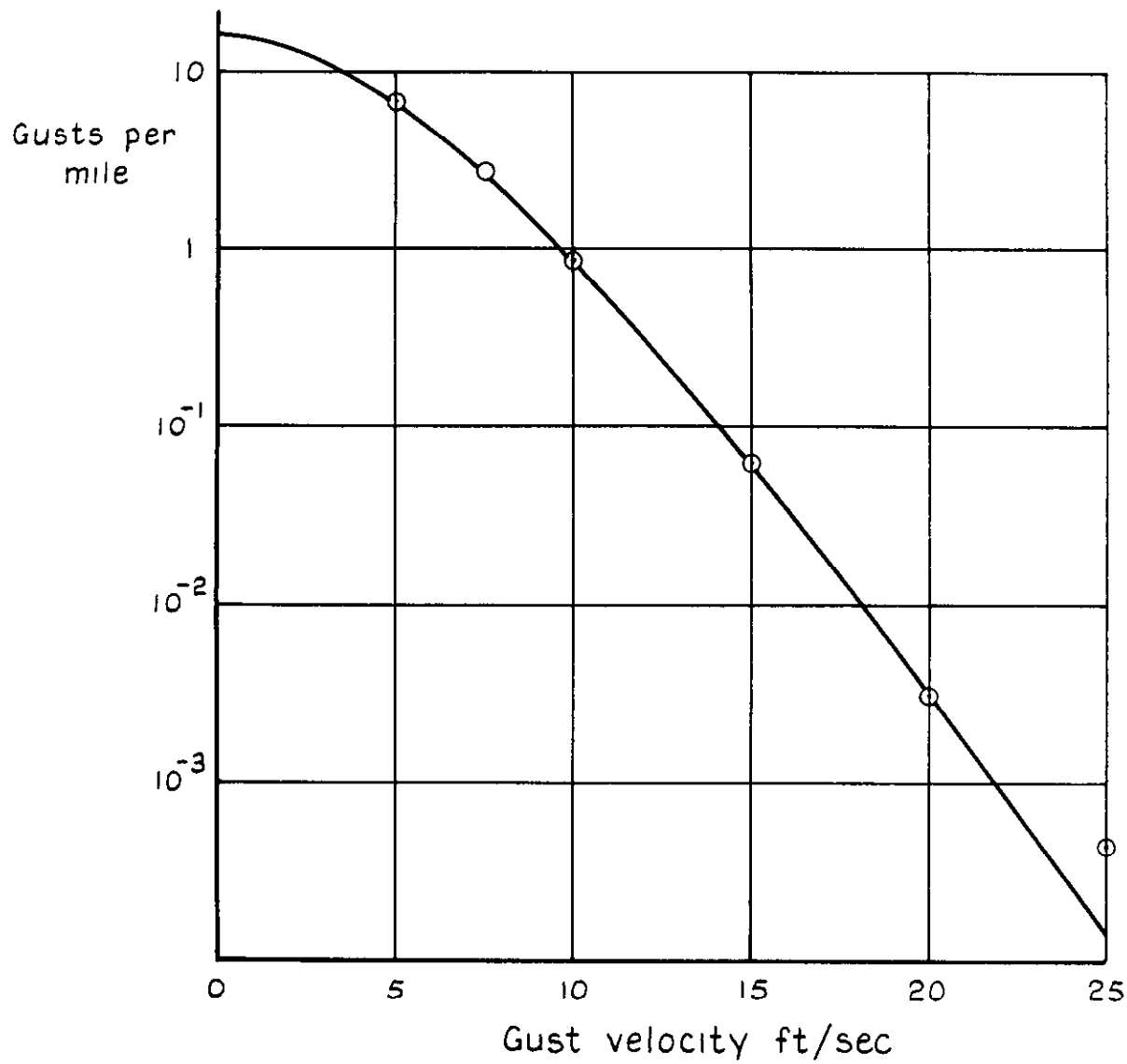
d Solar radiation 50-54 mW/cm²

Fig.7 contd



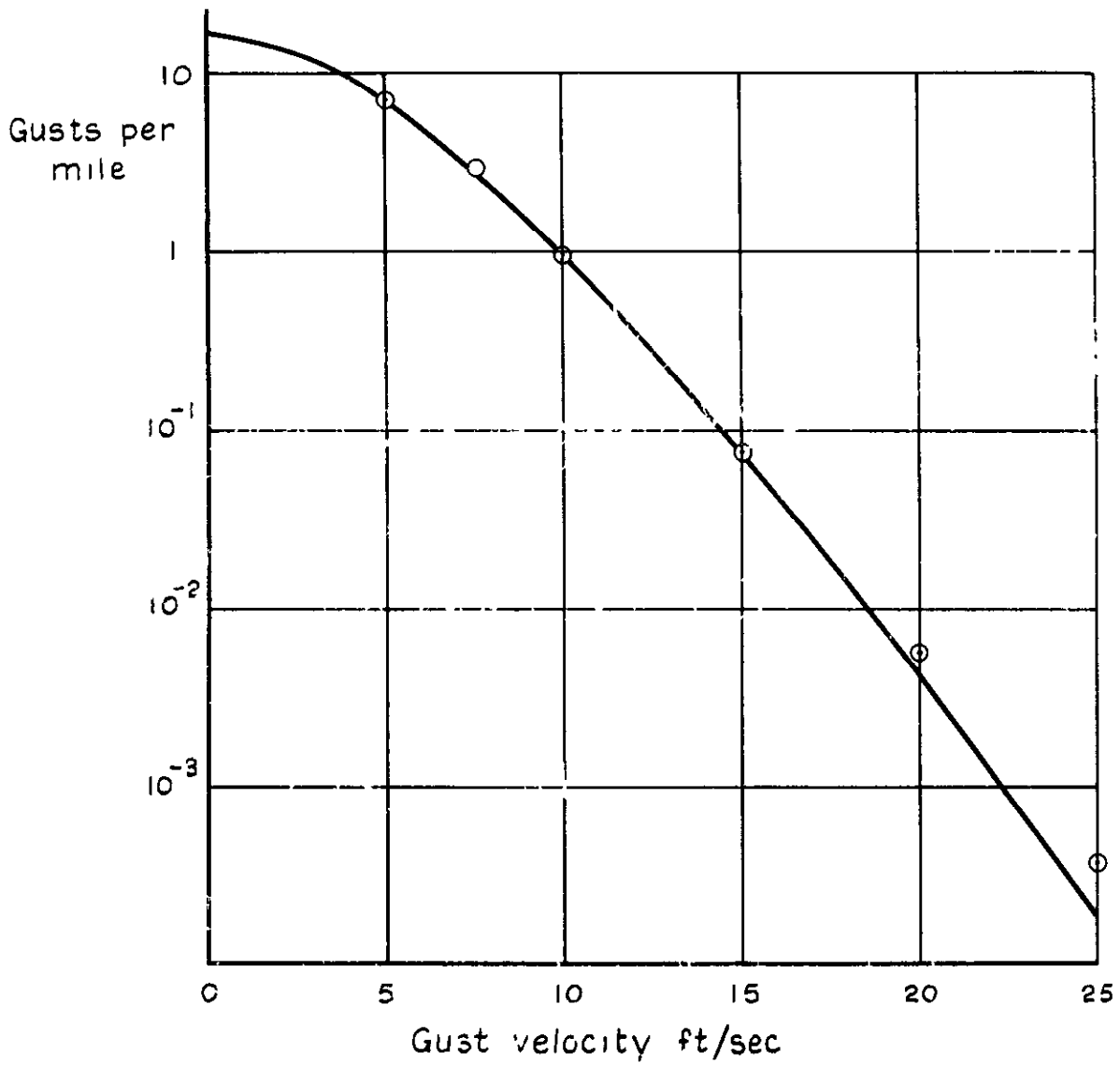
e Solar radiation 55-59 mW/cm²

Fig. 7 contd



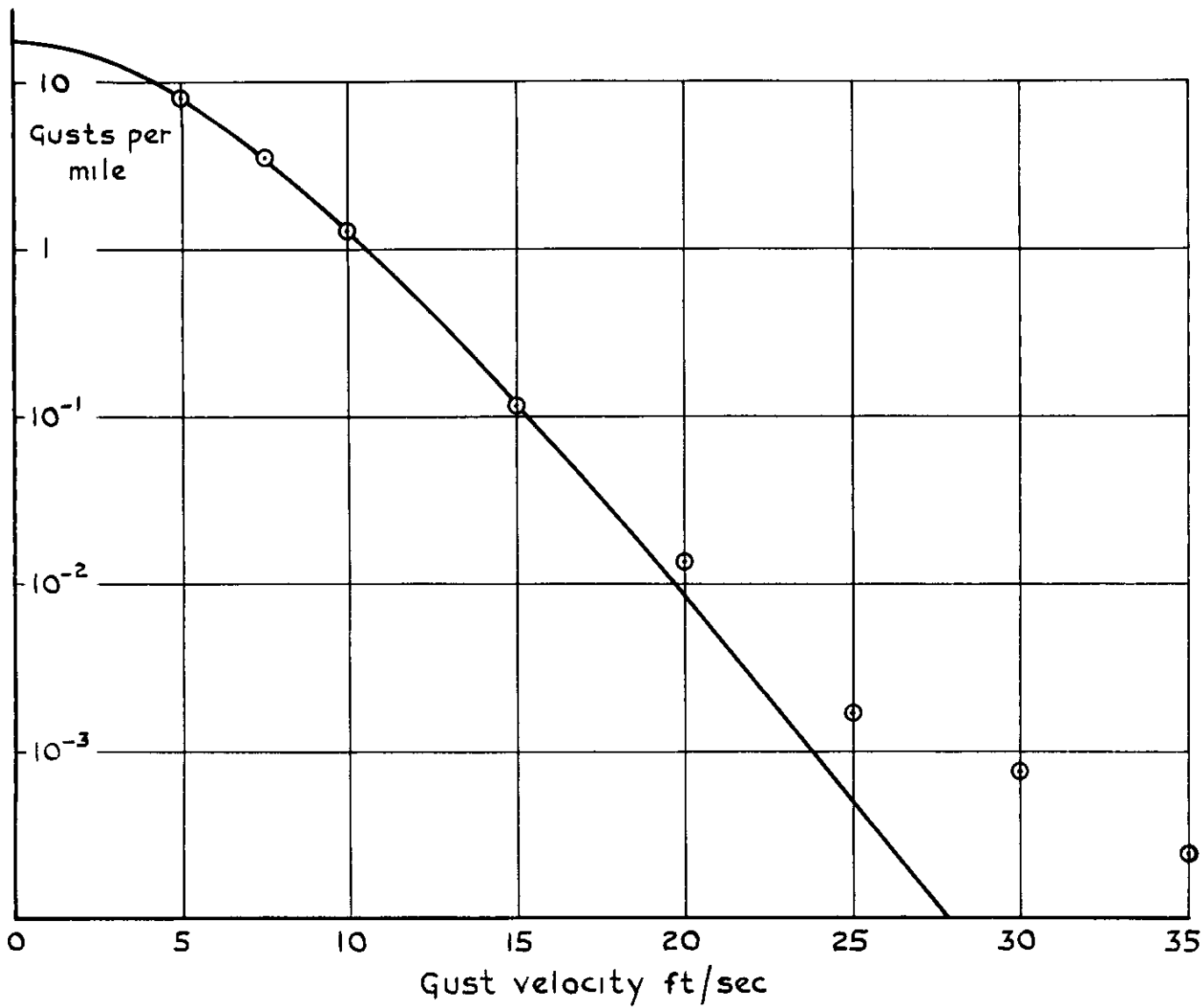
f Solar radiation 60-64 mW/cm²

Fig. 7 contd



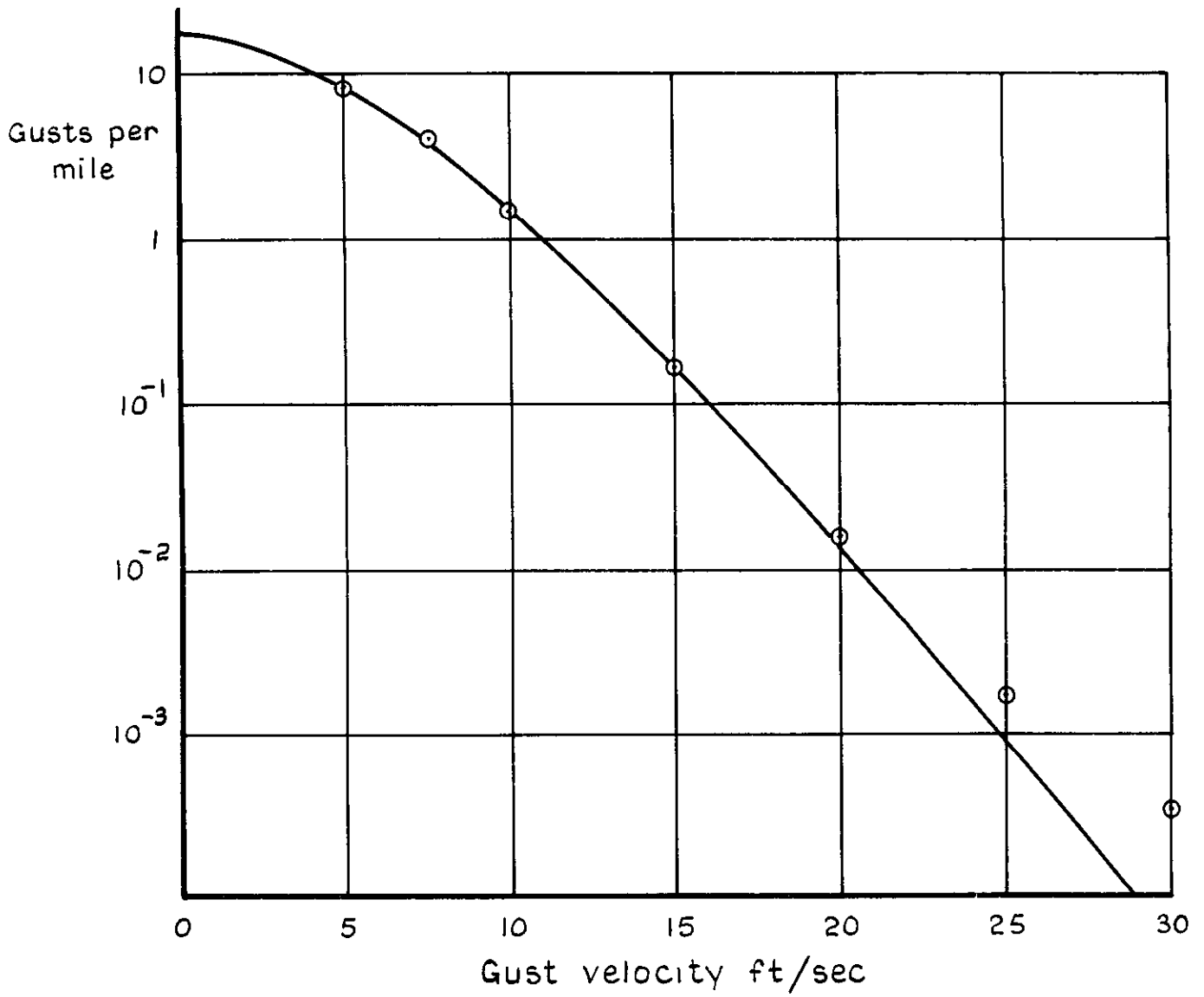
g Solar radiation 65-69 mW/cm²

Fig.7 contd



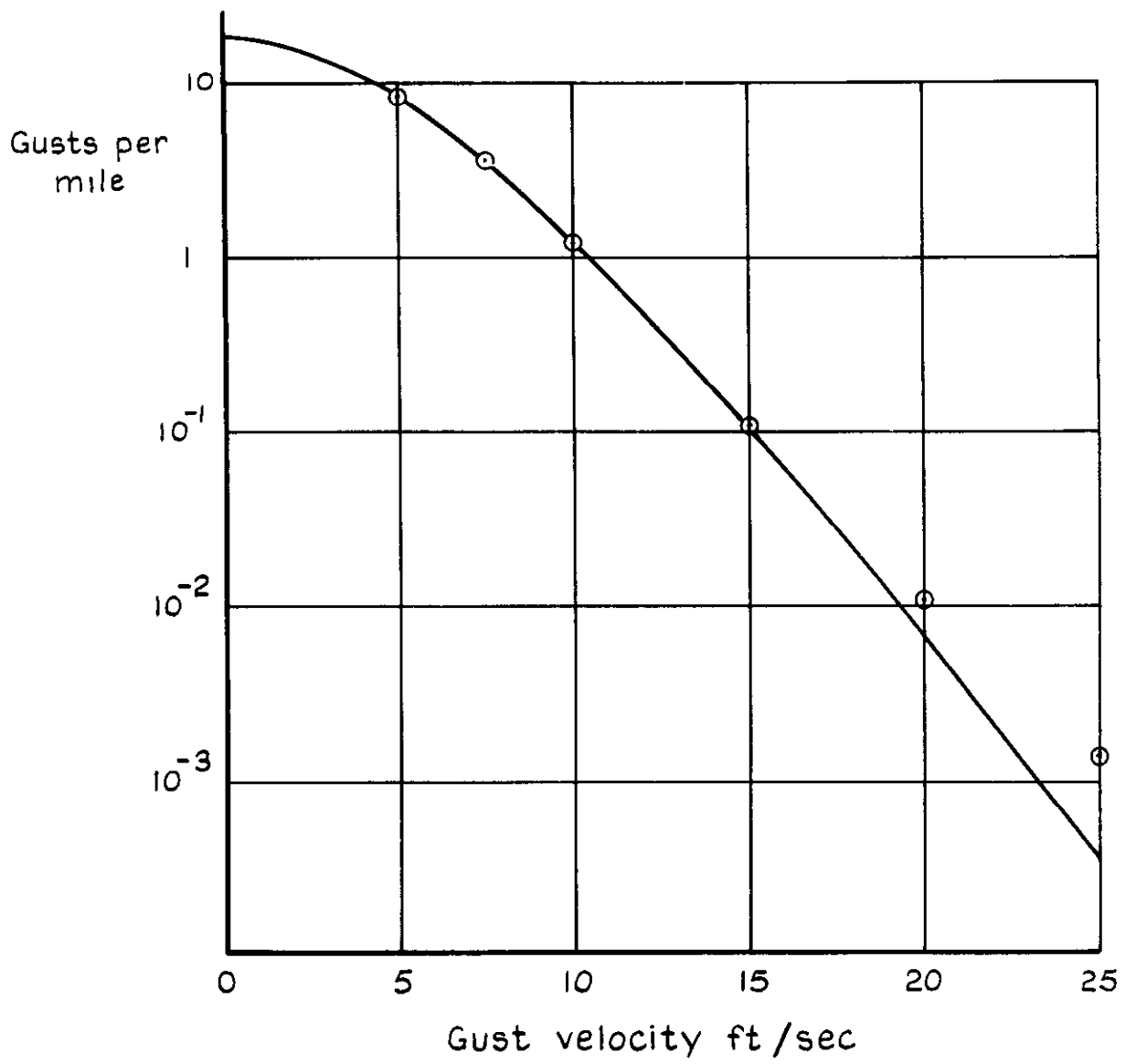
h Solar radiation 70-74 mW/cm²

Fig. 7 contd



i Solar radiation $75-79 \text{ mW/cm}^2$

Fig.7 contd



j Solar radiation 80-84 mW/cm²

Fig. 7 conclud

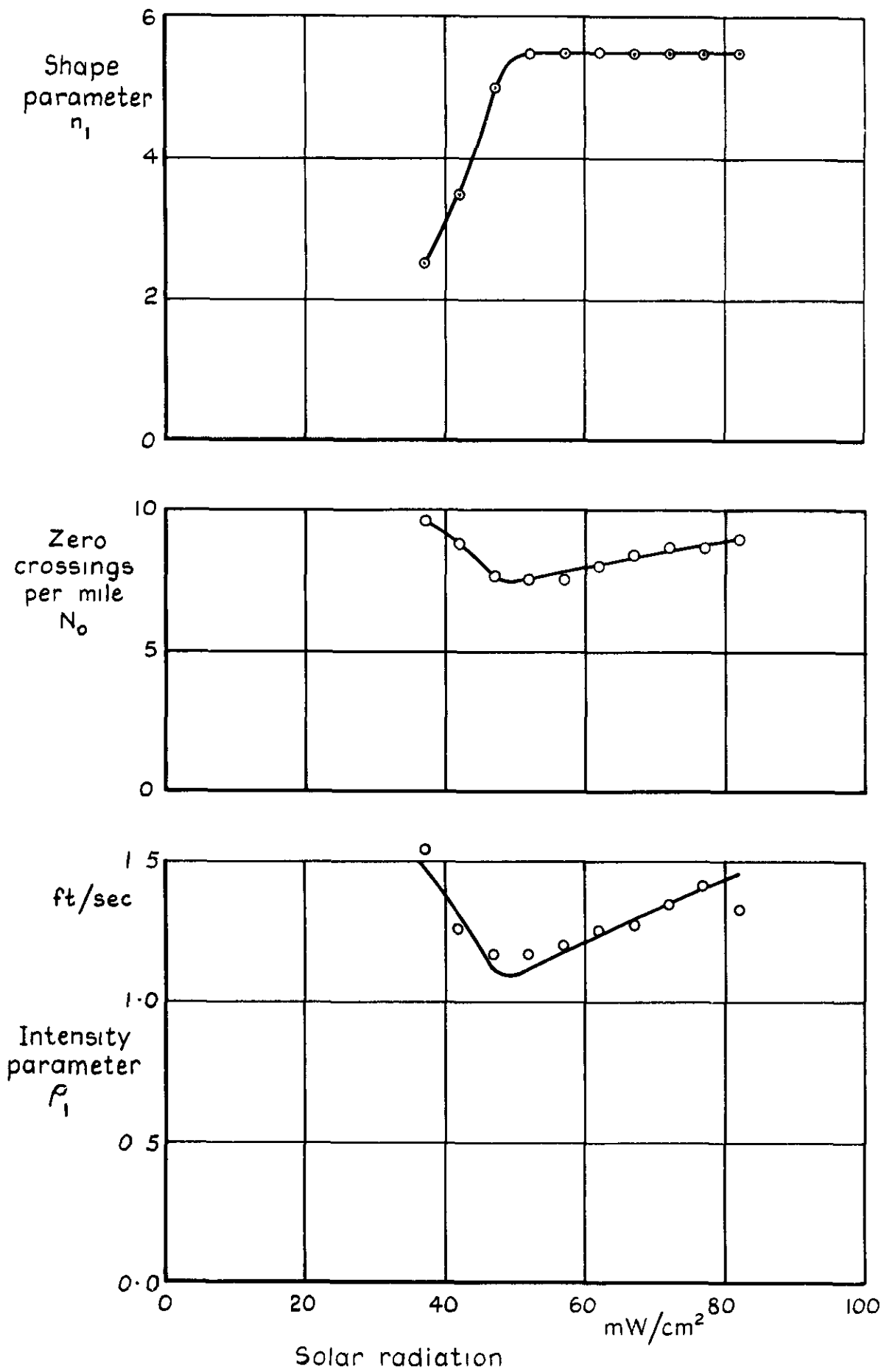
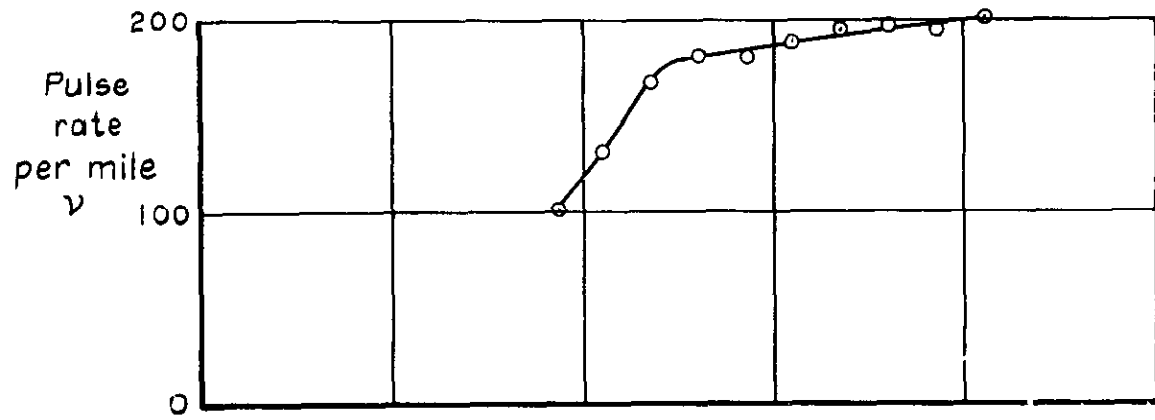
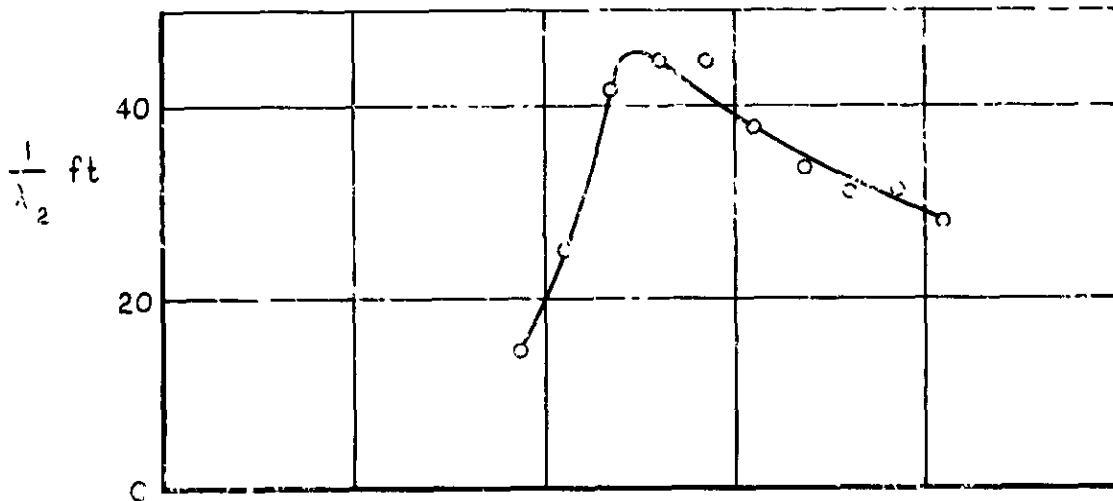


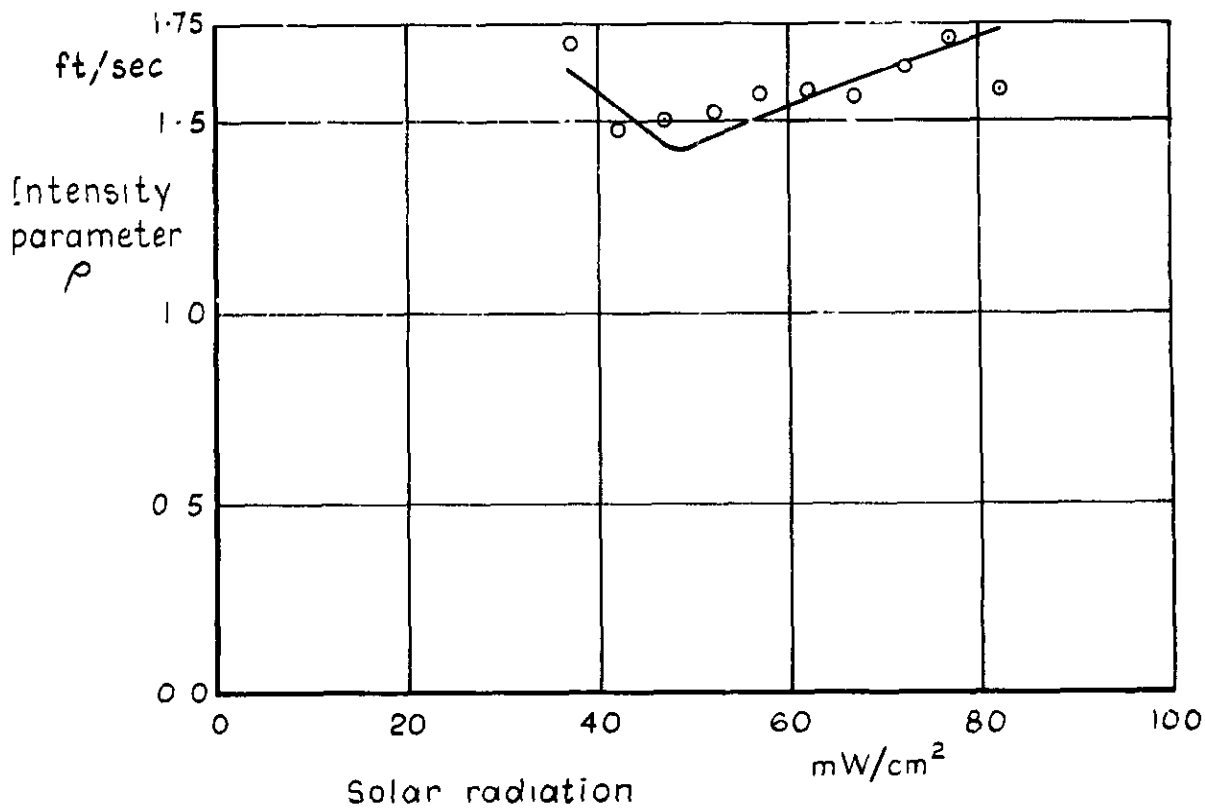
Fig. 8 "Swifter" midday flights over flat desert.
Parameters of fitted curves



a



b



c

Fig. 9 "Swifter" midday flights over flat desert.
Derived parameters

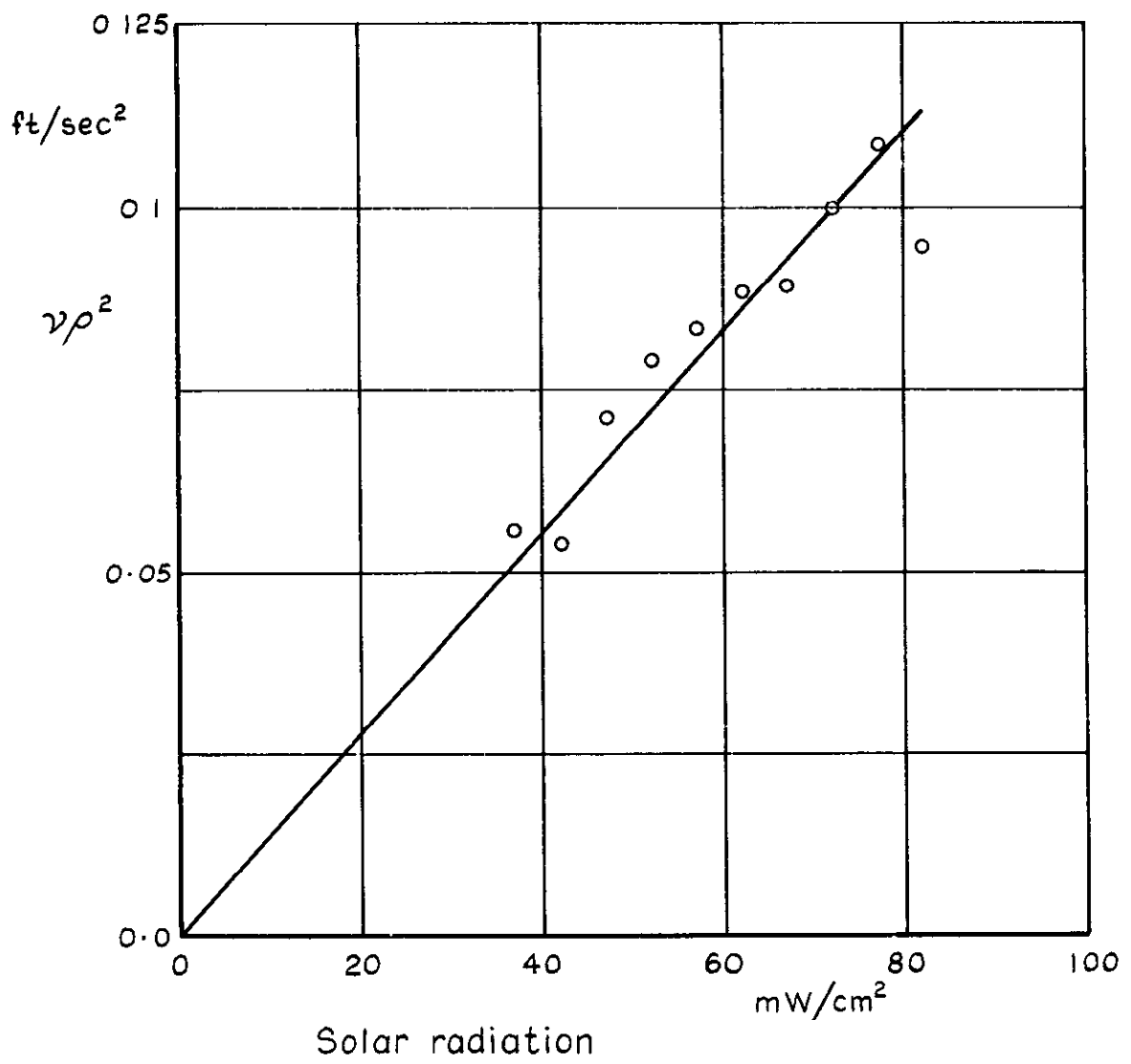
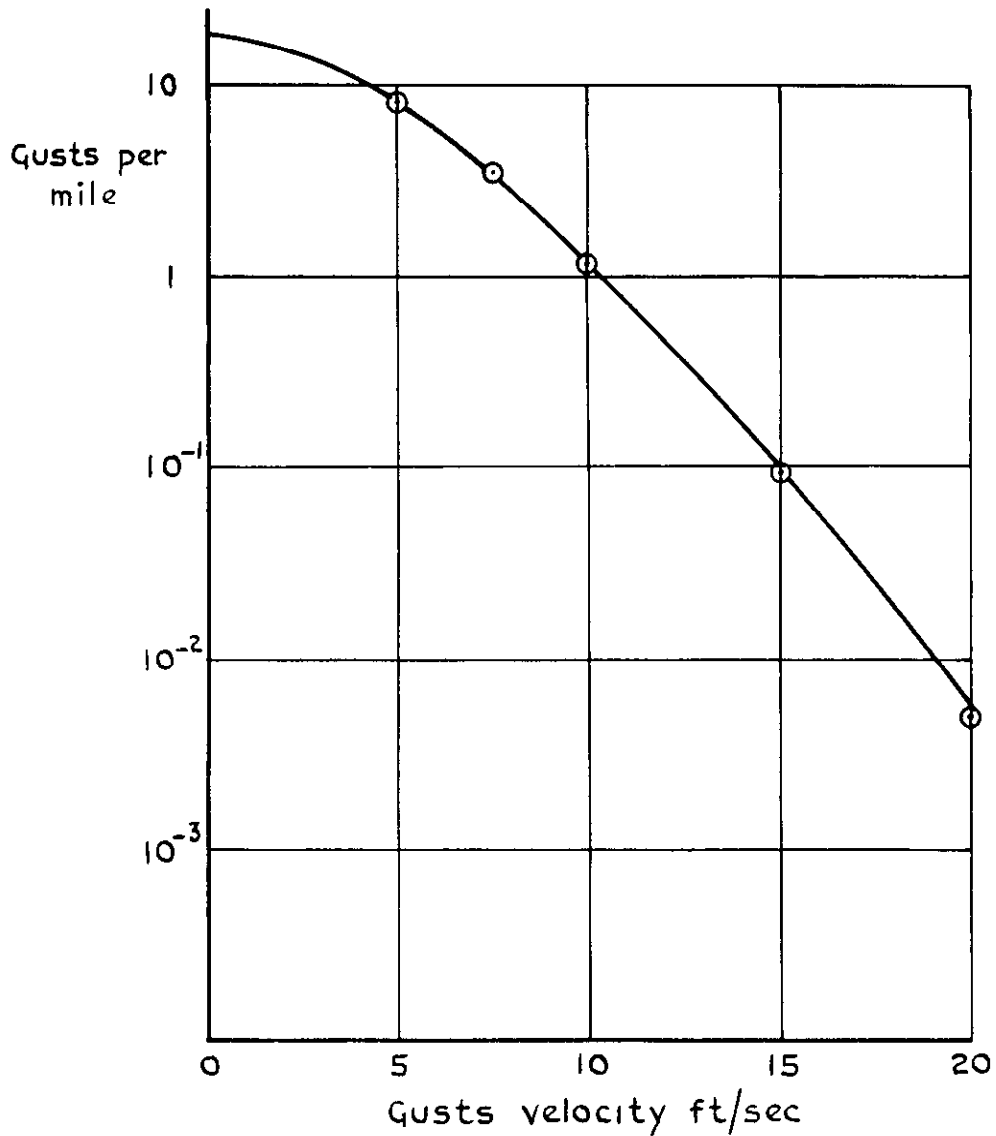
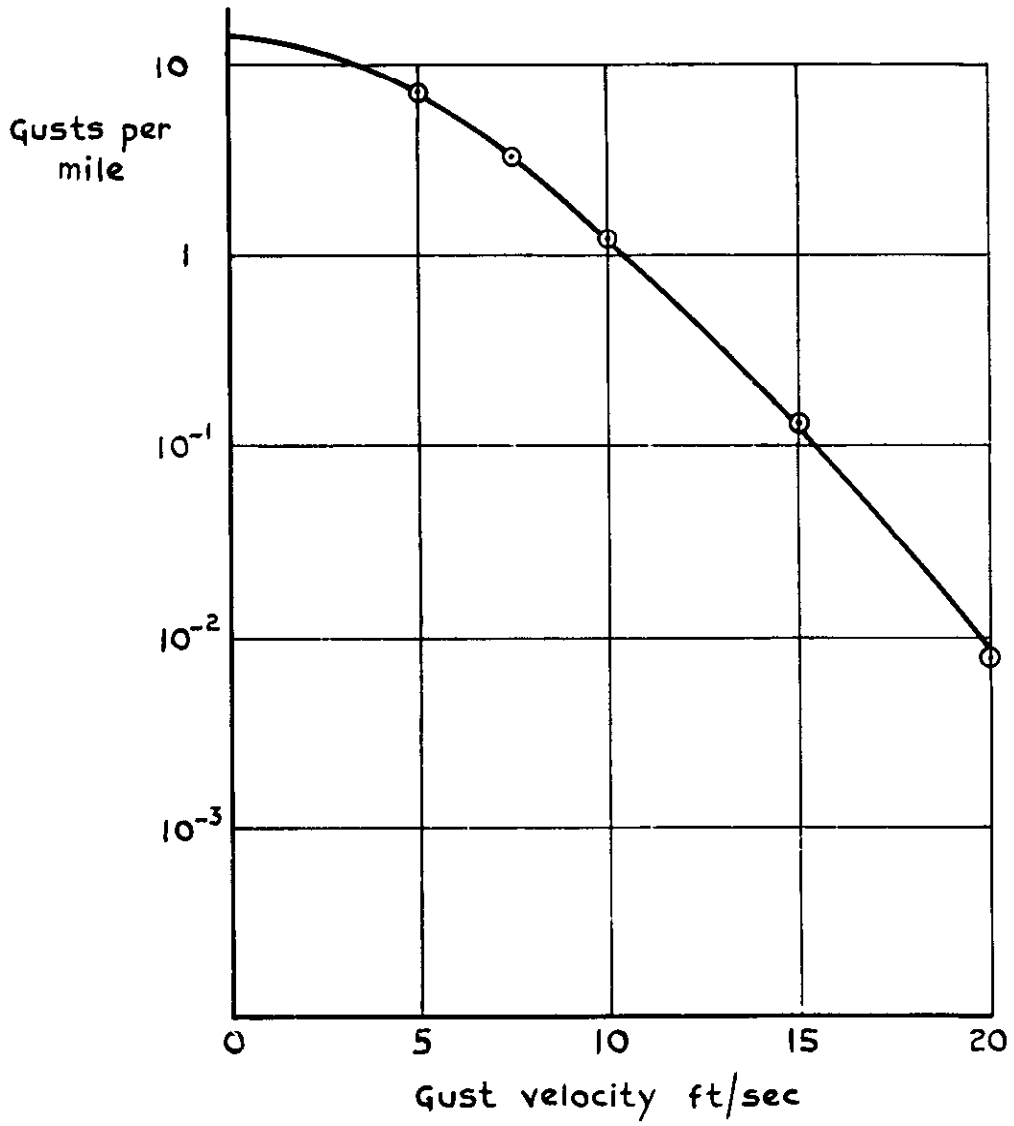


Fig.10 "Swifter" midday flights over flat desert.
Energy relationship



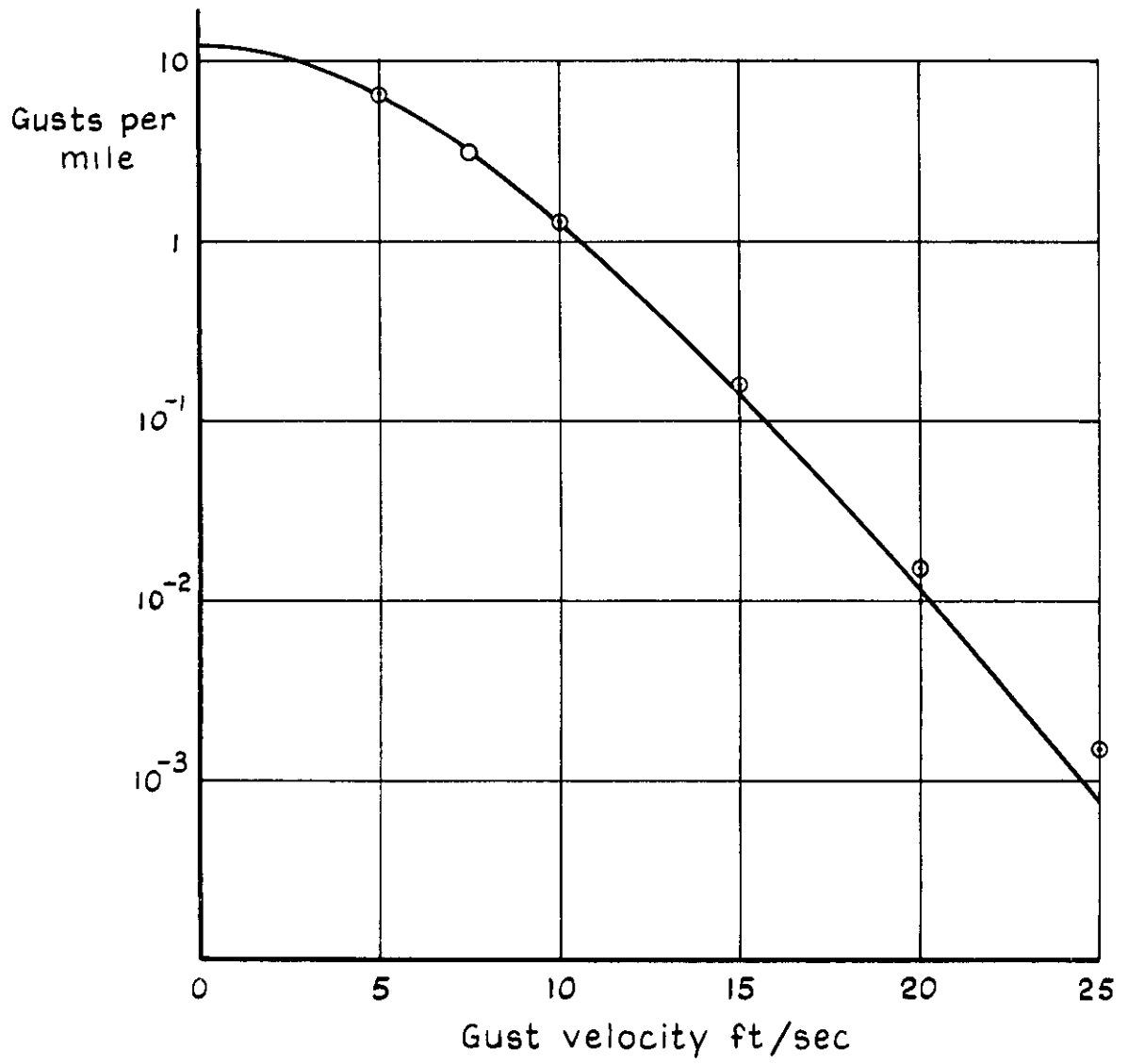
a 200 ft

Fig.II "Swifter" stacked sorties with solar radiation $\geq 65\text{mW/cm}^2$ over flat desert. Cumulative gust distributions



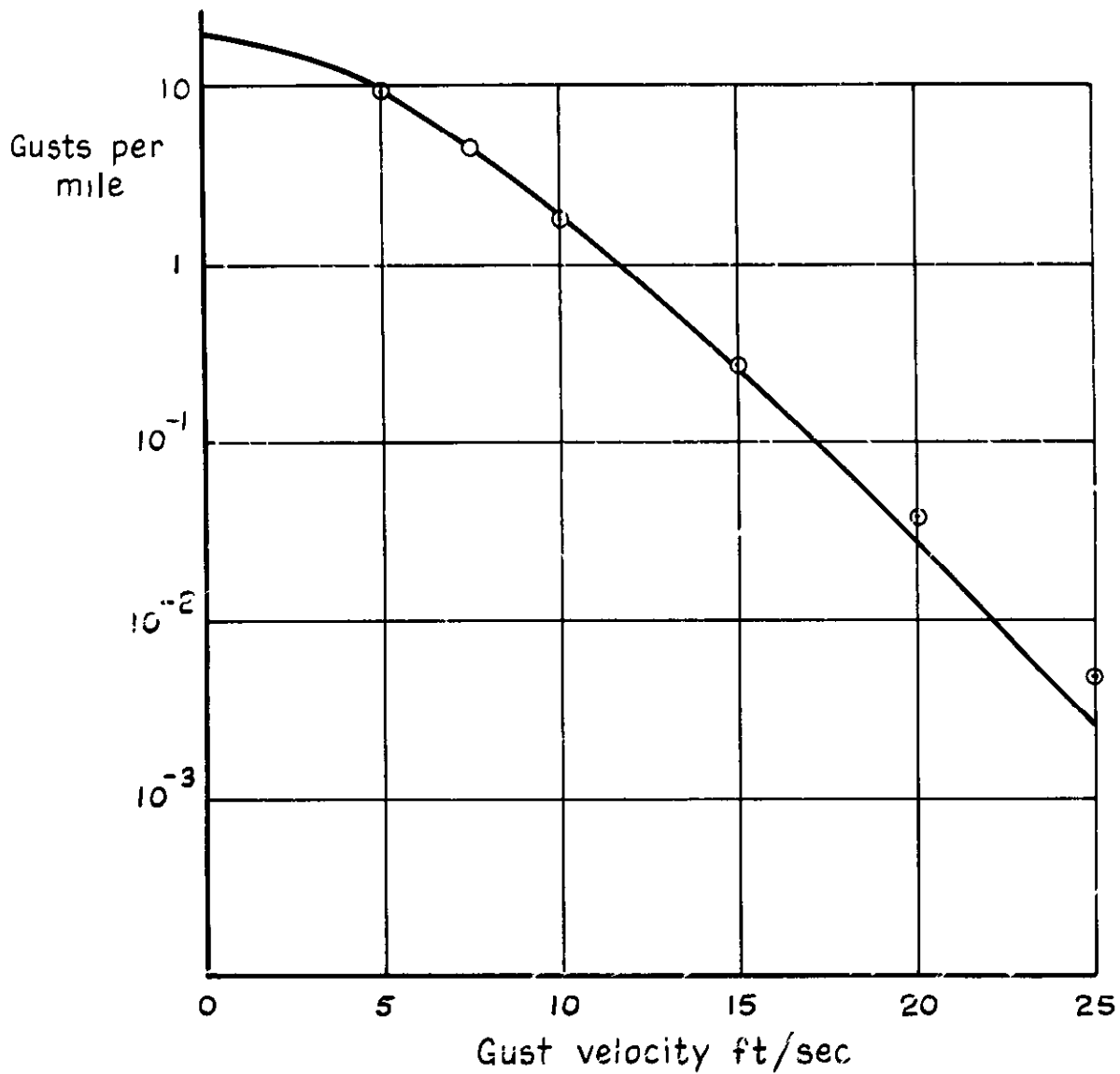
b 400 ft

Fig. II contd



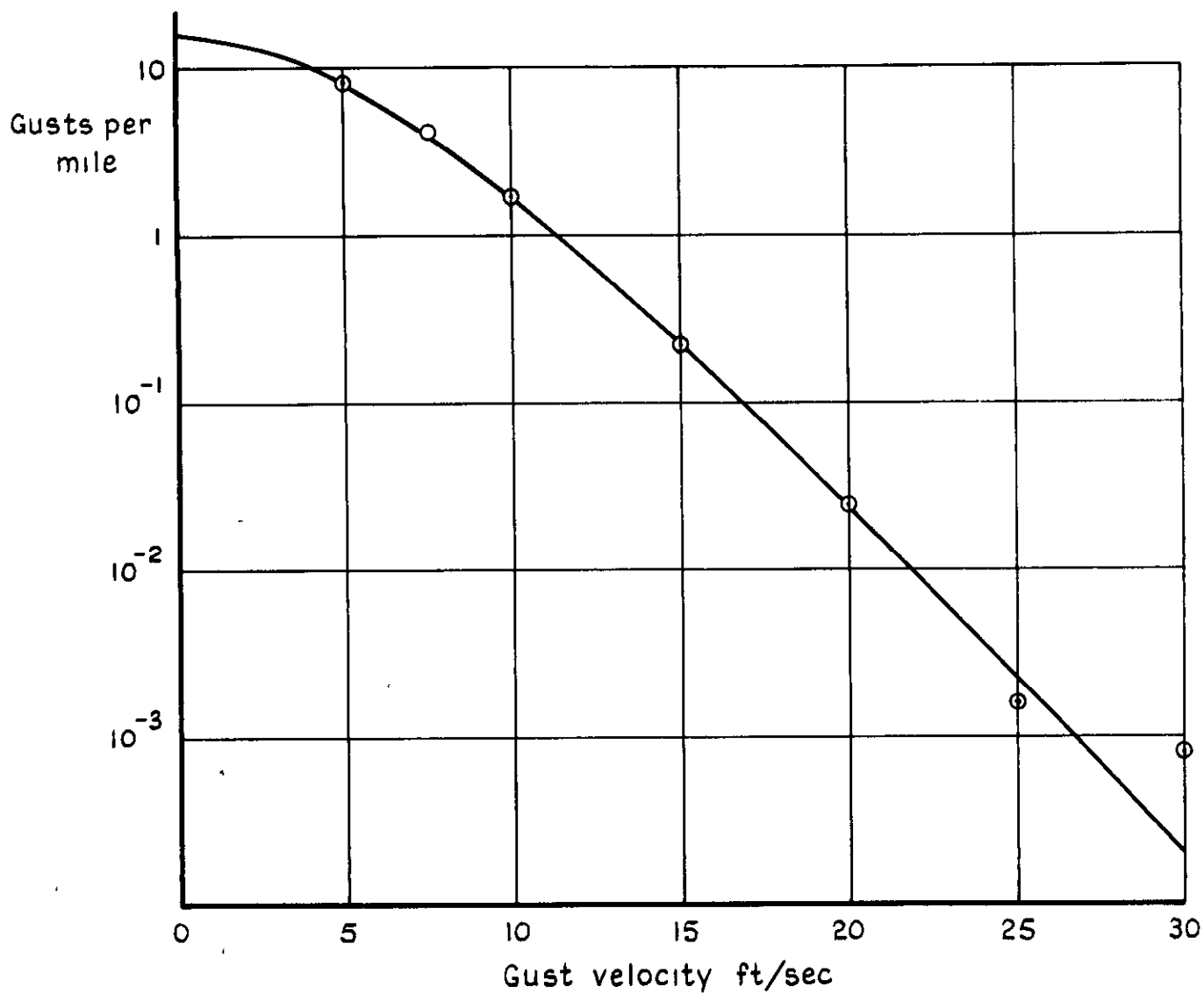
c 600 ft

Fig. 11 conclud



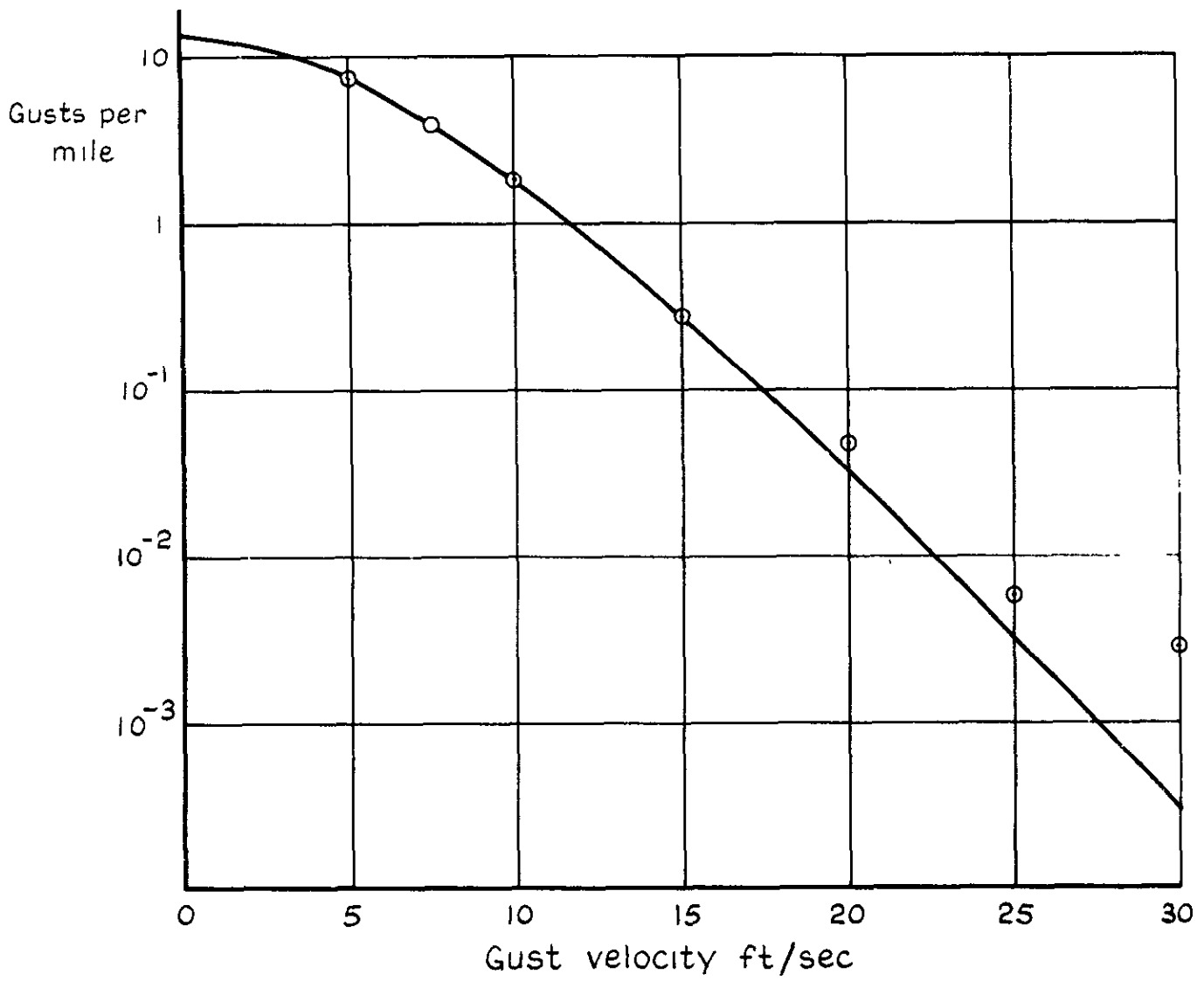
a 200 ft

Fig.12 "Swifter" stacked sorties with solar radiation $\geq 65 \text{ mW/cm}^2$ over hilly desert. Cumulative gust distributions



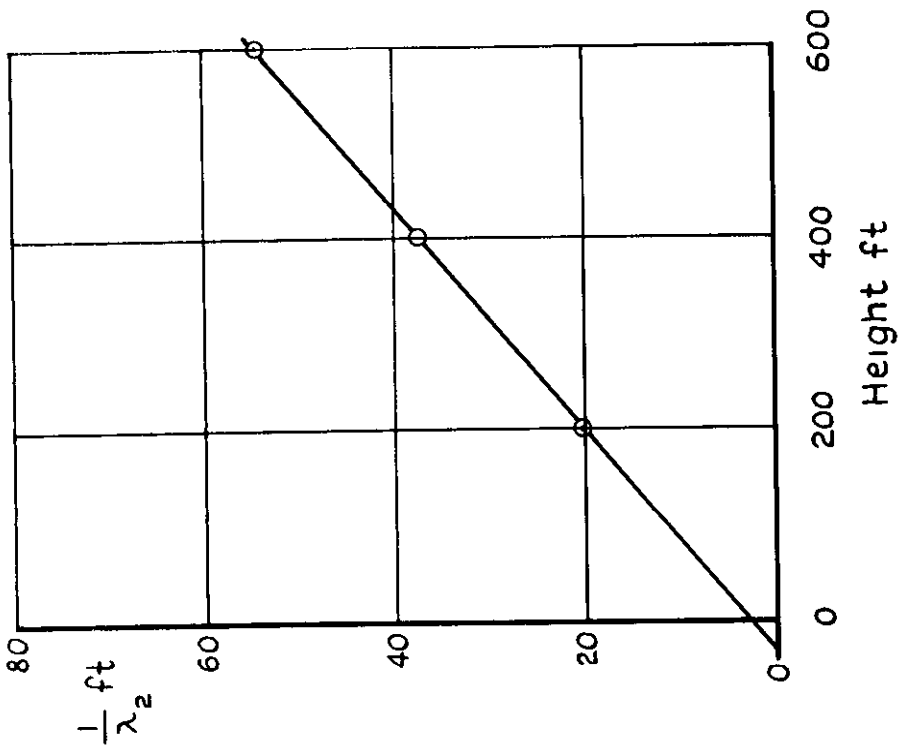
b 400ft

Fig. 12 contd

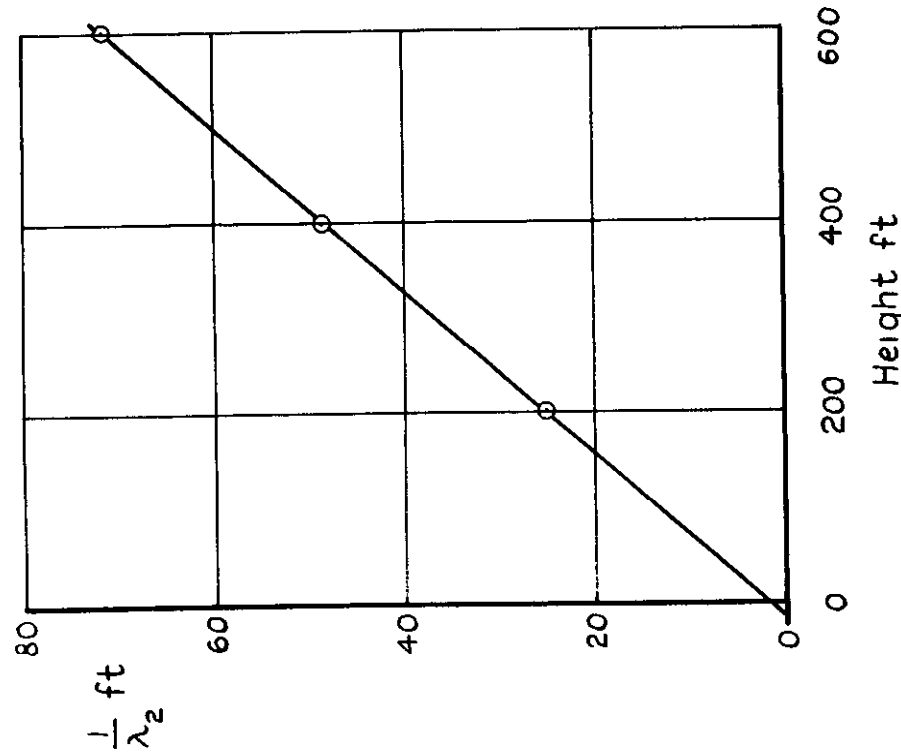


c 600 ft

Fig. 12 conclud

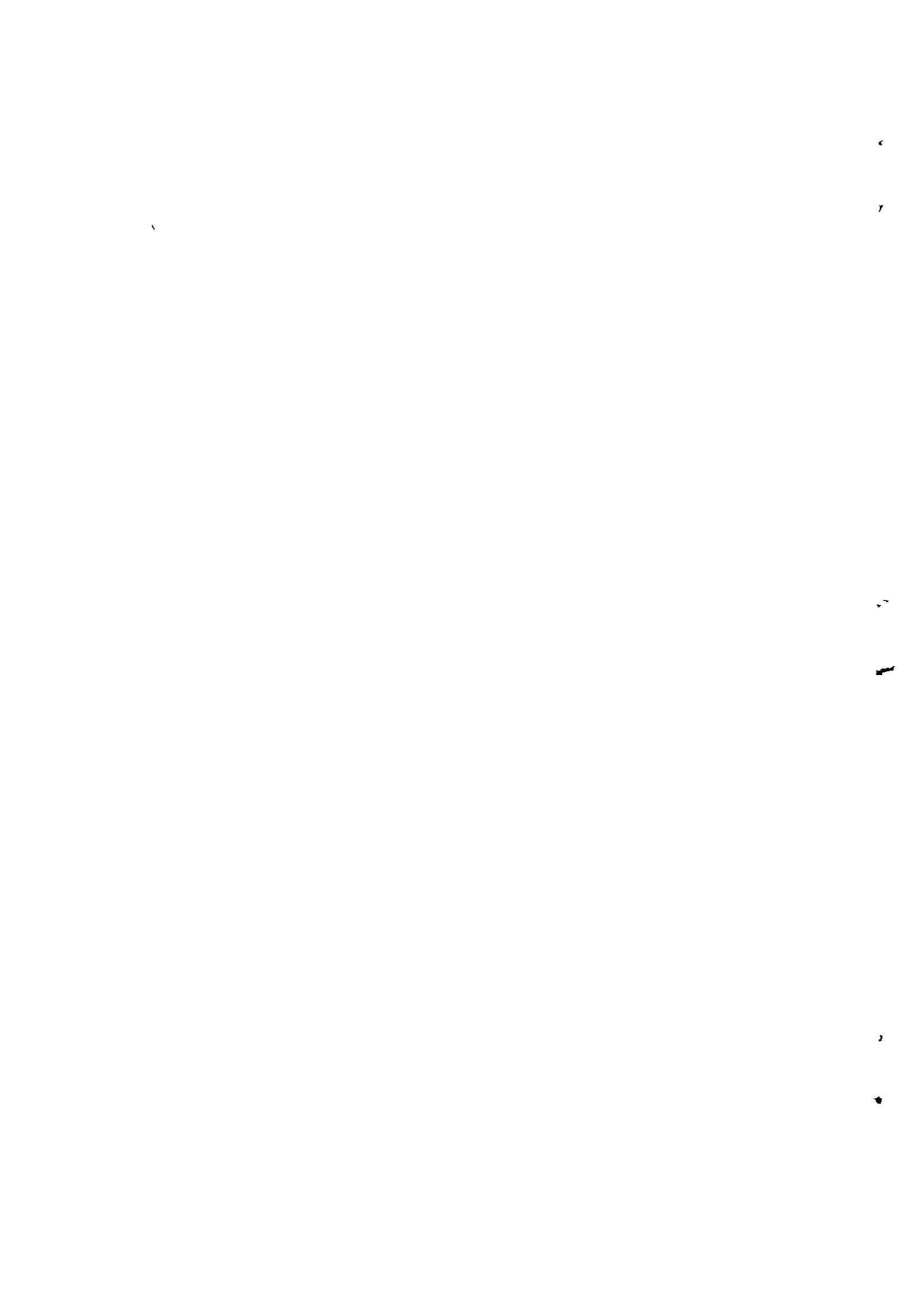


a Flat desert



b Hilly desert

Fig.13 "Swifter" stacked sorties (solar radiation $\geq 65 \text{ mW/cm}^2$).
Variation of $\frac{1}{\lambda_2}$ with height



A.R.C. C.P. No.1079
March 1969

Bullen, N. I.

GUSTS, DISCRETE AND INDISCRETE

For the analysis of gust loads on aircraft, a method is described in which the occurrence and magnitude of the loads are represented as random variables.

The paper begins with the discrete gust, and goes on to treat the case in which the disturbances are too frequent to be considered singly and become indiscrete. In the limit this leads to the usual results obtained from the spectral approach, but in the observational material examined this limit is not reached. The simple mathematical model developed here gives a consistent picture of the properties of observed gust load frequency distributions.

533.6.048.5 :
551.551 :
519.242 .
519.251 .
5.001.57

A.R.C. C.P. No.1079
March 1969

Bullen, N. I.

GUSTS, DISCRETE AND INDISCRETE

For the analysis of gust loads on aircraft, a method is described in which the occurrence and magnitude of the loads are represented as random variables.

The paper begins with the discrete gust, and goes on to treat the case in which the disturbances are too frequent to be considered singly and become indiscrete. In the limit this leads to the usual results obtained from the spectral approach, but in the observational material examined this limit is not reached. The simple mathematical model developed here gives a consistent picture of the properties of observed gust load frequency distributions.

533.6.048.5 :
551.551 :
519.242 .
519.251 :
5.001.57

A.R.C. C.P. No.1079
March 1969

Bullen, N. I.

GUSTS, DISCRETE AND INDISCRETE

For the analysis of gust loads on aircraft, a method is described in which the occurrence and magnitude of the loads are represented as random variables.

The paper begins with the discrete gust, and goes on to treat the case in which the disturbances are too frequent to be considered singly and become indiscrete. In the limit this leads to the usual results obtained from the spectral approach, but in the observational material examined this limit is not reached. The simple mathematical model developed here gives a consistent picture of the properties of observed gust load frequency distributions.

533.6.048.5 :
551.551 :
519.242 :
519.251 :
5.001.57

2
12

12
13
14

15
16

C.P. No. 1079

© *Crown copyright 1970*

Published by

HER MAJESTY'S STATIONERY OFFICE

To be purchased from

49 High Holborn, London w c 1
13a Castle Street, Edinburgh EH 2 3AR
109 St Mary Street, Cardiff cf1 1JW
Brazenose Street, Manchester 2
50 Fairfax Street, Bristol BS1 3DE
258 Broad Street, Birmingham 1
7 Linenhall Street, Belfast BT2 8AY
or through any bookseller

C.P. No. 1079

SBN 11 470279 9